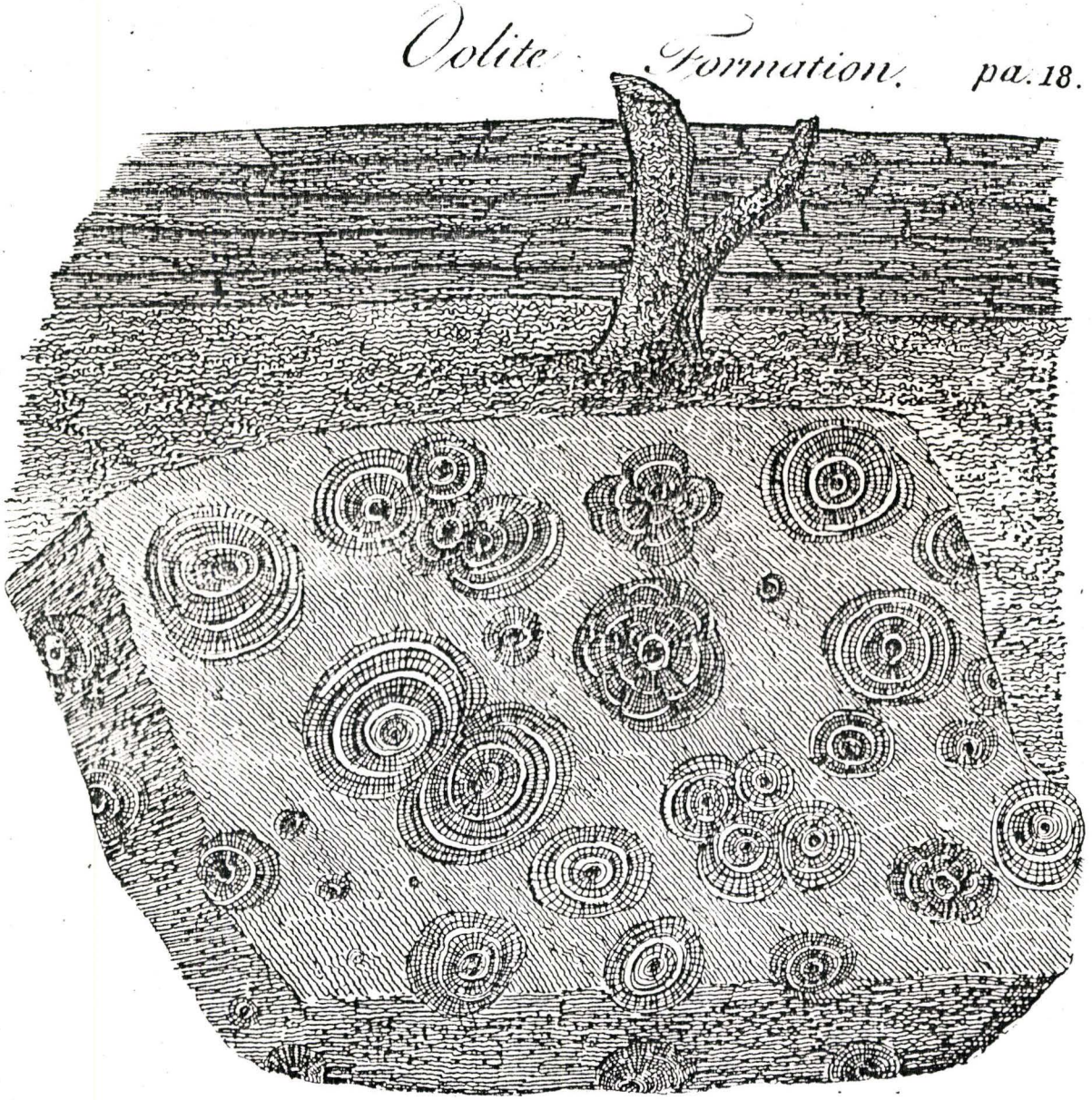

Frontispiece: engraving of stromatolites in the Upper Cambrian, Saratoga Springs, New York, from Steel (1825).

ALGAL MATS AND CRYPTALGAL STRUCTURES, BOCA JEWFISH, LAC, BONAIRE, NETHERLANDS ANTILLES

BY

BRIAN R. PRATT

Submitted to the Department of Geology, in partial fulfillment of the requirements for the degree Honours Bachelor of Science

McMaster University

May, 1976

ABSTRACT

Algal mats form a variety of sediment-stabilizing cryptalgal structures in the Boca Jewfish area of the Lac, Bonaire. These structures are related to the blue-green algal communities that comprise the mats, desiccation during intertidal periods and current action. Variation in these parameters produces a zonation of external morphologies of cryptalgal structures. Sediment is agglutinated onto mucilage secreted by fine filaments of blue-green algae in subtidal and intertidal oncolites. Sediment is trapped and enmeshed by blue-green algae in the rigid smooth mat. Subtidal colloform mats hold sediment loosely by entrapment and agglutination onto mucilagenous algal sheaths. The sediments of the tufted mat zone are caught and bound by large sticky filaments. Lithification of oncolites and chunks of smooth mat occurs in the intertidal by growth of pore-destroying fibrous aragonite cement. Indurated crust pavements that are found in the study area appear to have been cemented in the intertidal and supratidal environment. Cementation here is principally cryptocrystalline aragonite.

In the present regressive stage in the Lac, there has not been sufficient time for significant vertical accretion in the smooth and tufted mat zones.

Honours Bachelor of Science (1976)

Geology

Title: Algal mats and cryptalagal structures, Boca Jewfish, Lac, Bonaire, Netherlands Antilles

Author: Brian R. Pratt

Supervisor: Dr. M. J. Risk

Number of Pages: vii, 100

TABLE OF CONTENTS

LIST OF FIGURES

ACKNOWLEDGEMENTS

I would like to thank Dr. M. J. Risk (McMaster University), for his supervision and guidance throughout the study, and for critically reading initial drafts of the thesis. I especially thank D. R. Kobluk (McMaster University), who discovered the study area, for his advice, suggestions and help in the field, in the lab and for critically reading initial drafts. I am grateful to J. Whorwood (McMaster University), for his tremendous help in the preparation of photographs, though any lack of quality is entirely the fault of the author. Dr. I. Kristensen and the staff of the Caribbean Marine Biological Institute (CARMABI) of the Netherlands Antilles provided equipment and accommodation on Bonaire, and supervised the shipment of samples. I thank Dr. P. Hoffman (Geological Survey of Canada) and Dr. H. J. Hofmann (Universite de Montreal), for helpful discussions. Financial support was received from the National Research Council (grant to Dr. M. J. Risk), the Ontario Petroleum Institute, and the Department of Geology, McMaster University. I also thank the Bedford Institute of Oceanography (Halifax), for supplying plastic case liners, the staff of the Electron Microscope Facilities of the McMaster University Medical Centre and Department of Metallurgy, and D. G. Reid for photographic assistance. Amoco Canada Petroleum Company Ltd. (Calgary), covered the cost of typing and reproduction.

CHAPTER I

INTRODUCTION

Algae are a large and diverse group of plants, with a geologic range that begins in the Precambrian (Barghoorn and Tyler, 1965; Barghoorn and Schopf, 1966; Hofmann, 1975) and extends throughout the Phanerozoic. The algae can be classified as either eukaryotic or prokaryotic; eukaryotes have a nucleus and cell organelles; prokaryotes do not have a distinct nucleus and internal organelles (Schopf et al, 1973). Eukaryotic algae are divided into ten phyla (Chapman and Chapman, 1973), two of which are of direct interest in this study: Rhodophyta (red algae) and Chlorophyta (green algae). Certain members of the Rhodophyta and Chlorophyta are able to secrete calcium carbonate skeletons; these organisms are referred to as calcareous algae (Johnson, 1961).

The blue-green algae belong to the Cyanophyta, and, together with the bacteria, comprise the prokaryotes. The Cyanophyta do not secrete calcium carbonate skeletons, yet they play important roles in the formation of many sedimentary carbonate rocks. Assemblages of blue-green algae form mats in shallow sub-tidal, intertidal, and low supratidal coastal marine areas and also in waters that range from brackish to fresh. Filamentous and coccoid blue-green algae construct cohesive algal mats by trapping and binding sedimentary particles. Sediments of algal mats may be internally laminated or non-laminated; this internal fabric is termed cryptalgal (Aitken, 1967) and distinguishes algal mats from structures produced by calcareous algae.

Precambrian cryptalgal structures are the earliest known structures to have been constructed undoubtedly by organisms. Cryptalgal structures have been found as far back as the late Archaean (Henderson, 1975; Schopf et al, 1971) and are evidence for the early existence of prokaryotic life. Since the Precambrian, eukaryotic life has dramatically increased in complexity and diversity, and yet modern cryptalgal carbonate structures analogous to Precambrian forms are found today.

Stromatolites, oncolites and algalaminites are three types of cryptalgal structures. Algalaminites are planar in morphology (Aitken, 1967); the blue-green algal origin of fossil forms is inferred from their fossil content and similarity to the fabrics of modern planar algal mats (Aitken, 1967). Oncolites are formed by a mat growing around an intermittently mobile nucleus and have in general a spheroidal shape (Hofmann, 1969). Stromatolites are distinct stationary cryptalgal structures that have positive relief in the form of heads, domes or branching forms (Aitken, 1967). An additional type, "thrombolite", was described by Aitken (1967) as a structure lacking internal lamination. Stromatolites, oncolites, thrombolites, and algalaminites can be grouped as a whole by depositional texture as algal boundstones (Dunham, 1962), or petrographically as algal biolithites (Folk, 1959, 1962). Many classifications of cryptalgal morphologies have been proposed; these are thoroughly reviewed in Hofmann (1969). The most accepted classification is that of Logan et al (1964), as it can be applied to both ancient and modern

cryptalgal structures. The practice of using generic nomenclature for cryptalgal structures began during the nineteenth century, although applying Linnéan names to organosedimentary structures such as these is of dubious validity (Hofmann, 1969, 1973; Hoffman, 1973).

Increased understanding of fossil forms and comparative work on recent carbonate sediments has permitted differentiation of cryptalgal structures from other morphologically similar biogenic structures, such as calcareous red algal nodules (rhodoliths, rhodolites; these are discussed in Bosellini and Ginsburg, 1971 and Toomey, 1975), foraminifera (Gürich, 1907), sponges (Seely, 1906), and stromatoporoids (Steinmann, 1911) as well as laminated structures produced by purely sedimentary or concretionary processes.

HISTORICAL BACKGROUND

The affinities and origin of cryptalgal carbonate structures were a problem for many years after they were first described by Steel (1825) from the Upper Cambrian at Saratoga Springs, New York (Frontispiece). The Saratoga Springs locality was redescribed by Hall (1883) who interpreted the stromatolites as produced by protozoa and called them Cryptozoon proliferum.

The first true Precambrian stromatolite group to be named generically was Archaeozoon (Eozoon) acadiense Matthew 1890 from the Green Head Group of New Brunswick (Figure 1). Prior to this, Eozoon canadense Dawson 1864 was described from several localities of the Precambrian Grenville Province of eastern Canada by Sir William Logan during the late 1850's and early 1860's. Dawson (1875) summarized the contemporary controversy over this "fossil". Hofmann (1971) presents a discussion of Eozoon in light of later evidence which suggests that Eozoon is of inorganic origin.

The origin of cryptalgal structures remained obscure, though still considered fossils, and different forms were named; the genera were collected under the Spongiostromidae of the Protozoa by Gürich (1907). The word "Stromatolith" was introduced by Kalkowsky (1908) to refer to a bed or accumulation of "Stromatoids". The orders "Oncolithi" and "Stromatolithi" were introduced by Pia (1927) for mobile and attached cryptalgal structures respectively. Pia (1927) placed these orders in the newly created family Spongiostromata of the Class Schizophyceae.

While studies of fossil cryptalgal structures were being carried out without proof as to their origin, algal-induced precipitation in hotsprings of minerals such as silica and calcium carbonate was described by Cohn (1862) at Karlsbad and by Weed (1889) at Yellowstone Park, Wyoming. These were compared with stromatolitic deposits of Belguim and Germany by Reis (1908). Calcareous nodules formed by blue-green algae in freshwater lakes and streams were examined by several early workers such as Clark (1900) and Roddy (1915). Walcott (1914) first demonstrated convincingly the algal origin of ancient stromatolites by comparisons with these freshwater nodules.

Figure 1:

Archaeozoon (Eozoon) acadiense Matthew 1890 from the Precambrian Green Head Group, St. John, New Brunswick. See Hofmann (1974) for further discussion of this stromatolite locality.

A. Longitudinal view of stromatolite columns. Lens cap is approximately 6 cm across.

B. Tangential view of stromatolite columns, showing concentric laminations.

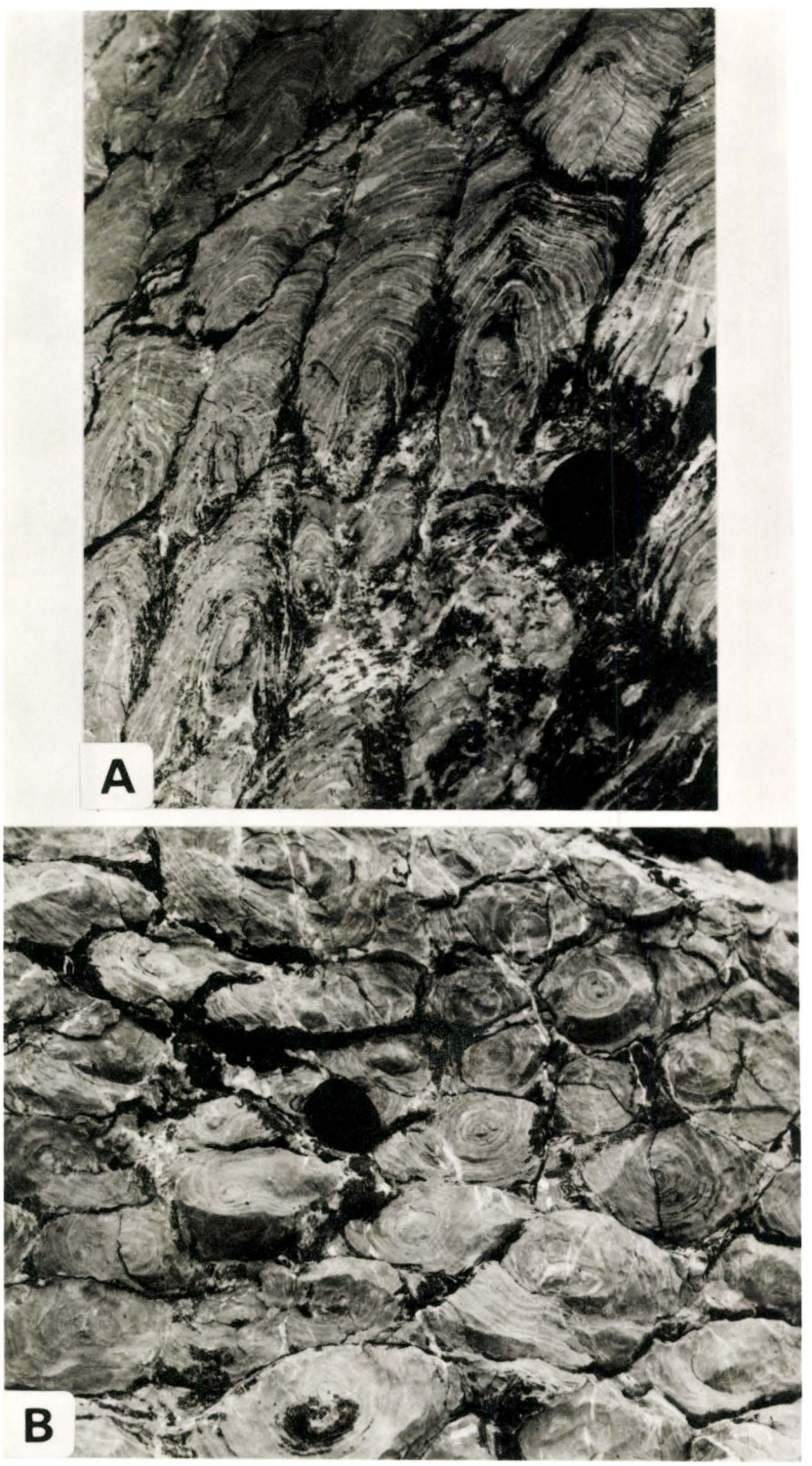
A
B

The first description of modern marine cryptalgal carbonates and the environmental factors influencing their growth was given by Black (1933) from Andros Island in the Bahamas; Ginsburg et al (1954) described a second occurrence of modern algal mats in the Florida Keys. Since then, modern marine cryptalgal carbonates have been described from many tropical and subtropical areas, such as the Persian Gulf (Kendall and Skipwith, 1968), Western Australia (Logan, 1961; Davies, 1970; Logan et al, 1974), Bahamas (Monty, 1965a,b, 1967, 1972; Neumann et al, 1970) and Bermuda (Gebelein, 1969). Algal mats are not restricted to warmer climates and have been found in the temperate zone (Hommeril and Rioult, 1965).

Recent studies of modern and ancient cryptalgal structures have shown that they are of considerable use in paleoecological, paleosedimentary and paleogeographical interpretations of ancient rock sequences. The shape and fabric of cryptalgal carbonate structures is controlled by a complex interplay of many environmental and sedimentological factors (Logan et al, 1964). Cryptalgal carbonates may also be considered as a distinct facies in a sequence of shallow-water carbonate rocks, and have been used in reconstructions of ancient shorelines by many workers (e.g.: Roehl, 1967; Laporte, 1967; Walker, 1972; Lucia, 1972; Hoffman, 1974).

The present study is an examination of modern cryptalgal carbonate structures from the Boca Jewfish, Bonaire, Netherlands Antilles.

CHAPTER II

REGIONAL SETTING

Bonaire, Netherlands Antilles, is located in the Caribbean Sea (Figure 2) at Long. 68°25'W., Lat. 12°6'N., about 100 kilometres off the north coast of Venezuela (Figure 3). It is approximately 265 square kilometres in area (Figure 4) and has a maximum relief of 243 metres, with some areas below sea level.

Bonaire has a semi-arid climate; the mean annual temperature is 27°C with a 6 degree variation (Sibley and Murray, 1972). The annual rainfall on the island varies considerably, with an average of about 51 centimetres, over half falling in the rainy season, September to January (Westermann and Zonneveld, 1956, cited in Deffeyes et al, 1965; Sibley and Murray, 1972).

Folded Cretaceous igneous rocks comprise the core of the island. These are overlain unconformably by a thin sequence of Cretaceous clastics and Eocene carbonates, and primarily by Plio-Pleistocene limestones and dolomites (de Buisonjé, 1974). These carbonates are terraced, particularly on the eastern side of the island; this terracing is similar to other Quaternary terraces reported from other Caribbean islands, and is due to an interplay of depositional and erosional processes associated with (Quaternary) sea level fluctuations (de Buisonjé, 1974). Inclined Plio-Pleistocene beds are found on the western side of the island; these are considered to exhibit a primary dip, and are composed of reef-derived talus (de Buisonjé, 1974). These beds are partially dolomitized (Deffeyes et al, 1965). Dipping Pleistocene eolianites are also found on the western side of the island (de Buisonjé, 1974). The terraced limestones are composed predominantly of calcareous algae and corals; they are fossil fringing reef depositis (de Buisonjé, 1974).

The island is fringed by a living coralgal reef. Along the shore of the southern part of the island, a storm-deposited barrier of coral rubble has isolated several shallow hypersaline lakes, the largest of which is the Pekelmeer. The Pekelmeer has been well studied and is the site of Holocene dolomite and evaporite formation (Deffeyes et al, 1965; Lucia, 1968; Murray, 1969; v.d. Meer Mohr, 1972).

On the southeast coast of Bonaire there is a large shallow lagoon, the Lac (Figure 5). The Lac is rimmed by mangroves; behind these, on the landward side, karstified Pleistocene bedrock outcrops. The Lac is protected from the open ocean to the east by a linear fringing coralgal reef and beach ridges of coral rubble and reef- and lagoon-derived carbonate sands. The lagoon is very shallow with a maximum depth of about three metres (Figure 6). Ocean currents enter mainly via a natural channel, Boca di Lac, through the coralgal reef. The water temperature is approximately 30°C. Salinity throughout most of the Lac is normal marine ($\sim 35‰$), though hypersaline conditions are found in some of the shallows in the mangrove swamps (Wagenaar Hummelinck and Roos, 1969; v.d. Meer Mohr, 1972).

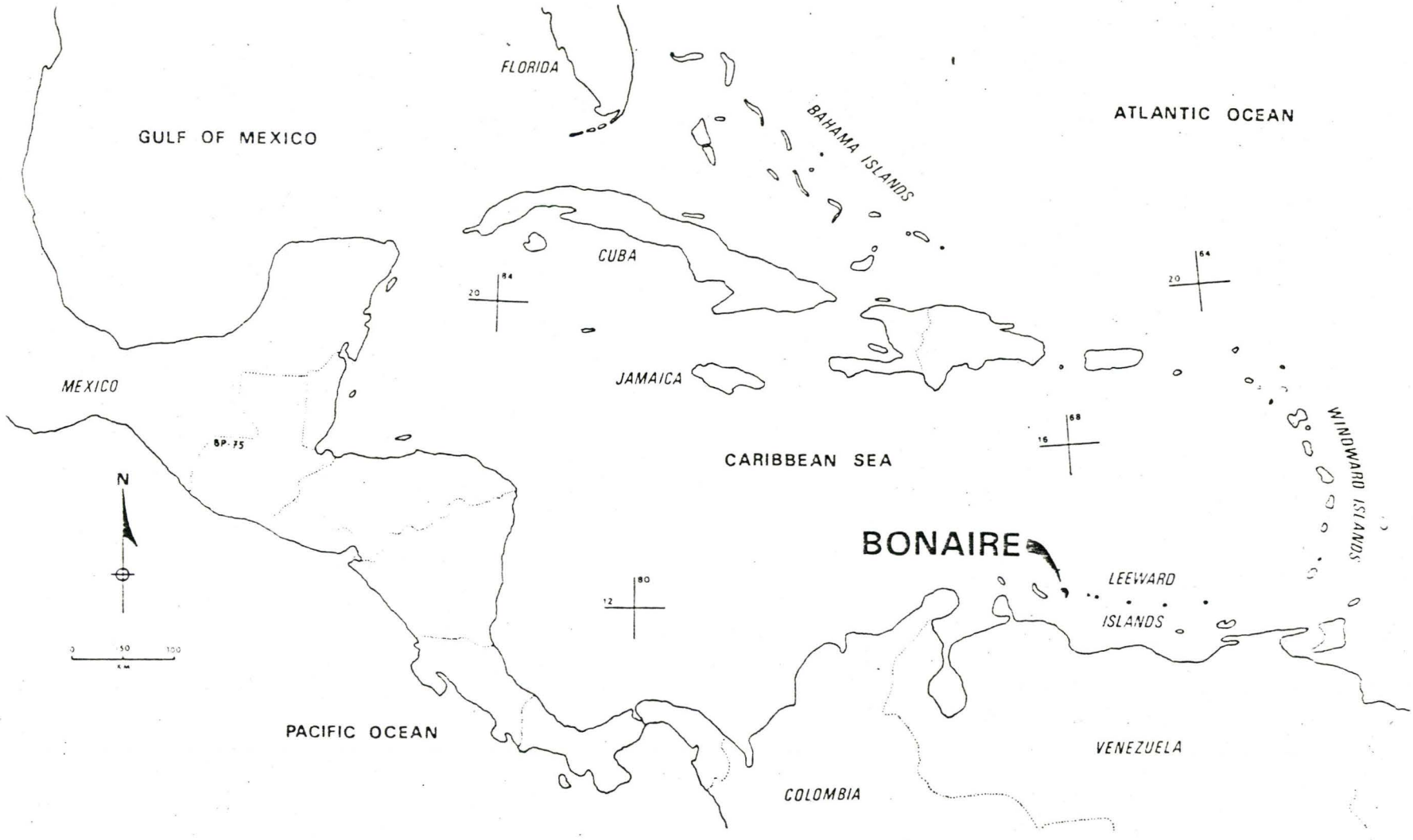

Fig. 2. Location map of Bonaire, Netherlands Antilles.

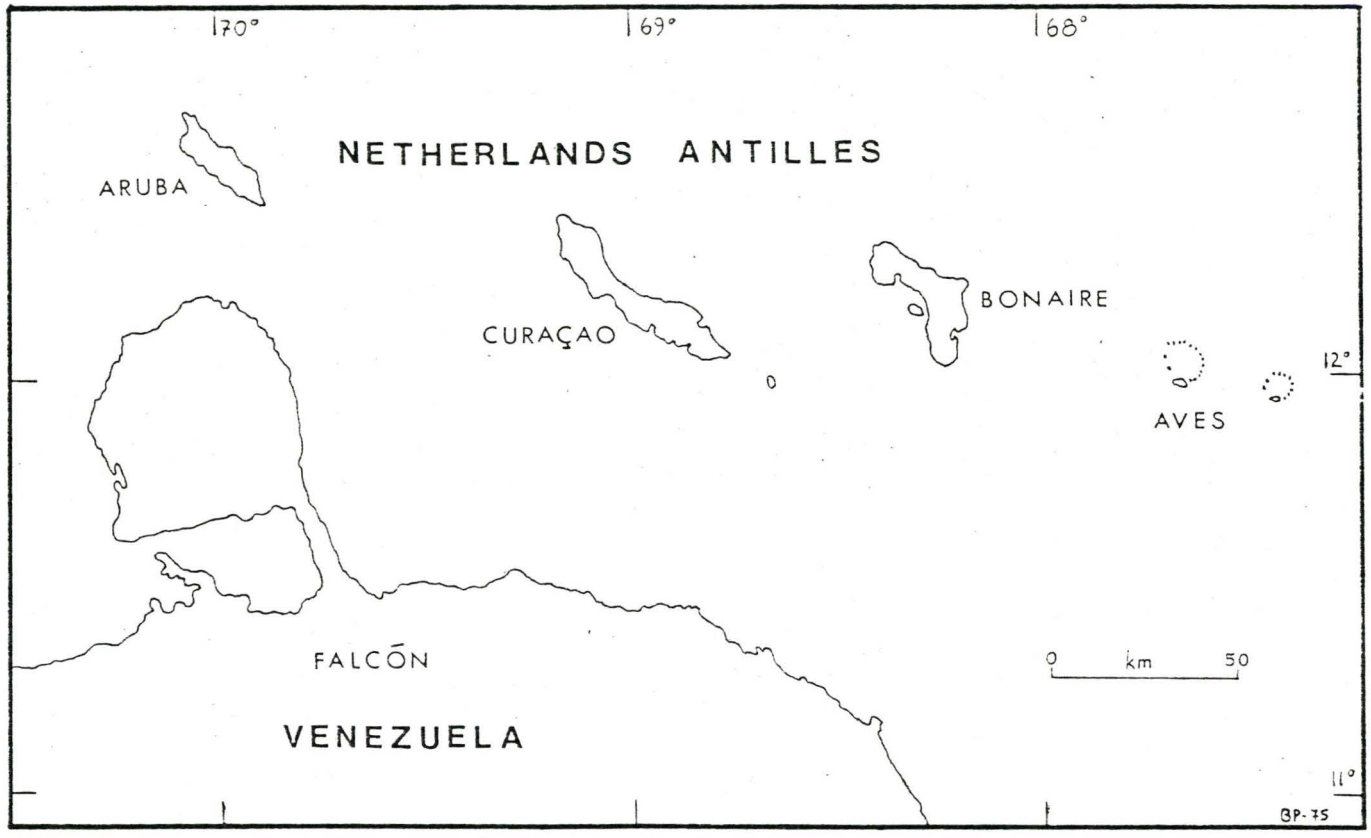

Fig. 3. Location of islands of the Netherlands Antilles.

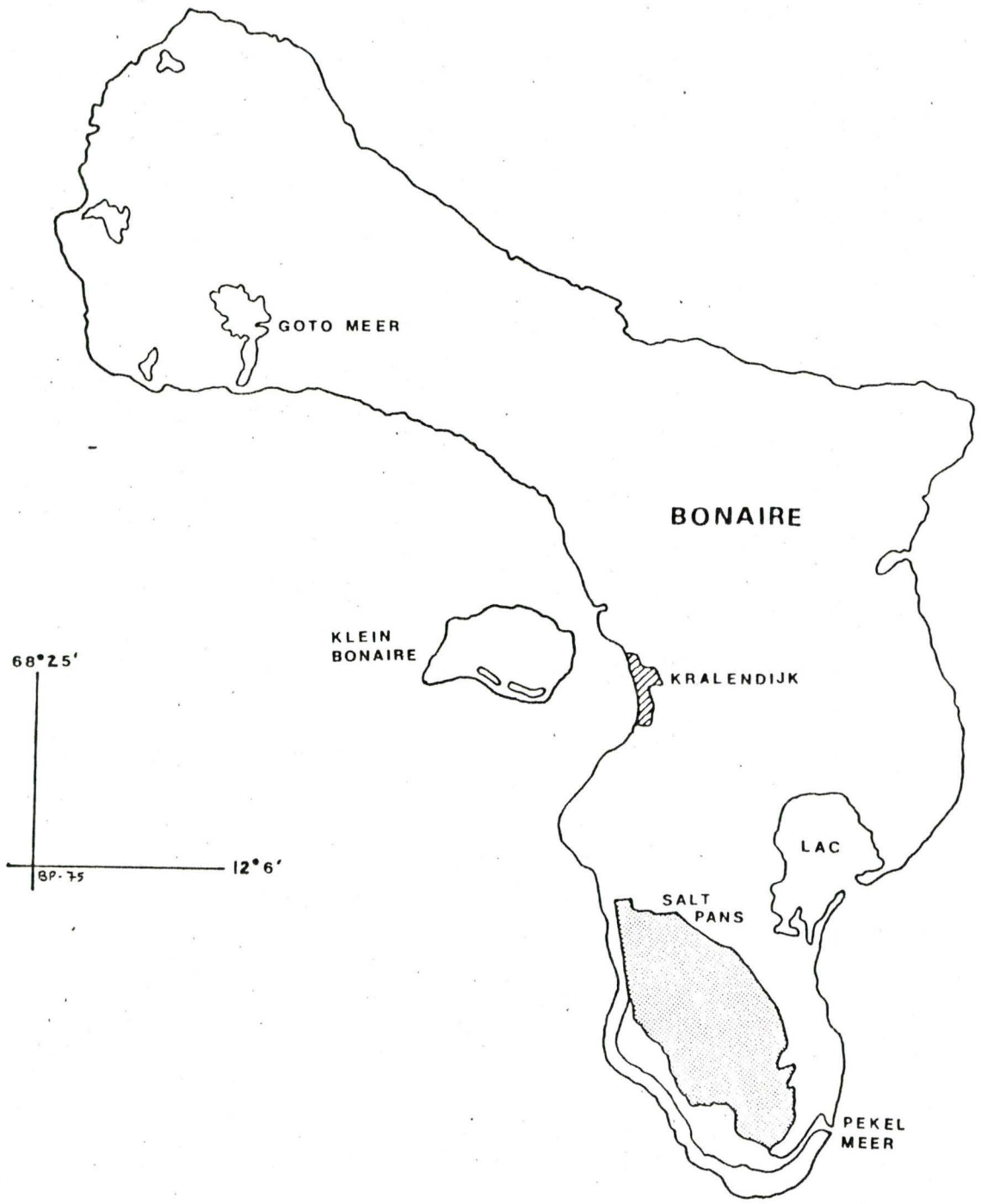

Fig. 4. The island of Bonaire, showing location of the Pekelmeer and the Lac.

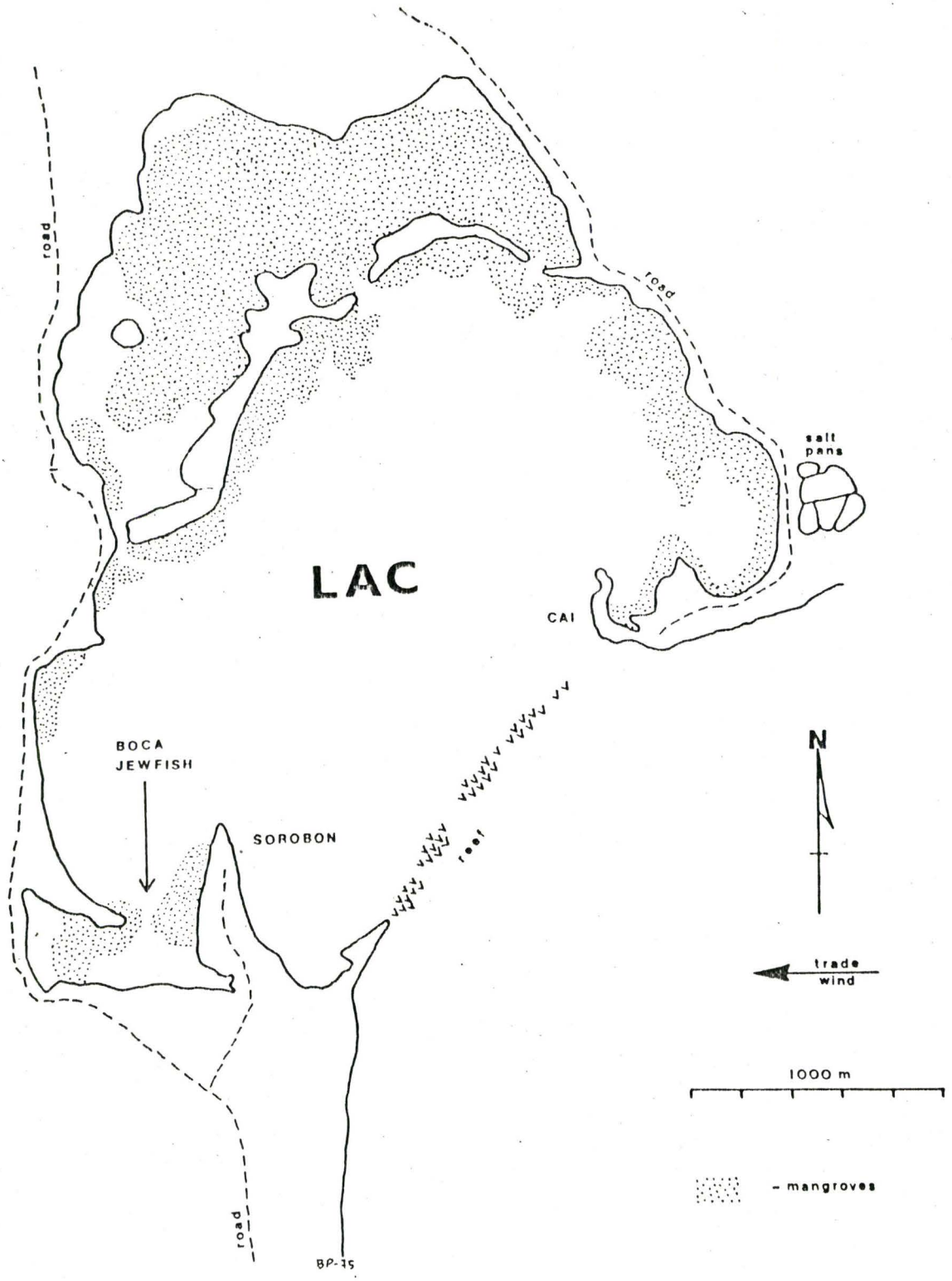
road
road
salt pans
LAC
CAI
BOCA JEWFISH
SOROBON
road
road
BP-15
N
trade wind
1000 m
- mangroves

Fig. 5. The Lac

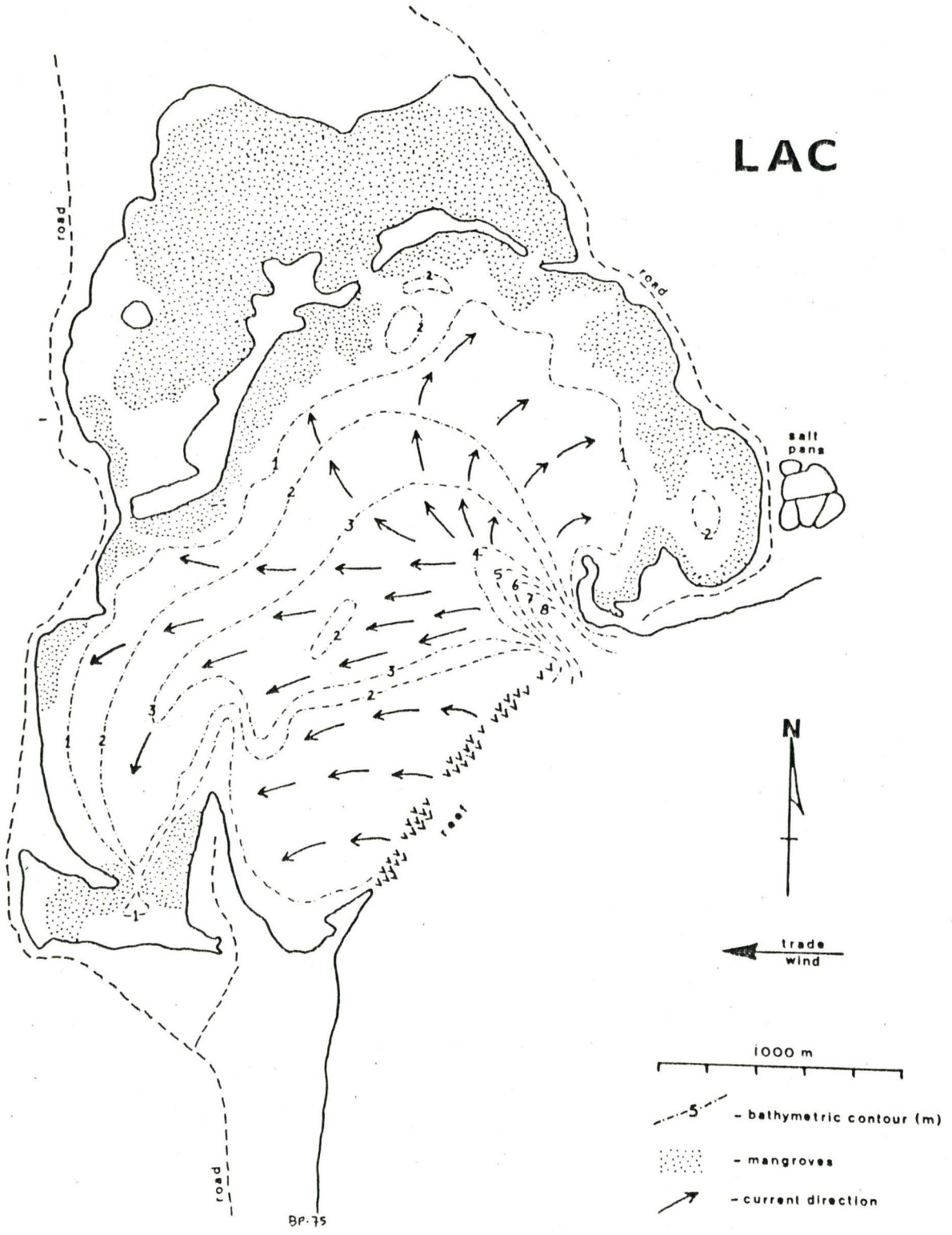

Fig. 6. Approximate depth contours and water current directions of the Lac, after Wagenaar Hummelinck and Roos (1969).

The flora and fauna of the Lac have been studied by Wagenaar Hummelinck and Roos (1969) and v.d. Hoek et al (1972). The sediments of the main part of the Lac are dominantly sand-sized carbonate particles and are extensively bioturbated; conical mounds produced by the burrowing shrimp Callianassa sp. are abundant. The benthos consists of Thalassia testudinum (Figure 7), Halimeda opuntia (calcareous Chlorophyta), coralline (calcareous red) algae (Zaneveld, 1958) (Figure 7), other non-calcareous Chlorophyta, Porites sp., various echninoderms, and the large gastropod Strombus gigas. The mangroves around the edges are made up of Rhizophora sp. and Avicennia sp. The sediments of the mangrove swamps are rich in organic detritus. Acetabularia crenulata (calcareous Chlorophyta) is found growing on mangrove roots; Batophora (Chlorophyta) is common in the swamps. The paucity of molluscs in the Lac is noticeable (Wagenaar Hummelinck and Roos, 1969; Sibley and Murray, 1972) though Strombus gigas is found commonly in the subtidal and is a food source for the local people. Cerithium sp. has been reported living in the salt pans on the northern spit that protects the Lac from the ocean (v.d. Meer Mohr, 1972).

The Boca Jewfish is a small subsidiary bay of the Lac near the Sorobon spit (Figure 8); water depth is less than 1 metre deep. Mangroves (Rizophora sp.) rim the edges of the Boca Jewfish and the shore of Sorobon. The tidal range is about 32 cm (Wagenaar Hummelinck and Roos, 1969); intertidal flats occur along the shores of the Boca Jewfish to Sorobon (Figure 9). Cryptalgal carbonate structures have been found in subtidal, intertidal and supratidal environments of the Boca Jewfish (v.d. Meer Mohr, 1972; v.d. Hoek et al, 1972), and in other areas along the south and west shores of the Lac (v.d. Meer Mohr, 1972; Sibley and Murray, 1972).

METHODS

Field work was carried out in July, 1975. Preliminary examination was undertaken of the subtidal, intertidal and supratidal environments of the Lac in the Boca Jewfish area; on the basis of these observations, sampling sites A, B and C in the intertidal and supratidal areas were chosen; site A was studied and sampled intensively; sites B and C were examined in less detail.

Site A is a sand spit 1.8 square km in area on the south shore of the Lac and separates the Boca Jewfish from the main lagoon. Samples were taken at 35 m intervals (determined by pacing) along a 250 m transect erected along the length of the spit (Figure 10). At sample station B6, a transect perpendicular to the main transect was made; sampling on this transect was carried out at irregular intervals.

The procedure at sample stations B1 to B9, T2 to T4, T6, and T7 was as follows:

- a 30 cm long, 3.5 cm diameter vertical core of algal mat and underlying sediment was taken with plastic core liners.

- a block of algal mat and underlying sediment, 5 to 10 cm square and 3 to 5 cm deep was cut out and the vertical face photographed.

Figure 7:

Subtidal algal benthos of the Lac, off Sorobon.

A. Branching calcareous red (coralline) algal clusters in Thalassia testudinum bed. The red algal clusters range from 5 cm to 10 cm in diameter; the Thalassia blades are about 1 cm to 2 cm across. Water depth is approximately 10 cm at low tide.

B. Thalassia blades and gelatinous oncolite (centre of photograph). The sandy substrate is held loosely by flocculent algal growth. Water depth is approximately 30 cm (Photograph courtesy of D. Kobluk).


A


B

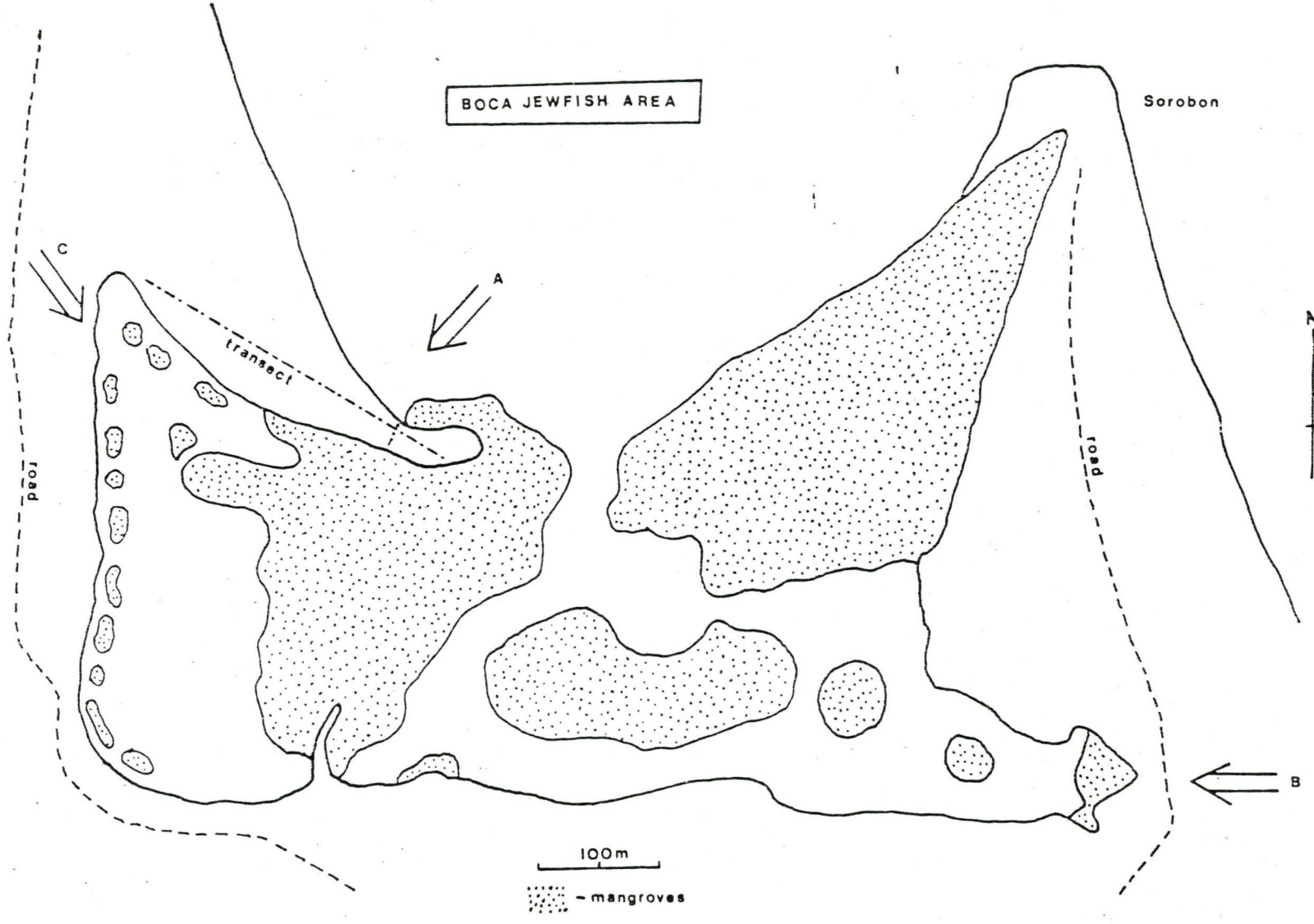

Figure 8: The Boca Jewfish area showing location of sample sites.

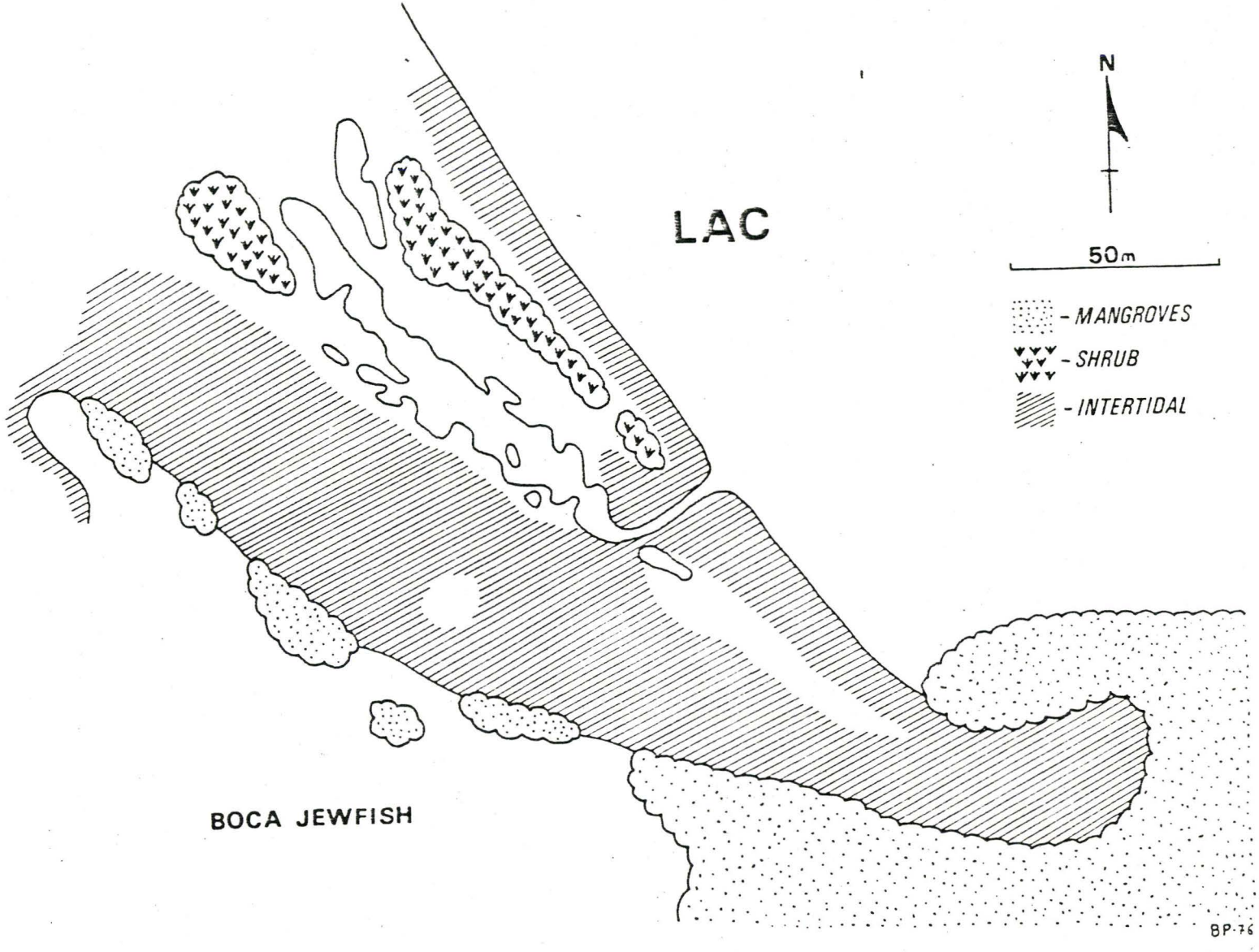

Figure 9: Sample site A showing the intertidal zone which is covered by water only at high tide.

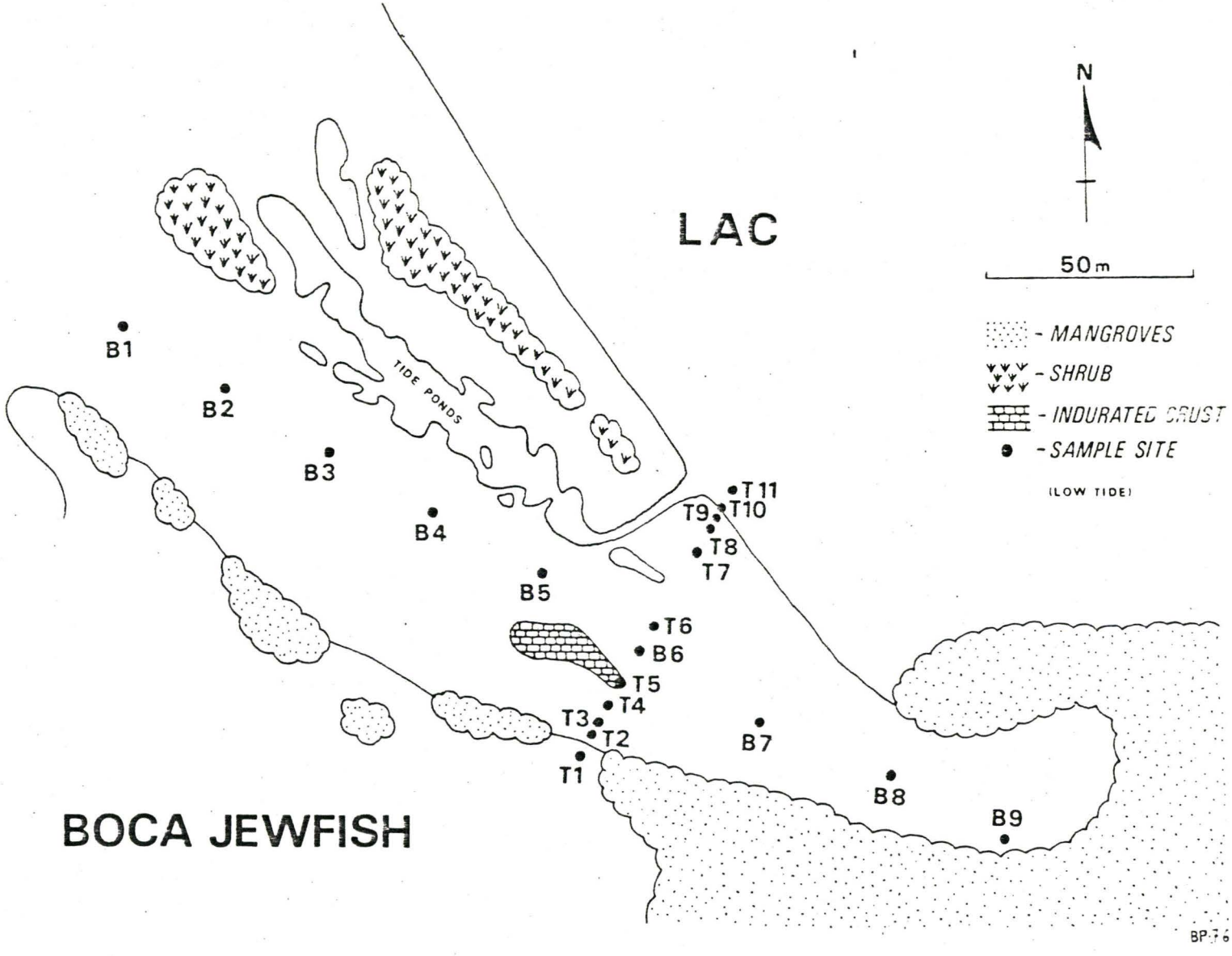

Figure 10: Sample stations of site A.

- small pieces of algal mat were preserved in 3% aqueous glutaraldehyde and 5% aqueous $CaCO_3$-buffered formaldehyde solutions.

- algal mat surfaces around the sample station were photographed.

Cores were not taken at stations T5, T8 and T9. At stations T1, T10 and T11, only samples of loose sediment were collected from the top several cm of substrate. The core samples were frozen while still in the plastic tubes. Loose sediment and blocks of mat and underlying sediments were air dried; after desiccation, the blocks were coated in polyester resin for protection during shipment.

At site B, the cryptalgal structures were photographed; one core was taken. At site C, cryptalgal structures were photographed and hand samples were collected.

Subtidal cryptalgal structures and sand samples were collected in the main lagoon of the Lac near Sorobon.

Thin sections of cryptalgal structures were prepared from specimens that were vacuum impregnated (see Milliman, 1974) with Ceiba-Geigy epoxy (resin RP-103, Hardener 956). The thin sections were stained for aragonite with Feigl's solution as outlined by Friedman (1959) and for organic material with malachite green (Kahle et al, 1973).

Mat surfaces were examined with the transmission and reflecting light microscope. Scanning elctron microscopy was carried out on an AMR model 1000 unit and on a Cambridge scanning electron microscope equipped with an EDAX unit (energy dispersive X-ray analyzer). Algal mat specimens were dehydrated in stages with ethanol after fixing with osmium tetroxide and washing with phosphate buffer (following the procedure outlined by Lukas, 1973); aluminium, gold and carbon coatings were used on various specimens.

Frozen sediment cores were cut longitudinally in half by making two parallel cuts along the length of the plastic core liner, lifting off the top half and skimming off the thawed sediment down to the level of the cuts. X-ray radiography was carried out on these sectioned cores, as well as on slices of gelatinous oncolites and indurated nodules, using a Macrotank K X-ray apparatus.

Several gelatinous oncolites were allowed to dry in air to examine features that might be expected to be preserved during fossilization.

Sediment bound in several gelatinous oncolites was removed from the organic matrix by soaking for several days in approximately 15% aqueous $CaCO_3$-buffered hydrogen peroxide solution. This sediment, and sediment from stations T10 and T11 were seived after drying at 100°F. The size fraction less than 62 μm was removed by wet-seiving; the larger fractions were dry-seived on a shaker for 10 minutes.

CHAPTER III

CRYPTALGAL STRUCTURES, BOCA JEWFISH

Subtidal Oncolites

Gelatinous oncolites (algal biscuits) commonly are found in the subtidal (less than 1 m) areas of the Sorobon spit and the Boca Jewfish beach (Figure 7B). The substrate is carbonate sand on which grow Thalassia testudinum, the codiacean (calcareous green) algae Halimeda opuntia, and patches of the branching coralline red alga Goniolithon sp. (as identified by v.d. Hoek et al, 1972 and Sibley and Murray, 1972). Oncolites are most common near, and in, the patches of Goniolithon sp. Oncolites were most commonly found growing on fragments of dead Goniolithon sp. (Figure 11C), and, more rarely, on blades of Thalassia testudinum. The oncolites have a yellow-brown colour and are rubbery to the touch. They are roughly hemispherical and normally rest convex upward on the sand bottom. Specimens were seen which ranged from 2.5 cm to 10.0 cm in diameter, and up to 4 cm in height (Figures 11, 41).

In cross-section, the oncolites show alternating organic-rich and sediment-rich laminations (Figures 11A, 41) in which elongate sediment grains are oriented with their long axes tangential to the laminations. The organic material is gelatinous and contains numerous algal filaments. Toward the centres of the oncolites, the sandy laminae are closely spaced (less than 0.5 mm) and the gelatinous laminae become thinner (Figure 11A). The gelatinous laminae thicken (up to 1 mm) toward the outer edges of the oncolites. The laminations are continuous and fairly regularly spaced. They are disrupted in places by burrowing organisms (possibly polychaetes).

The algal species found in these structures is dominantly Schizothrix calcicola.

Intertidal Oncolites, Site B

Numerous gelatinous oncolites are found in a small area in the low intertidal sand flats behind the Sorobon spit (site B) (Figure 12A). The sand flats contain tidal ponds that are protected from the Lac by mangrove thickets. The substrate where the oncolites are found is permanently wet, is not bound by a cohesive algal mat and is extensively bioturbated (by polychaetes?). The oncolites are firmly attached to hard objects, such as cemented intraclasts, that are found in the sand flat. The oncolites are hemispherical in shape (Figures 12B, C) and are yellow-brown in color. Several specimens have concave depressions in their upper convex surface (Figure 12B). The oncolites range in diameter from 0.9 cm to 6.0 cm. In some cases, large oncolites have formed by coalescence of smaller ones (Figure 12C). In cross-section, the oncolites consist of alternating sediment-rich and gelatinous layers. The sediment-rich layers are evenly spaced at intervals of about 1 mm; the centers are not sandier as found in the subtidal oncolites.

Figure 11:

Subtidal oncolites, less than 1 m, Sorobon.

A. X-ray radiograph of a vertical section of a subtidal oncolite showing denser core where the sand laminae are more closely spaced than in the outer parts. The tubular clear patch on the right side is a burrow (polychaete?). (Scale bar is 1 cm).

B. Upper surface of a subtidal oncolite.

C. Upper surface of a subtidal oncolite attached to a fragement of coralline algae. The holes in the oncolite may be burrows (polychaete?).

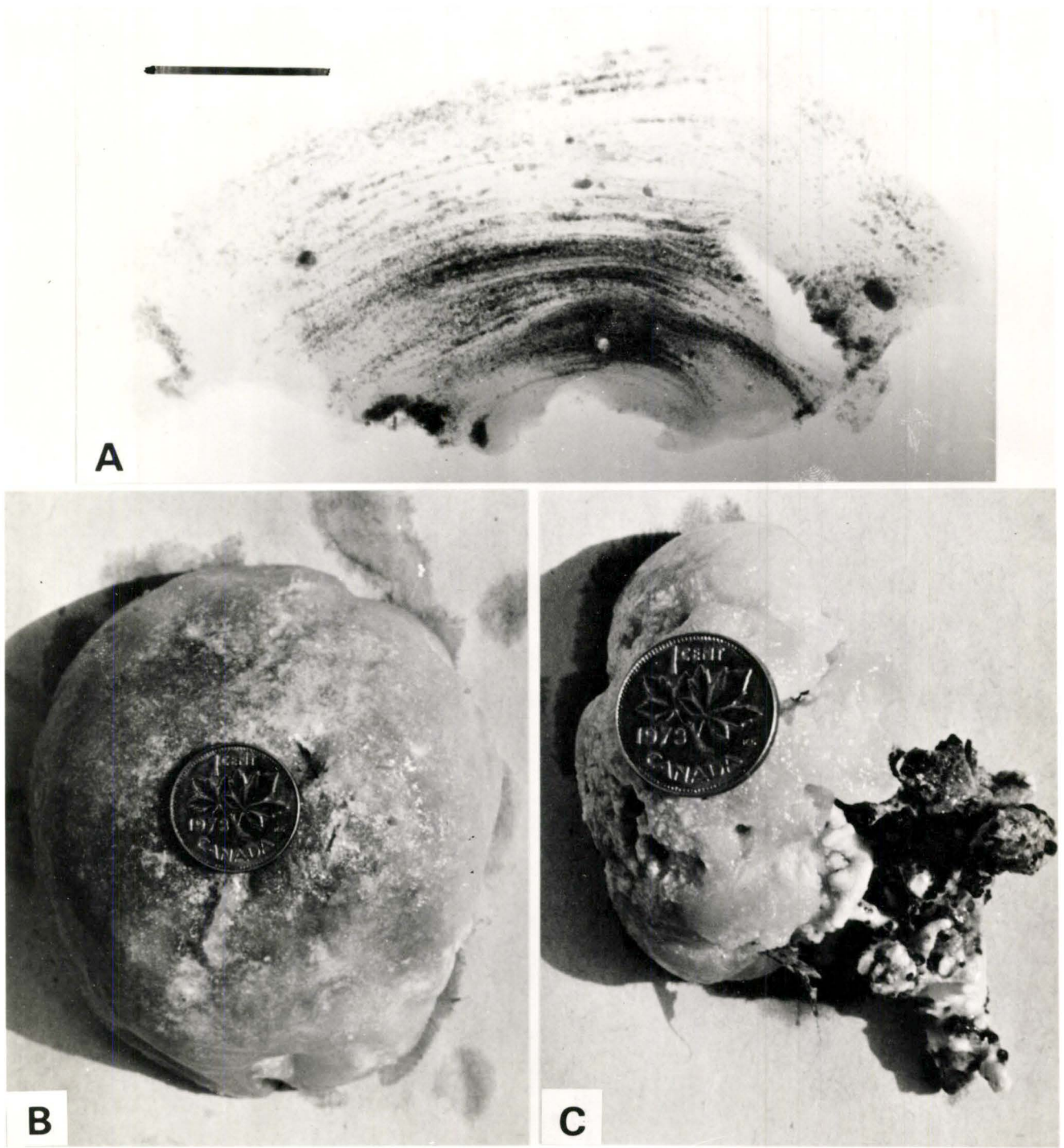
A
B
C

Figure 12:

A. Intertidal flats, tidal ponds, and mangroves, site B. The sediments are not bound by a cohesive mat, but patches of gelatinous oncolites are found.

B. Intertidal gelatinous oncolites, site B. Note concave depression in surface of oncolite to the left of the lens cap and large oncolite formed by coalescence of smaller oncolites to the right of the lens cap. (Lens cap is 5.8 cm in diameter).

C. Intertidal gelatinous oncolites, site B.

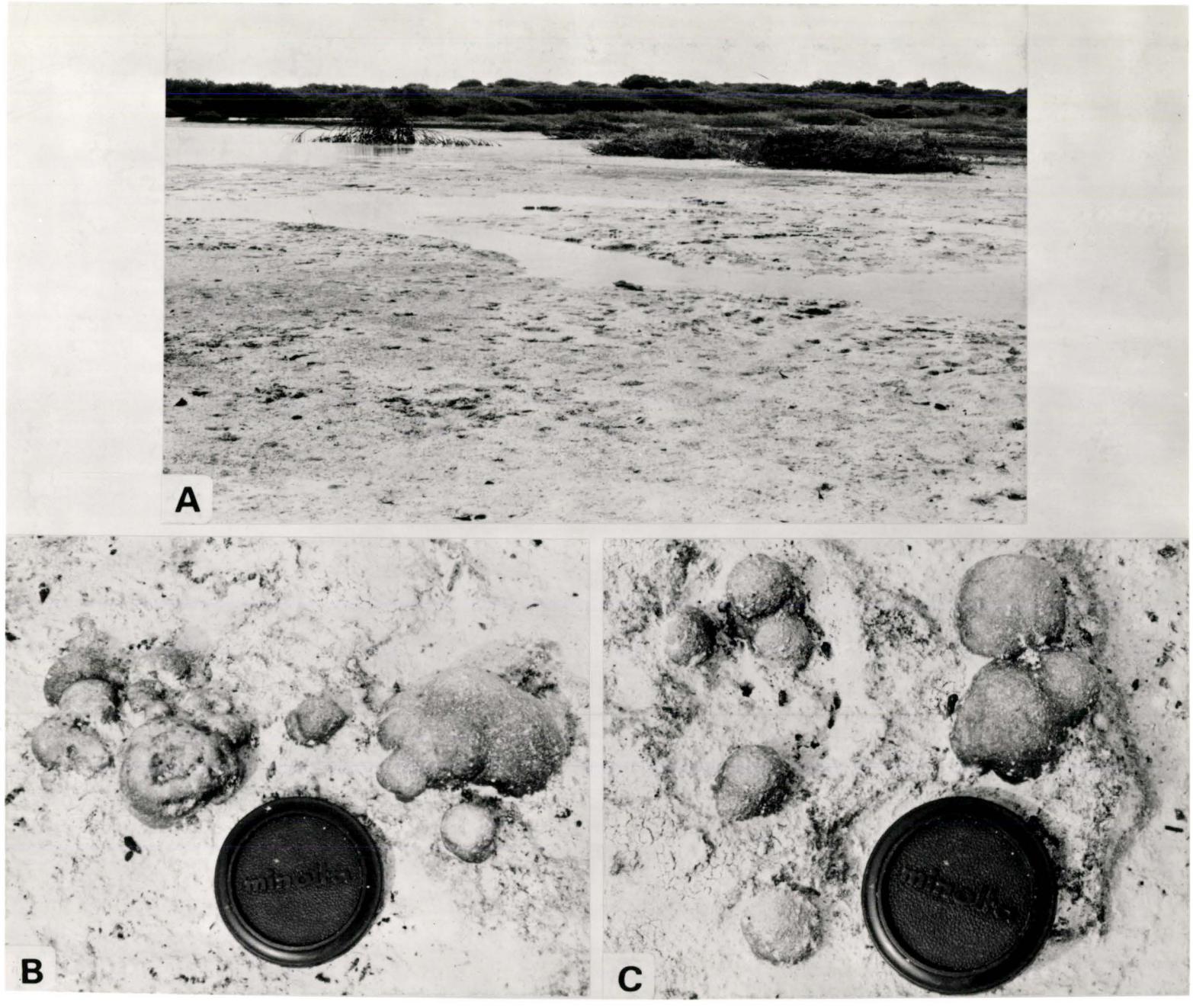
A
B
C

Intertidal Oncolites, Site A

Gelatinous oncolites are found in the low intertidal area of Boca Jewfish on a small part of the beach in the vicinity of sample point T9 (Figure 13A). This beach faces east and is exposed to the winds and waves blowing across the Lac. The small patch of sand on which the oncolites are found is bounded by the tidal channel on the north and the mangrove thicket on the south. The oncolites are exposed only for a short time during low tide. They are loose and mobile on the sand substrate which is extensively burrowed by polychaetes (?) and the fiddler crab Uca sp.

The oncolites have a flattened irregular hemispherical shape (Figure 13B); many are overturned (Figure 13C). They are gelatinous in texture in the lower part of the intertidal and become increasingly indurated higher in the intertidal, until rock-hard lithified nodules occur. The oncolites are up to 10 cm in diameter. They are constructed of concentric sandy laminae (Figure 13C, 41) in which the sediment grains are bound together by the gelatinous mucilagenous organic material. The oncolite nuclei, when present, are fragments of the lithified nodules (Figure 13C, 41). In many cases, coalescence of smaller oncolites has occurred to form larger lobate oncolites. The sands bound by these oncolites are better sorted than the sands of the beach and subtidal; large sand grains are not bound. Schizothrix calcicola appears to be the principle sediment-binding algae in these structures.

Intertidal Nodules, Site A

The sandy gelatinous oncolites of the lower intertidal of the Boca Jewfish beach grade in the degree of induration upwards in the intertidal to indurated nodules or lumps. Hard nodules frequently act as nuclei for the soft oncolites. The outer surface of the nodules is colonized by filamentous blue-green algae (Microcoleus sp.?) which impart a greenish or pinkish colour to the nodules' outer surface.

The nodules are very variable in shape (Figure 18D); they range from small fragments about 1 cm in diameter to large irregular lumps up to about 15 cm across. The nodules may possess concentric laminations (Figure 41), horizontal laminations (Figure 14A), or no visible internal laminations at all (Figure 14B).

The induration is due to aragonite cement, as determined by staining and crystal habit. This cement occurs as small acicular fibrous crystals coating grains and lining voids (Figure 14C,D). The constituent grains are predominantly Halimeda opuntia fragments.

Scanning electron microscopy reveals tangles of algal filaments binding the sediment grains (Figures 15, 16). The samples were not etched and thus the cement was not clearly visible. Many of the algal filaments

Figure 13:

A. Boca Jewfish beach (site A). Subtidal Lac is on the right. The car is sitting on smooth mat; the dark strip is the zone of indurated nodules. Between the zone of indurated nodules and the subtidal is the zone of gelatinous oncolites; this zone ends at the mangrove thicket in front of the car.

B. Gelatinous oncolites, site A. (Coin is 2 cm in diameter.)

C. Gelatinous oncolites, site A. Many are overturned revealing internal concentric sediment laminations. Oncolite in upper left is formed by coalescence of two smaller oncolites. Oncolite in lower part of the photograph has grown around a nucleus of indurated nodule fragment.

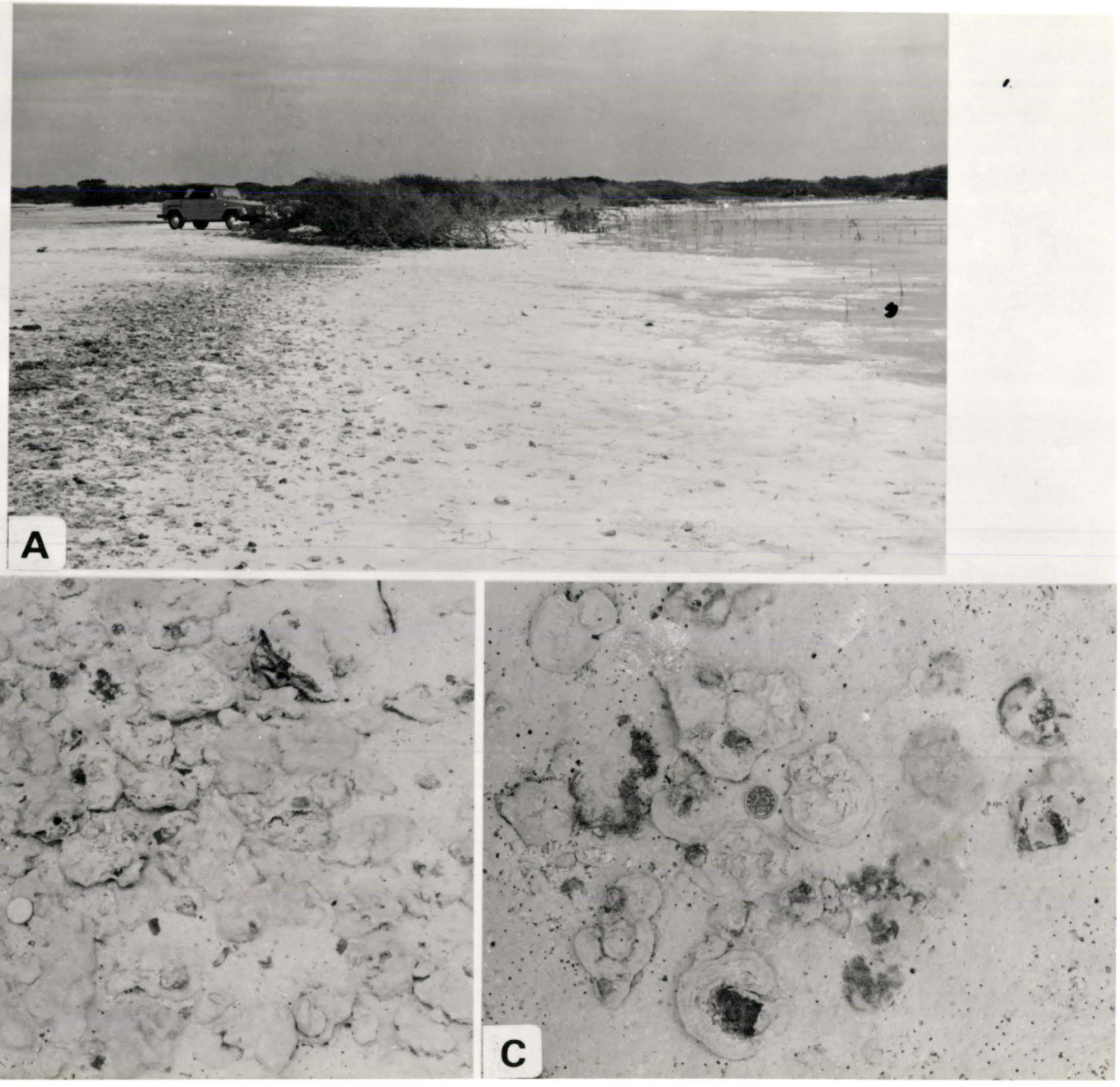
A
B
C

Figure 14:

A. X-ray radiograph of indurated cryptalgal nodule, site A, showing parallel horizontal laminations. The outer dark rim around the upper surface is due to superficial colonization by filamentous blue-greens (Scale bar is 1 cm).

B. X-ray radiographs of indurated cryptalgal nodule, site A, showing lack of internal lamination (termed "thrombolite" by Golubic, 1973). The upper dark rim is the superficial living blue-green algal layer (Scale bar is 1 cm).

C. Thin section (crossed polars) of Halimeda grains cemented by fibrous aragonite. Acicular aragonite also acts as a pore-filler in the utricles of Halimeda fragments (Scale bar is 19 μm).

D. This section (crossed polars) of Halimeda fragments coated by fibrous aragonite cement (Scale bar is 14 μm).

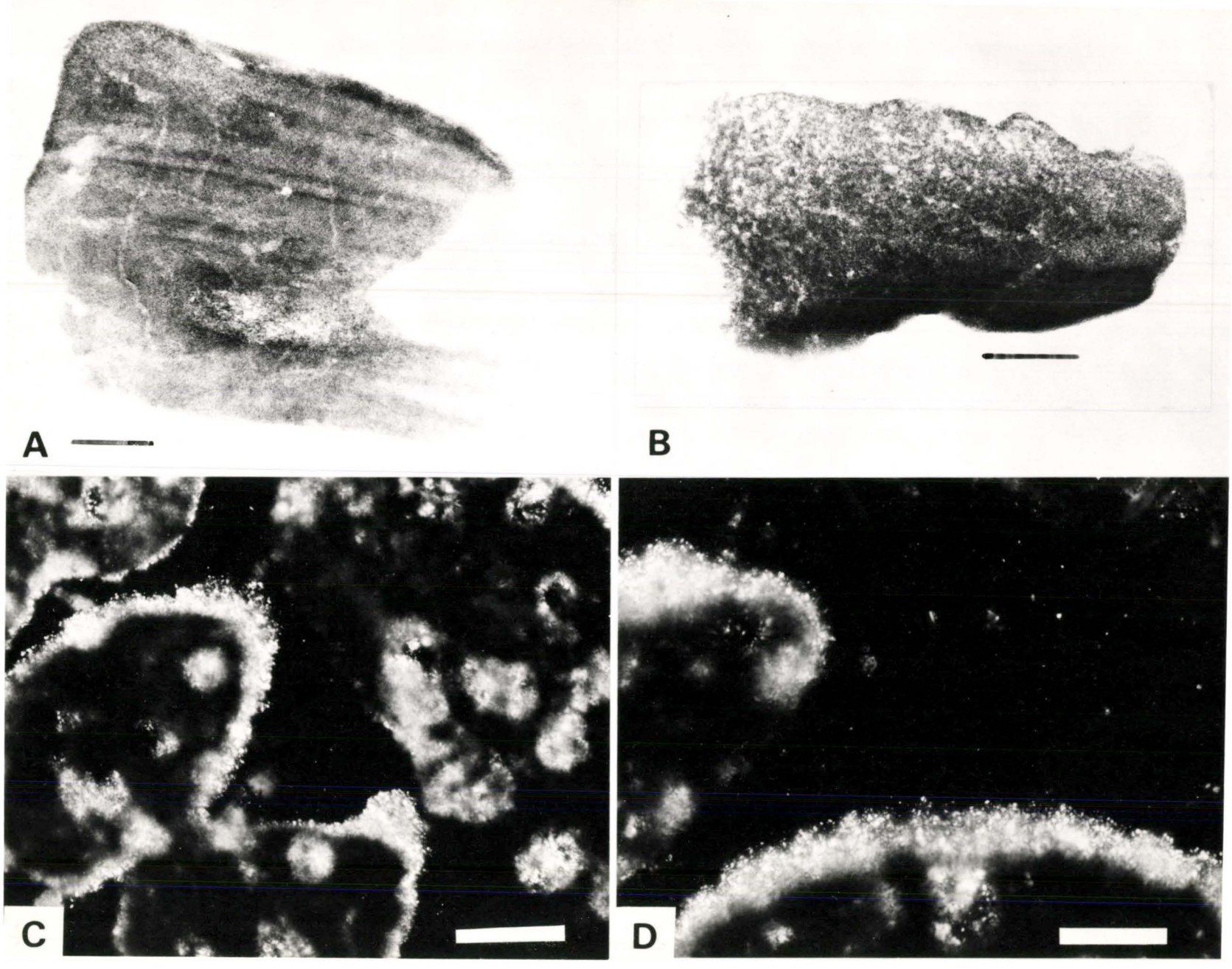
A
B
C
D

Figure 15:

Ultrastructure of cryptalgal indurated nodules.

A. Carbonate grains bound by algal filaments on the outer surface of the nodule (Scale bar is 61 µm).

B. Carbonate grain bound by masses of filaments (Scale bar is 31 µm).

C. Algal filaments (Scale bar is 15 µm).

D. Bundles of algal filaments (Scale bar is 6 µm).

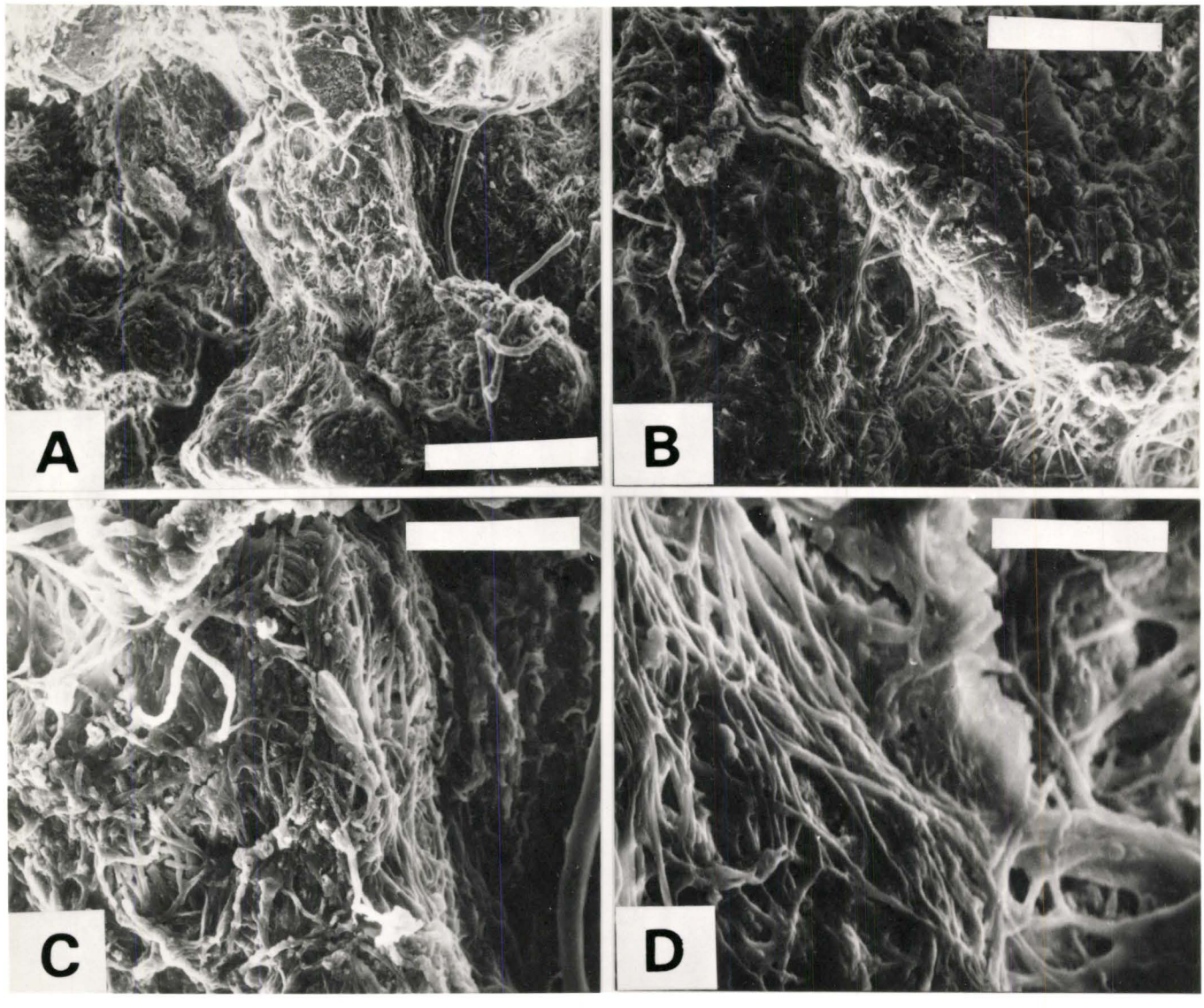
A
B
C
D

Figure 16:

Ultrastructure of cryptalgal indurated nodules.

A. Blue-green algal filaments on outer surface of nodule. Algal filaments are a mesh of strands; branching is common (Scale bar is 3 μm).

B. Blue-green algal filaments on outer surface of nodule. Adhering to the filaments in patches is micrite-sized carbonate. The origin of these carbonate grains is obscure; they may be physically trapped on the outer surfaces of the filaments, or they may have precipitated there (Scale bar is 3 μm).

C. Algal strands on the outer surface of a carbonate grain that has been extensively bored by endolithic microphytes. The algal strands have wrapped themselves around and bound a small carbonate grain (Scale bar is 15 μm).

D. Close-up of C, showing the carbonate grain bound by blue-green algal strands. These strands may be mucous strands rather than actual algal thalli (Scale bar is 6 μm).

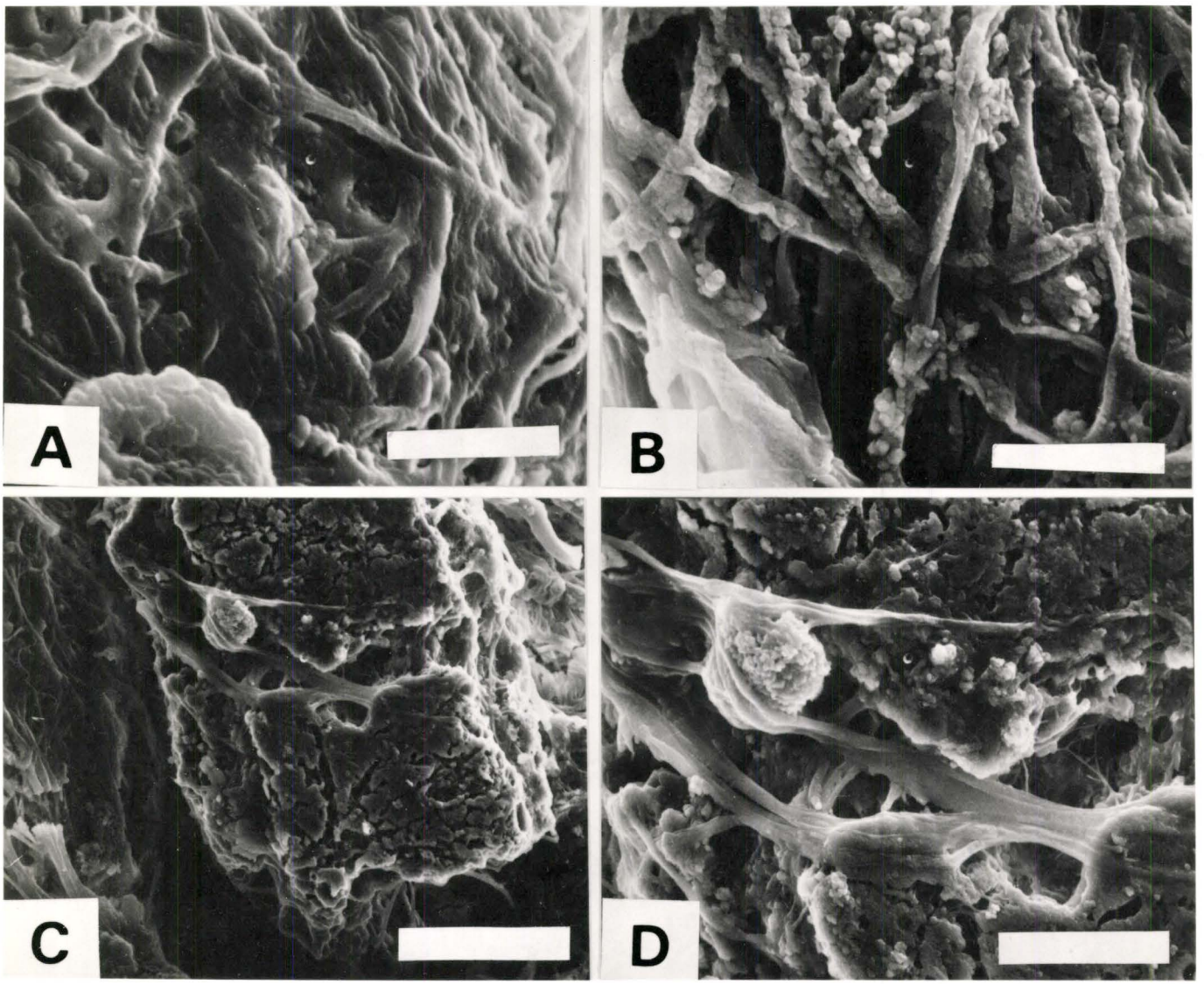
A
B
C
D

are coated with crusts or rinds of micrite-sized calcium carbonate (Figures 16B, 17B,C). EDAX of these filaments could not provide positive identification of this carbonate due to background noise.

Intertidal Smooth Mat, Site A

A smooth pink-coloured algal mat occurs in the upper intertidal zone around the tide channel at sample point T7. The smooth mat is nearly completely flat with few surface irregularities (Figure 19A,B). The seaward edge of this mat can either grade into unbound sands or can be a small eroded 'cliff' several cm high. Pieces eroded off the edge of the mat are scattered about the 'cliff' on the unbound sands seaward of the mat. The mat changes landward in the high intertidal to a small ridge of sūpratidal salt-encrusted sand. The sediments of this ridge are unlaminated internally and no algal mat is presently growing on it.

The internal cross-section of the smooth mat shows characteristic laminoid fenestral fabric that can be termed fenestral grain-framework (Logan et al., 1974) (Figure 18C). The laminations are relatively distinct and horizontal in the upper 2 cm, and sediments below this are not laminated. There is also a pronounced internal colour banding of pink and green algal layers. The sediments bound by the mat are mostly Halimeda opuntia fragments which are oriented parallel to the lamination.

These grains are bound dominantly by Schizothrix sp.(?) which secretes copious amounts of mucilagenous material. This material is stained green by malachite green and is seen in thin section as a network of strands that enmeshes and binds sediment grains (Figure 18C,D). This binding is very strong; the mat is rigid enough to support a vehicle driving on it. Electron microscope study shows this binding to be caused by masses of and smooth-walled tubular strands of organic mucilagenous material (Figures 18, 19, 20, 22). This material is seen to grow through utricles of Halimeda grains (Figure 23). The algal strands can be coated by a rind of micritic calcium carbonate (Figure 22D).

Higher in the intertidal, the upper surface of the mat is colonized by tufts of Microcoleus sp. filaments.

Tufted Mats

Intertidal tufted mats have the greatest areal extent of all the cryptalgal structures of the Lac. They cover most of the intertidal and lowermost supratidal flats behind the beach barrier at site A (Figure 24) as well as sites B (Figure 27) and C (Figure 28). The mat is a thin cohesive sheet (up to 0.5 cm thick). The mat has a leathery feel when damp, and is hard and brittle when dried out. It is easily detached from the underlying sediment. The mat's upper surface is green-black in colour and the underside is pinkish.

Figure 17:

Ultrastructure of cryptalgal indurated nodules.

A. Pore within cryptalgal nodule. Grains around the pore are cemented but the character of the cement is not clear as the specimen has not been etched. At the bottom of the photograph is a diatom skeleton (Scale bar is 15 μm).

B. Algal filament coated by a rind of micrite-sized calcium carbonate (Scale bar is 9 μm).

C. Close up of B. The fine-grained carbonate which coats the filament may be precipitated or passively bound (Scale bar is 4 μm).

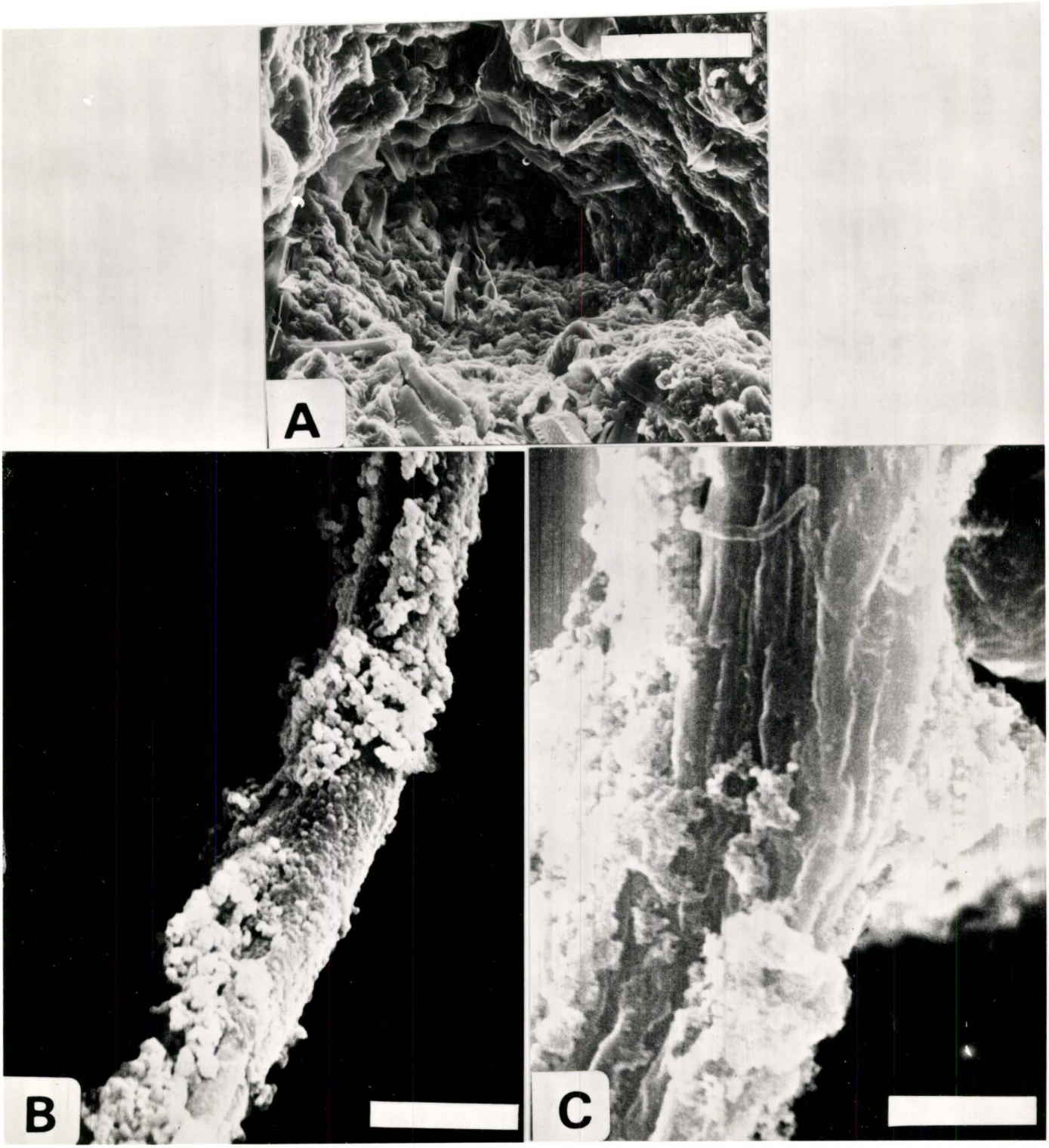
A
B
C

Figure 18:

A. Edge of the smooth mat. Unbound sands are to the left of the trowel. The edge is undercut by waves, causing pieces of smooth mat to be eroded off.

B. Eroded edge of smooth mat. (Coin is 2 cm in diameter).

C. Internal laminoid fenestral fabric of smooth mat. (Coin is 2 cm in diameter)

D. Indurated nodules. Dark colouration is due to surficial colonization by blue-green algae.

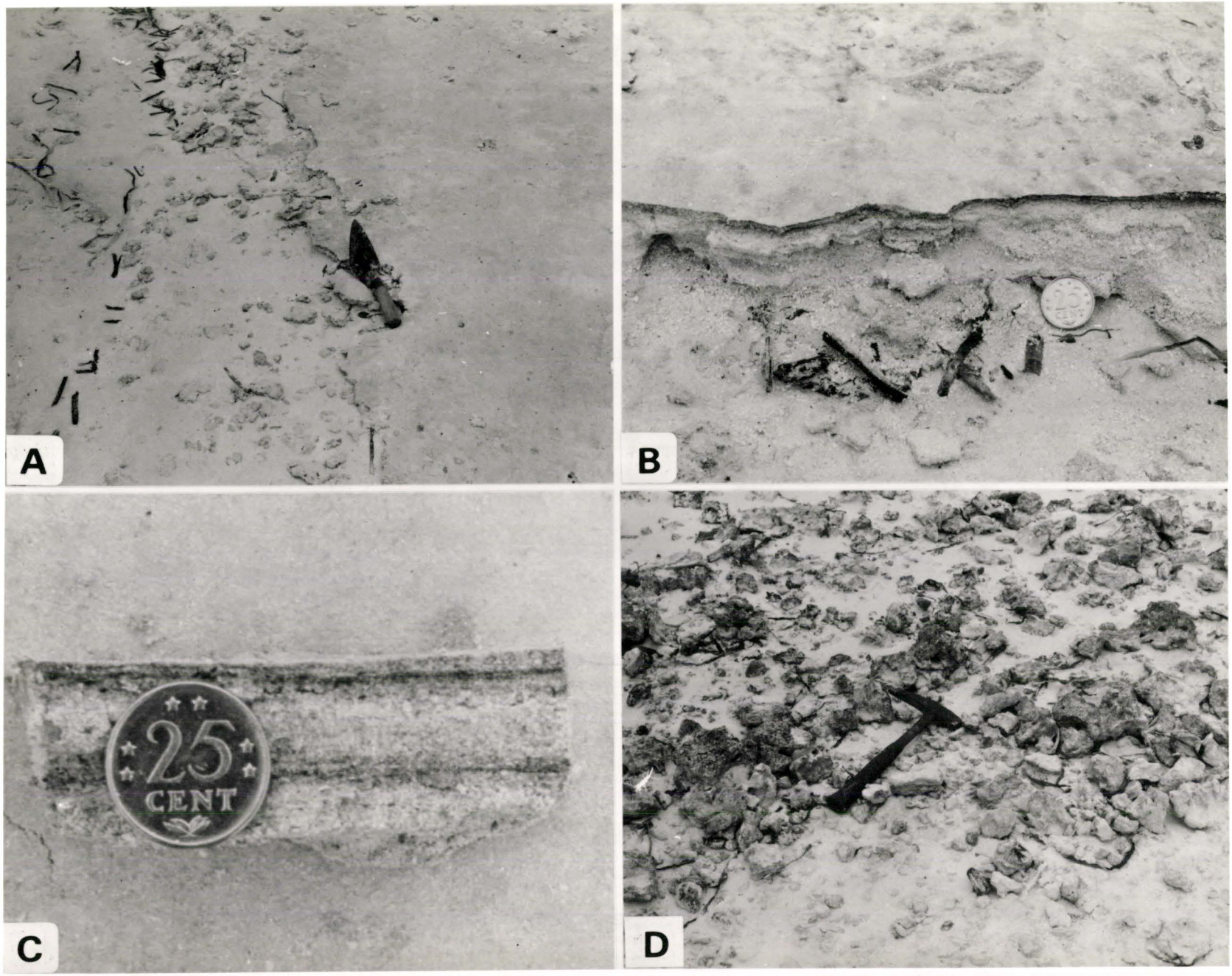
A
B
25
CENT
C
D

Figure 19:

A. Thin section (plane light) of tufted mat. Halimeda grains are bound by filaments of Microcoleus chthonoplastes (black horizontal stands in photographs) (Scale bar is 83 μm).

B. Close-up of A. Algal filaments are horizontal strands that have trapped and bound carbonate grains (Scale bar is 33 μm).

C. Thin section (plane light) of smooth mat. Halimeda opuntia grains are enmeshed and bound by a network of mucilagenous algal strands (Scale bar is 21 μm).

D. Thin section (plane light) of smooth mat (Scale bar is 20 μm).

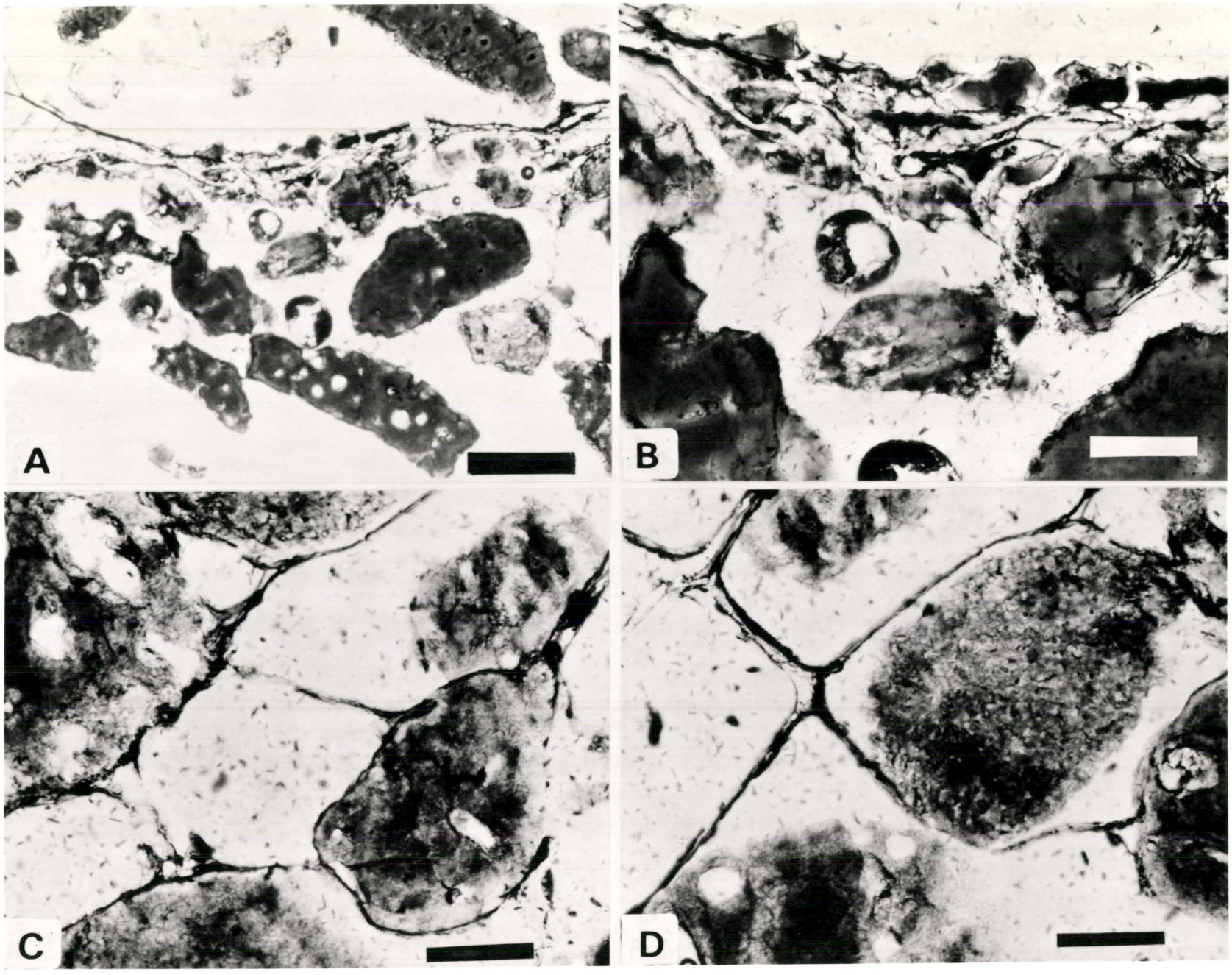
A
B
C
D

Figure 20:

Ultrastructure of smooth mat.

A. Sediment grains bound together by strands and masses of mucilagenous material. Halimeda grain upper left (Scale bar is ~~152~~ 175 µm).

B. Grains bound by mucilagenous masses and strands. The strands may be algal thalli (Scale bar is 70 µm).

C. Grains bound by mucilagenous masses (Scale bar is 35 µm).

D. Grains bound and enclosed by mucilagenous masses (Scale bar is 35 µm).

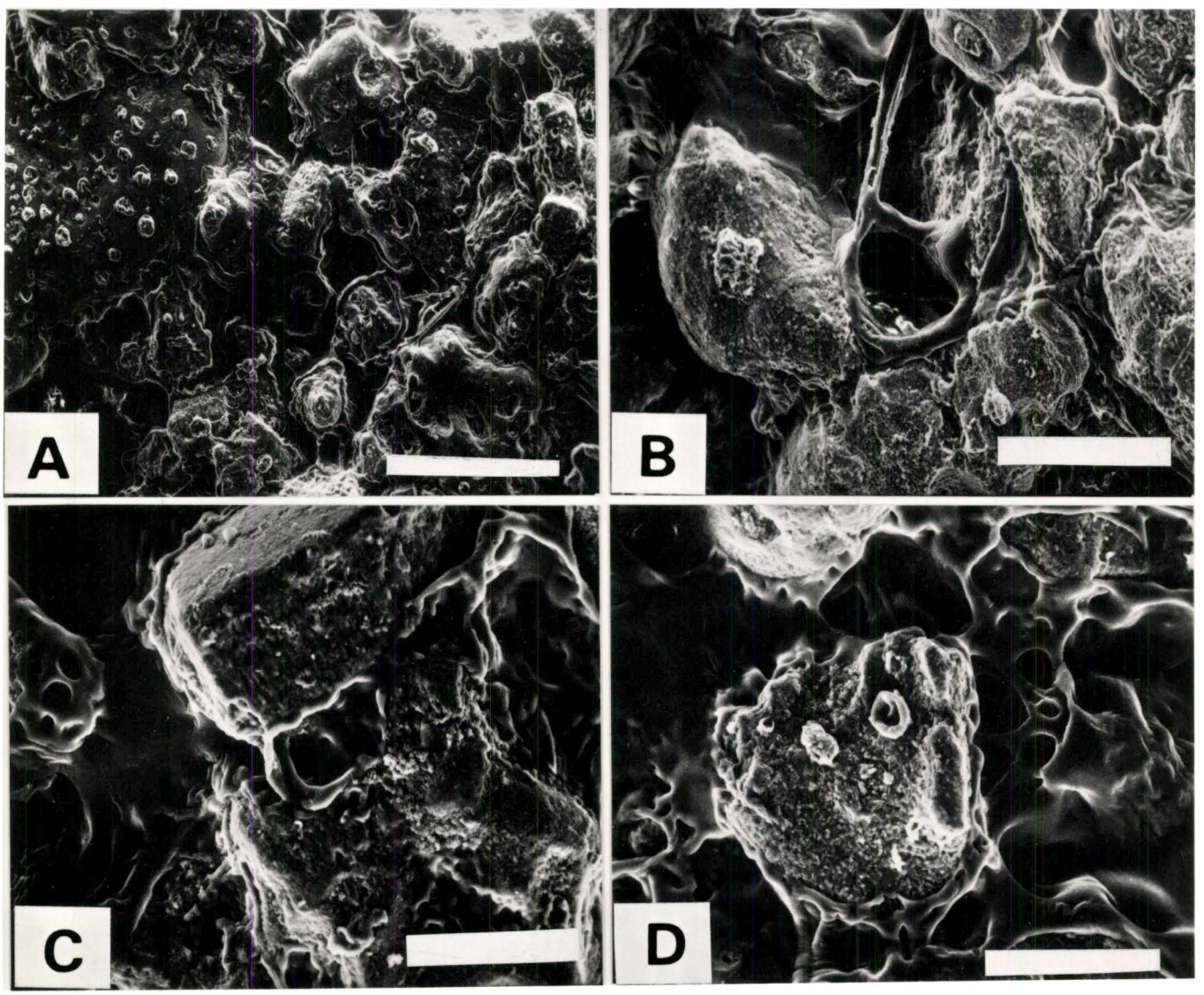
A
B
C
D

Figure 21:

Ultrastructure of smooth mat.

A. Grain bound by mucilage. Convoluted spherical organic structure in upper right may be part of the algal thallus (See Figure 21) (Scale bar is 35 µm).

B. Grains, mucilagenous strands and masses (Scale bar is 18 µm).

C. Grain enmeshed by mucilagenous strands (algal thallus?) (Scale bar is 18 µm).

D. Grains enmeshed in a network of mucilagenous strands (Scale bar is 35 µm).

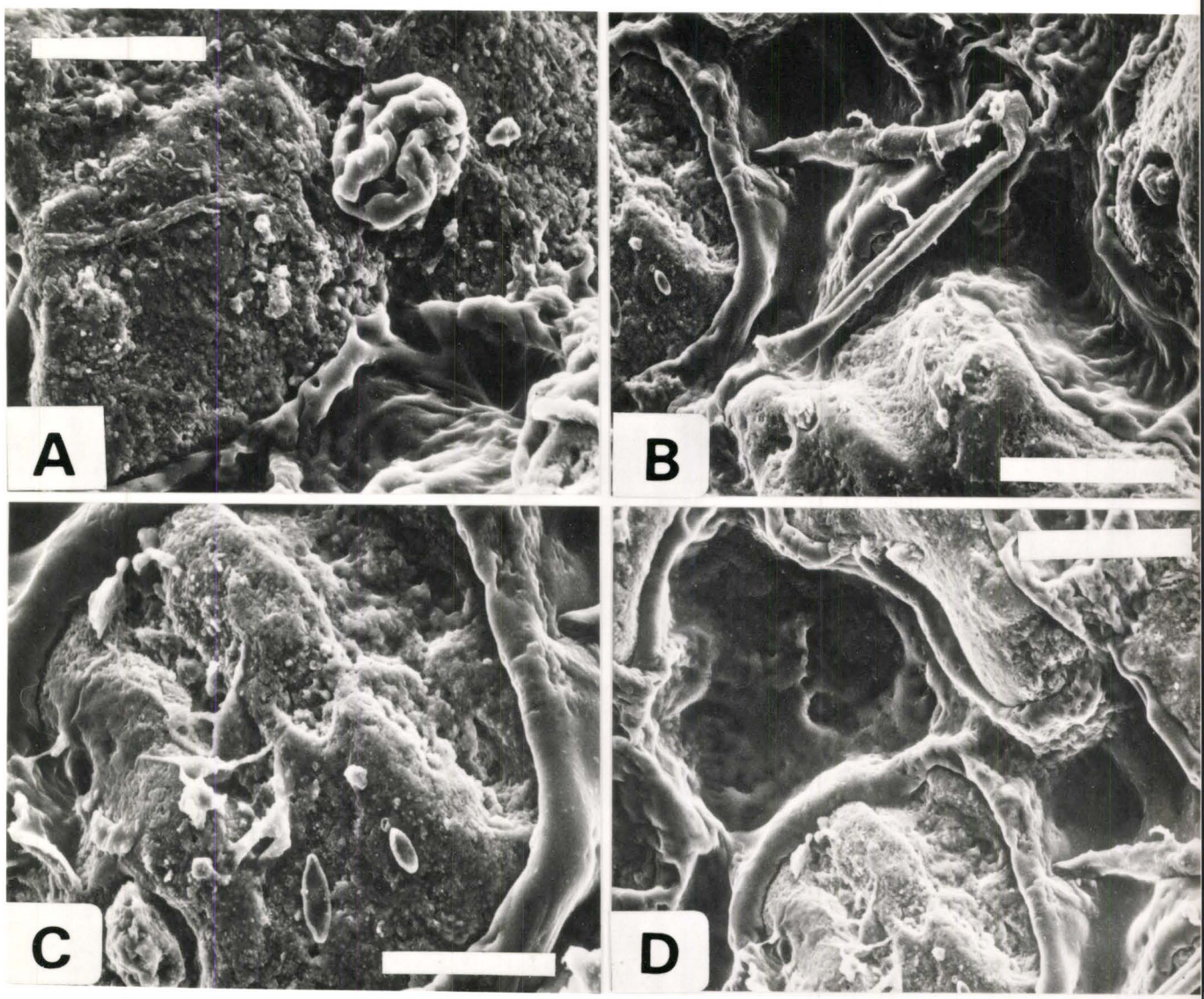
A
B
C
D

Figure 22:

Ultrastructure of smooth mat.

A. Mucilagenous strand, partly cut away revealing hollow internal structure. The branching strand appears to be the algal thallus and its mucilagenous outer sheath (Scale bar is 18 μm).

B. Mucilagenous strand binding carbonate grain (Scale bar is 18 μm).

C. Mucilagenous strand (Scale bar is 7 μm).

D. Mucilagenous strand partly coated by micrite-sized calcium carbonate. This carbonate may be precipitated in situ or has been trapped on the mucilagenous algal sheath (Scale bar is 18 μm).

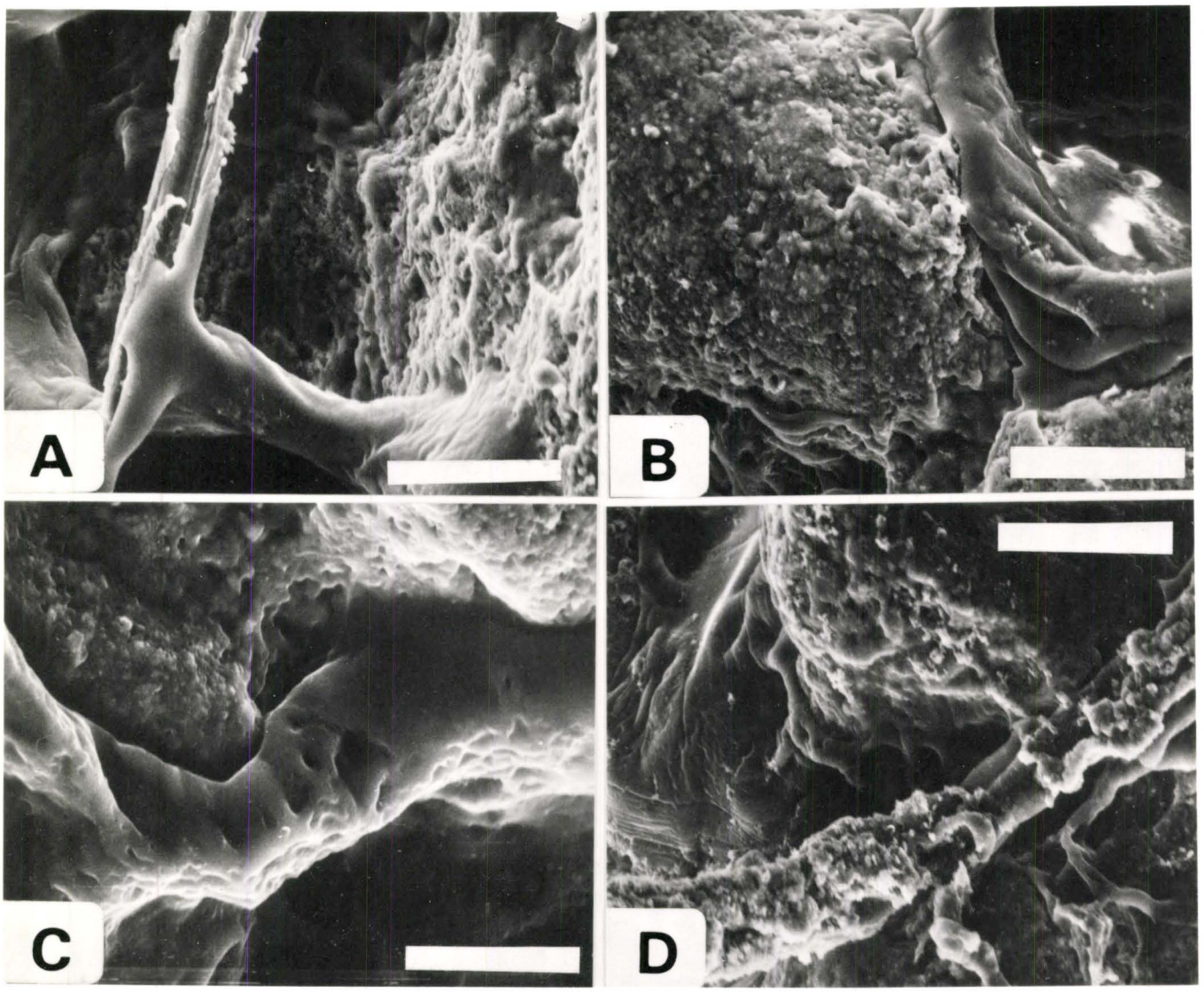
A
B
C
D

Figure 23:

Ultrastructure of smooth mat.

A. Halimeda grain with mucilagenous algal structures in the utricles. The surface of the grain is heavily bored by boring microphytes (algae?) (Scale bar is 70 μm).

B. Surface of Halimeda grain coated by a crinkly-textured mucilagenous organic mass (Scale bar is 18 μm).

C. Utricles of Halimeda grain (surface heavily bored). The utricle is lower part of photograph is occuped by a convoluted spherical mucilagenous algal structure (See Figure 19) (Scale bar is 18 μm).

D. Mucilagenous algal strands and convoluted spherical structures in Halimeda utricles (Scale bar is 18 μm).

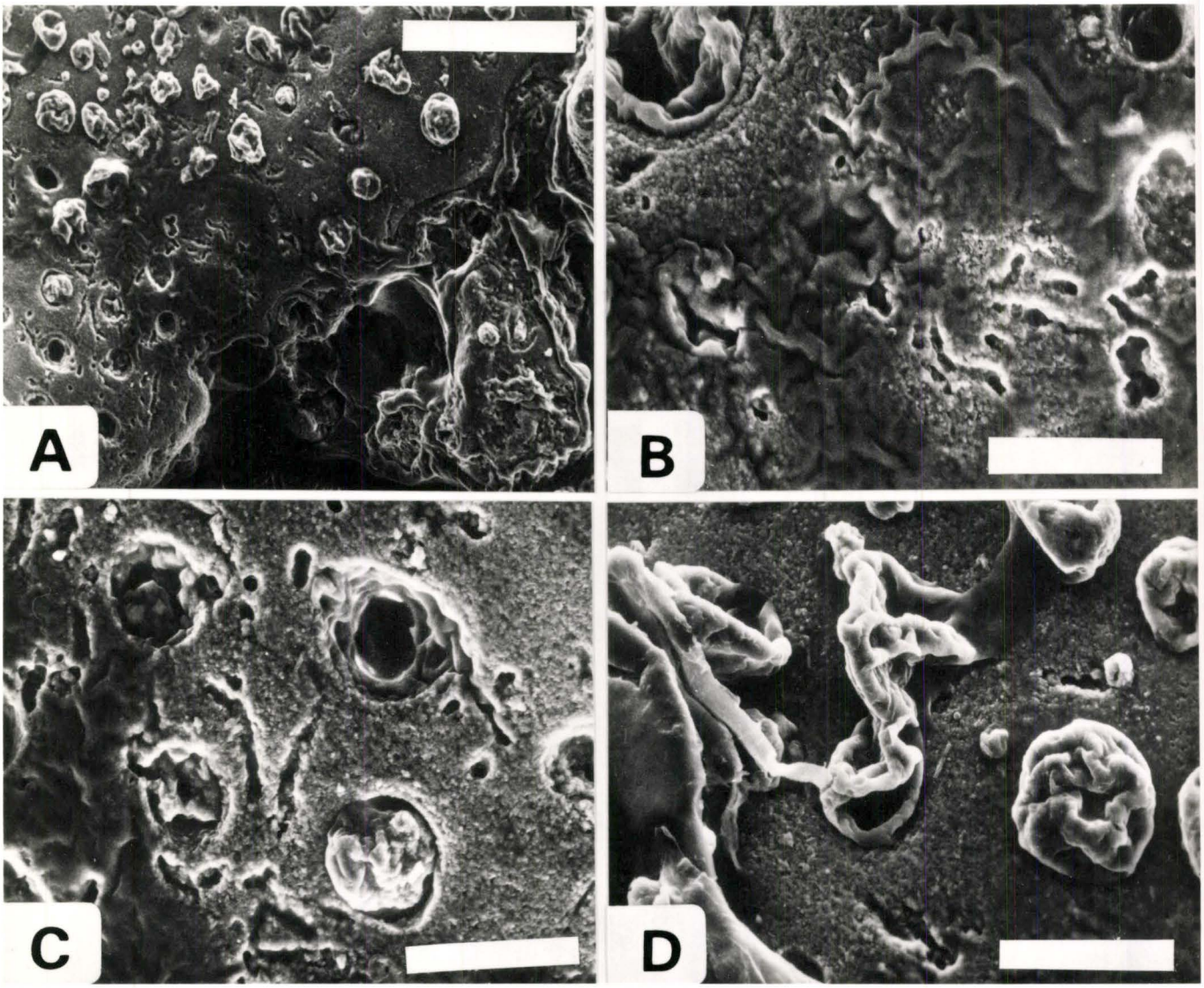
A
B
C
D

Figure 24:

Tufted mats of site A.

A. Looking NW along longitudinal transect from station B5.

B. Looking SE along longitudinal transect from station T4.


A
B

The tufted mat exhibits a wide variety of surface morphologies: shrunk, ripped, crinkled, blistered, curled, folded over, fragmented, cracked polygonally or a continuous sheet (Figures 25, 26, 27, 28). The continuous sheets can also have variously shaped pustules on the surface (Figure 25), in some cases connected to form small ridges several mm high. Sand collects in low spots of the mat between pustules or blisters.

The sediment grains, principally Halimeda opuntia fragments, are bound by tangles of algal filaments (Figures 19A,B, 29, 30). The dominant flora of this mat is Microcoleus chthonoplasts and Microcoleus tenerrimus (v.d. Hoek et al, 1972). Grains adhere to the mucilagenous sheaths of the filaments as well as having been physically trapped by the filaments. There is some evidence that suggests that calcium carbonate may precipitate in situ on algal sheaths and mucilage (Figures 30D, 31).

Intertidal Colloform Mats

Around the edges of tide ponds and the mangrove swamps of the Boca Jewfish area is found a pink coloured gelatinous mat which has an irregular surface. This colloform mat is not cohesive and is easily broken apart in the fingers. It is found in the lowermost intertidal and shallow subtidal areas that are well-protected from waves. The mat grades with the blackish green-coloured tufted mat of the higher intertidal (Figure 32A,B). The sediments under the mat do not show distinctive laminations; they are highly bioturbated (by polychaetes?) and the mat surface is breached by many burrow holes (Figure 31C). The following species of blue-green algae have been reported by V. D. Hoek et al (1972) from this mat: Entophysalis deusta (a coccoid form), Microcoleus chthonoplastes, M. tenerrimus and Lyngba aestuarii (Figure 32D).

Figure 25:

Tufted mat surface morphologies, site A.

A. Tufted mat skrunken and cracked into desiccation polygons.

B. Desiccation polygons ripped up by waves and cast about as intraclasts.

C. Tufted mat shrunken and curled by desiccation. Underlying sediments are exposed.

D. Desiccated and curled tufted mat.

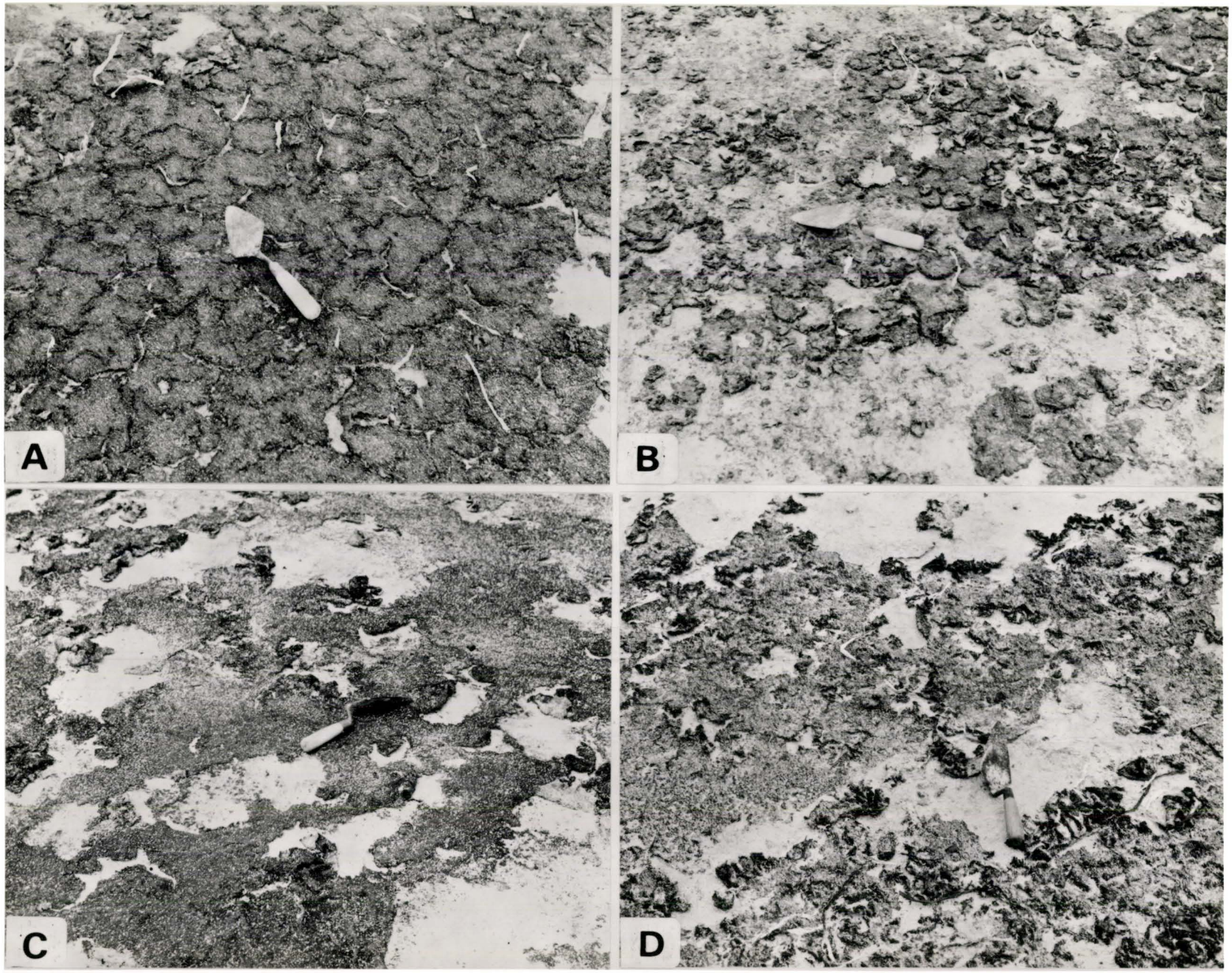
A
B
C
D

Figure 26:

Tufted mat surface morphologies:

A. Continuous tufted mat surface. (Coin is 2 cm across)

B. Continuous mat surface with tufts aligned parallel to wave direction. (Coin is 2 cm across).

C. Continuous mat with a blistered surface. (Coin is 2 cm across)

D. Continuous mat with a wrinkled alignment of tufts. (Coin is 2 cm across).

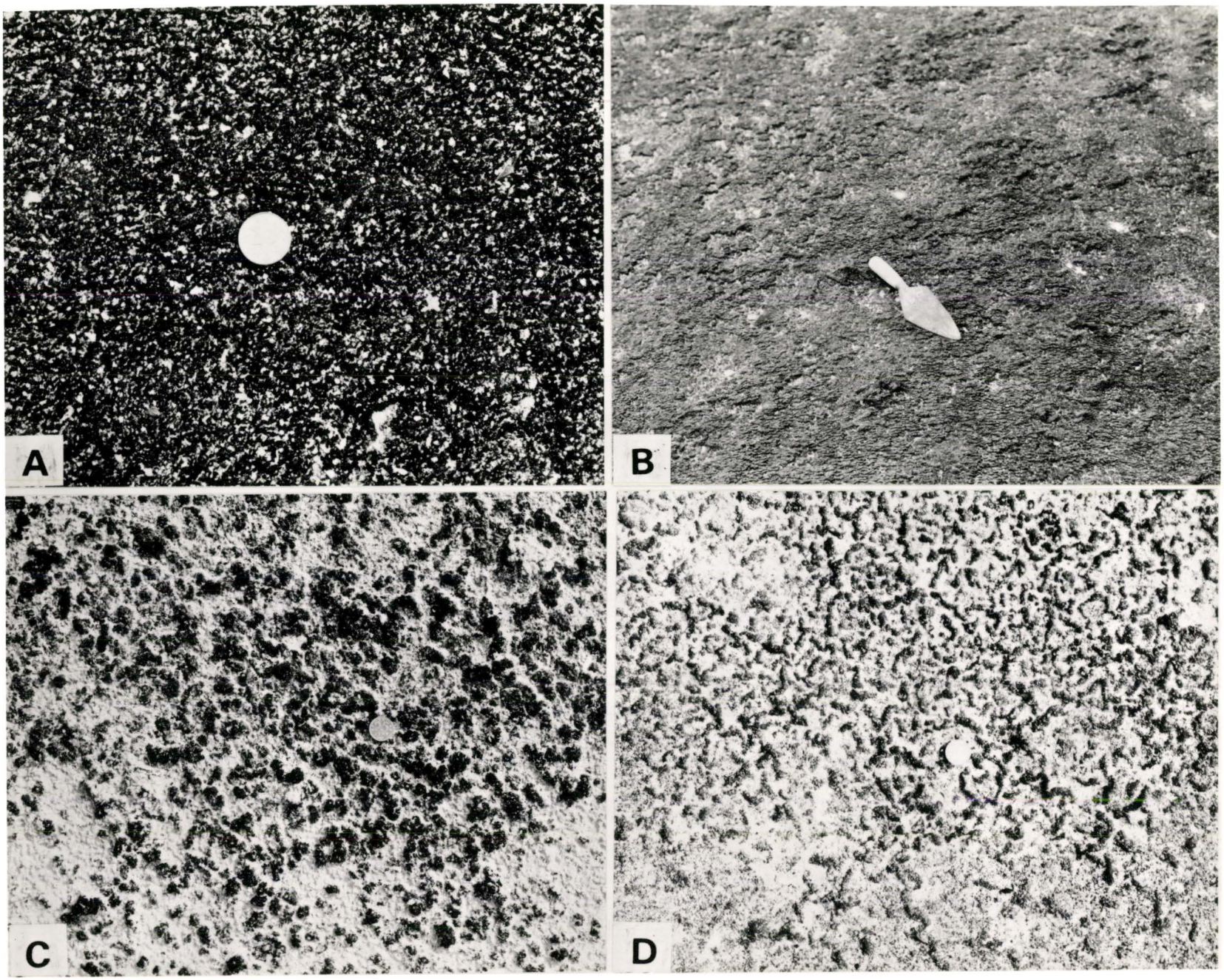
A
B
C
D

Figure 27:

Tufted mats of site B.

A. Site B showing gradation of dark-coloured tufted mat to light-coloured colloform mat. Indurated crust is in lower right. Mangrove thickets protect the area from winds and waves off the Lac.

B. Thick continuous carpet of tufted mat, extensively burrowed by the fiddle crab Uca sp.

C. Tufted mat shrunk by desiccation.

D. Tufted mat blistered by desiccation.

E. Tufted mat shrunk and blistered by desiccation.


A


B


C


D

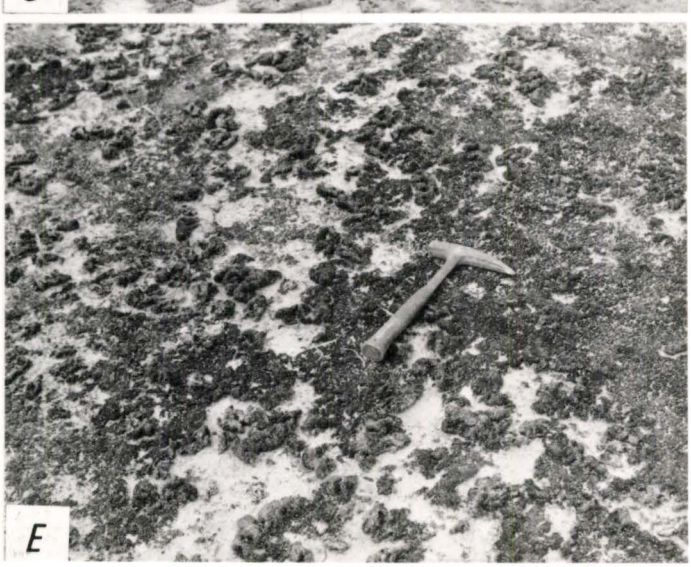
E

Figure 28:

Tufted mats of site C.

A. Site C showing indurated pavement in foreground, tufted mat in middleground and mangrove thickets and waters of the Boca Jewfish in background.

B. Tufted mat with a crinkled convoluted surface. (Coin is 2 cm across).

C. Tufted mat in the form of desiccation polygons.

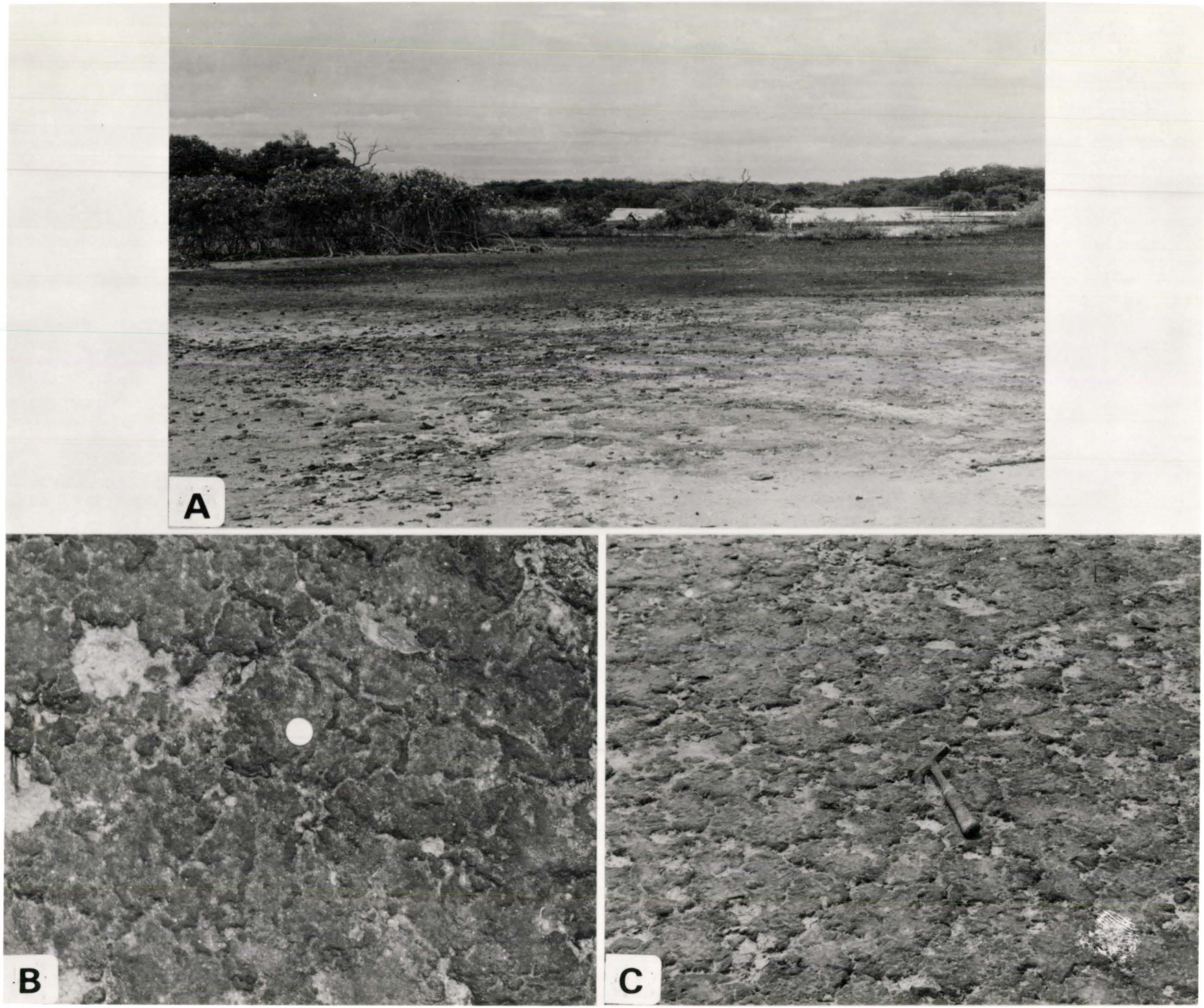
A
B
C

Figure 29:

Microcoleus spp. filaments binding sediment grains in the tufted mat.

A. (Scale bar is .5 mm).

B. (Scale bar is .7 mm).

C. (Scale bar is .6 mm).

D. (Scale bar is .6 mm).

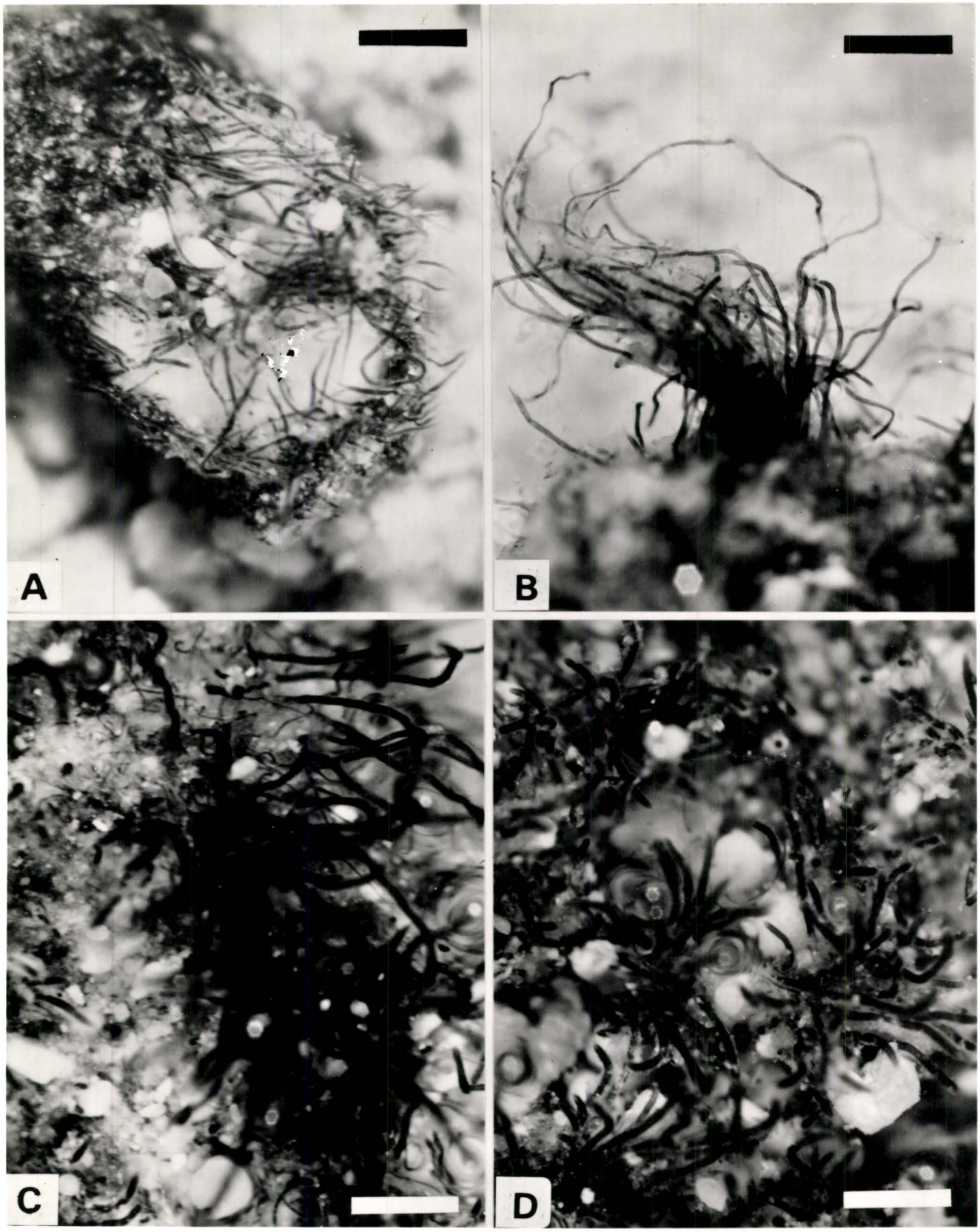
A
B
C
D

Figure 30:

Ultrastructure of tufted mat.

A. Sediment grains bound in the mat (Scale bar is 61 μm).

B. Algal filaments in the mat (Scale bar is 48 μm).

C. Filament and mucilagenous masses (Scale bar is 14 μm).

D. Branching filament. Part of the filament seems to have calcified by calcium carbonate precipitation within the algal thallus and growth of calcium carbonate crystals around the filament, similar to the manner of calcification of endolithic algae as reported by Schroeder (1972) and Kobluk (1976) (Scale bar is 5 μm).

E. Algal filament covered by a ragged organic material (Scale bar is 5 μm).

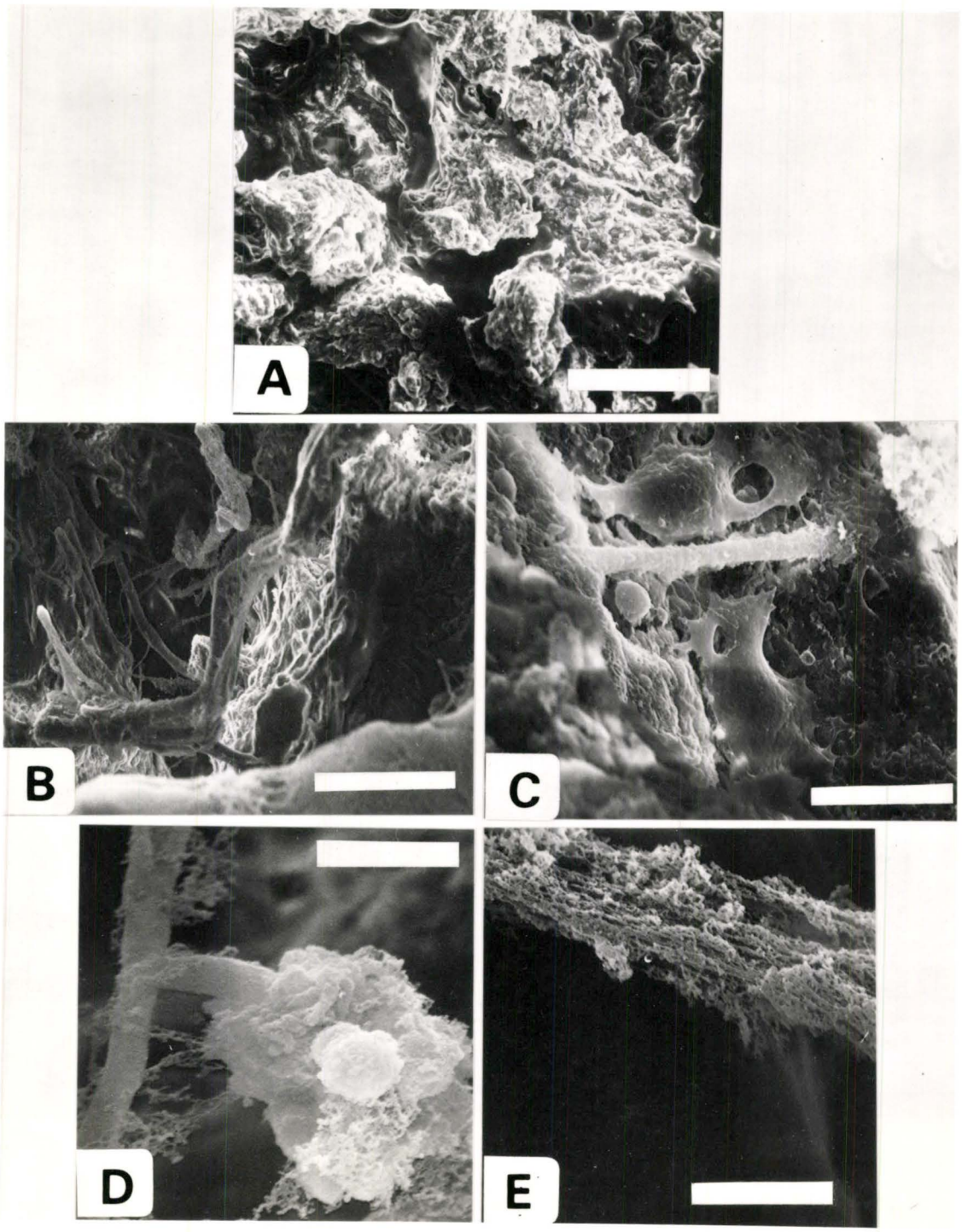
A
B
C
D
E

Figure 31:

Ultrastructure of tufted mat.

A. Sediment grains bound by filaments and mucilage (Scale bar is 30 μm).

B. Algal filament projecting from mucilagenous mass. The filament is partly coated by micrite-sized calcium carbonate (Scale bar is 15 μm).

C. Mucilagenous mass with very small grains (of calcium carbonate?) adhering to the surface (Scale bar is 6 μm).

D. Close-up of C. The material, if calcium carbonate, is either precipitated in situ or has been trapped onto the sticky mucilagenous mass (Scale bar is 3 μm).

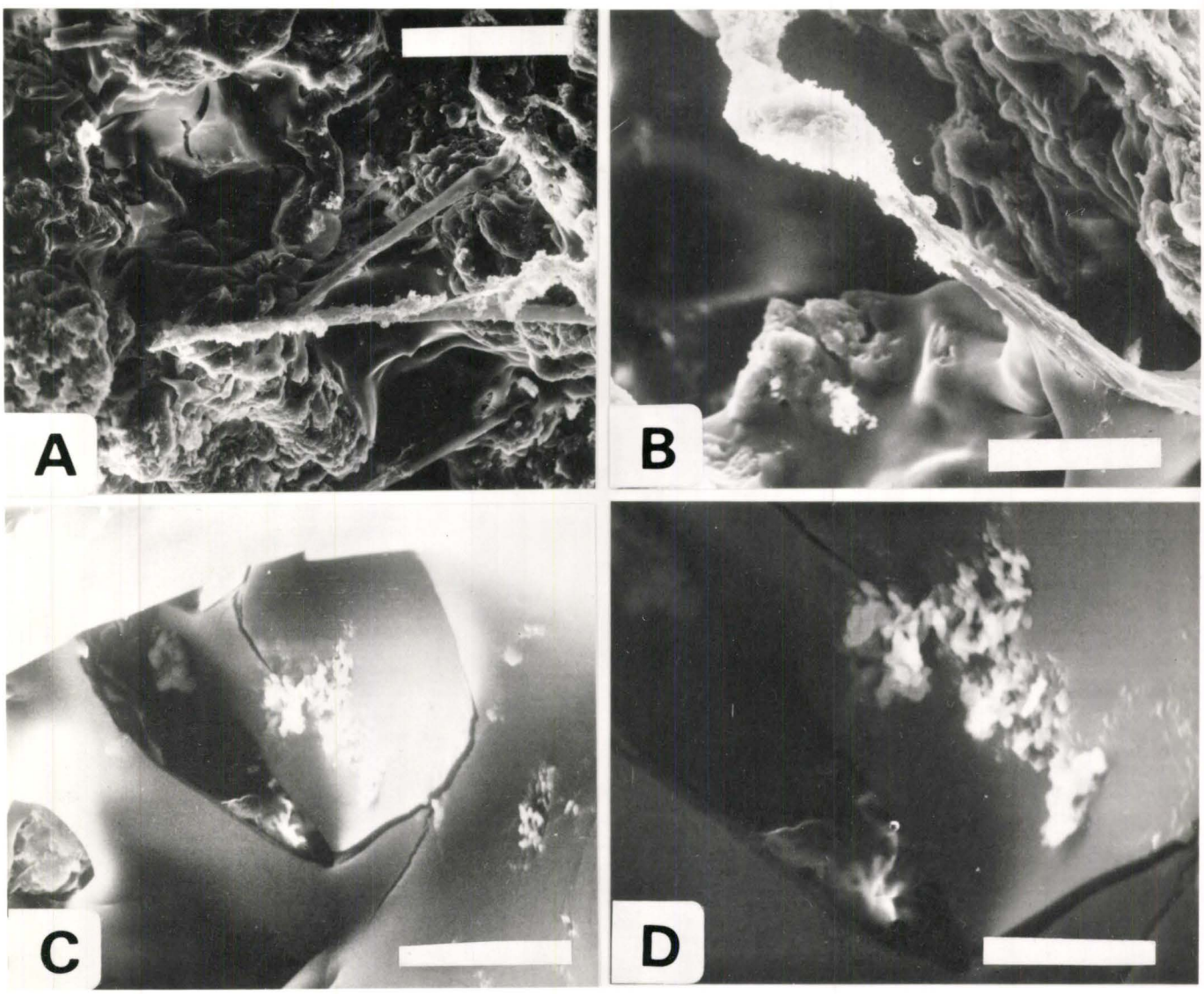
A
B
C
D

Figure 32:

Aspects of colloform mat.

A. Edge of tufted mat zone, site A, showing gradation to colloform mat (colonized here by mangrove shoots) and mangrove thicket behind.

B. Tufted mat grading to colloform mat and to mangroves, site A. Mangrove rhizomes have taken root in the colloform mat zone.

C. Surface of colloform mat, showing damage by burrowing organisms. The black-coloured areas on the surface are tufts of Microcoleus sp. algae.

D. Lyngbya sp. filaments with carbonate grains adhering to them (Scale bar is .4 mm).


A


B

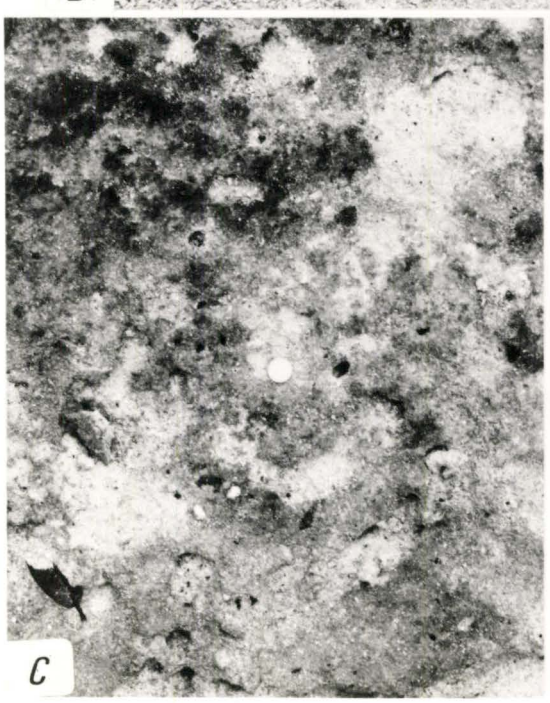
C


D

Indurated Crust

A discontinuous layer of lithified carbonate (cemented grainstone) is present at the surface and at shallow depths within the sediments of the Boca Jewfish area. Sediments above and below the crust are unlithified (Figure 34C). The crust varies from 2 to 6 cm in thickness. The crust is exposed at the surface in several spots in the intertidal and supratidal of the three sampling sites (Figure 33). The intertidal crust outcrop was sampled at station T5 of site A. The crust was reached at a depth of about 25 cm at station B1 of site A. In the intertidal zones, the surface of the crust is pitted (Figure 33) and is black in colour because of endolithic algal infestation. In the supratidal of site C, the crust occurs as an extensive pavement; the indurated crust has fractured and buckled into a 'teepee' type of structure (Figures 34A, 35). Fragments of crust and algal mat litter the crust surface (Figure 34A). These plates of crust have planar upper surfaces which are grey in colour; the lower surface is white to cream coloured, and is irregular. The upper surface may be pitted or lumpy; the lumpy surface can very similar to the irregular surface of nearby living tufted mats (Figure 34B). In cross section, the crust has a laminoid fenestral fabric. The indurated crust consists mostly of skeletal fragments and peloids cemented by cryptocrystalline aragonite (Figure 34D). It appears to be the same crust reported by Sibley and Murray (1972) from the Cas di Meeuchi in the southeast part of the Lac.

Zonation of Cryptalgal Structures, Site A

From the subtidal Lac across the beach and intertidal flat to the mangroves of the Boca Jewfish, there is a zonation of cryptalgal structures (Figures 36, 37). Subtidal Lac sands are stabilized by Thalassia testudinum, other grasses, and flocculent algal growth. Subtidal gelatinous oncolites are found in the shallows. The substrate of the lowermost intertidal of the beach, just higher than the Thalassia patches, is unbound bioturbated calcarenite. Higher in the intertidal, gelatinous calcarenitic oncolites rest on the sand. These become progressively more indurated shoreward, to cryptalgal nodules. At the highest part of the intertidal of the beach is the smooth mat zone, the seaward edge of which is eroded in places. The smooth mat zone grades

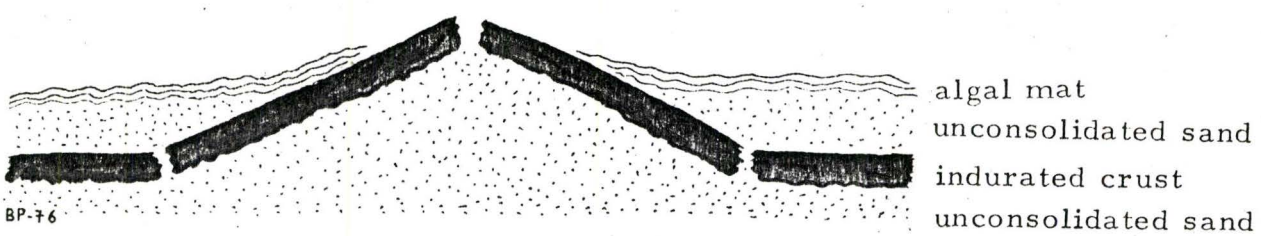

Fig. 35: Sketch of brecciated crust that has buckled into a teepee structure. Sediments over and under the crust are unlithified; tufted mat is present on sediments above the crust.

Figure 33:

Indurated crust, Boca Jewfish.

A. Exposed indurated crust, intertidal, site B. Tufted mat surrounds the pitted crust surface. (Lens cap is 5.8 cm across).

B. Irregular upper surface of indurated crust, intertidal, site B. Desiccated pieces of tufted mat have curled up and are scattered about.

C. Indurated crust pavement, low supratidal, site C.

D. Indurated crust pavement of site C, chipped by hammer blows. Tufted mat grows in patches where unlithified sediment has accumulated.

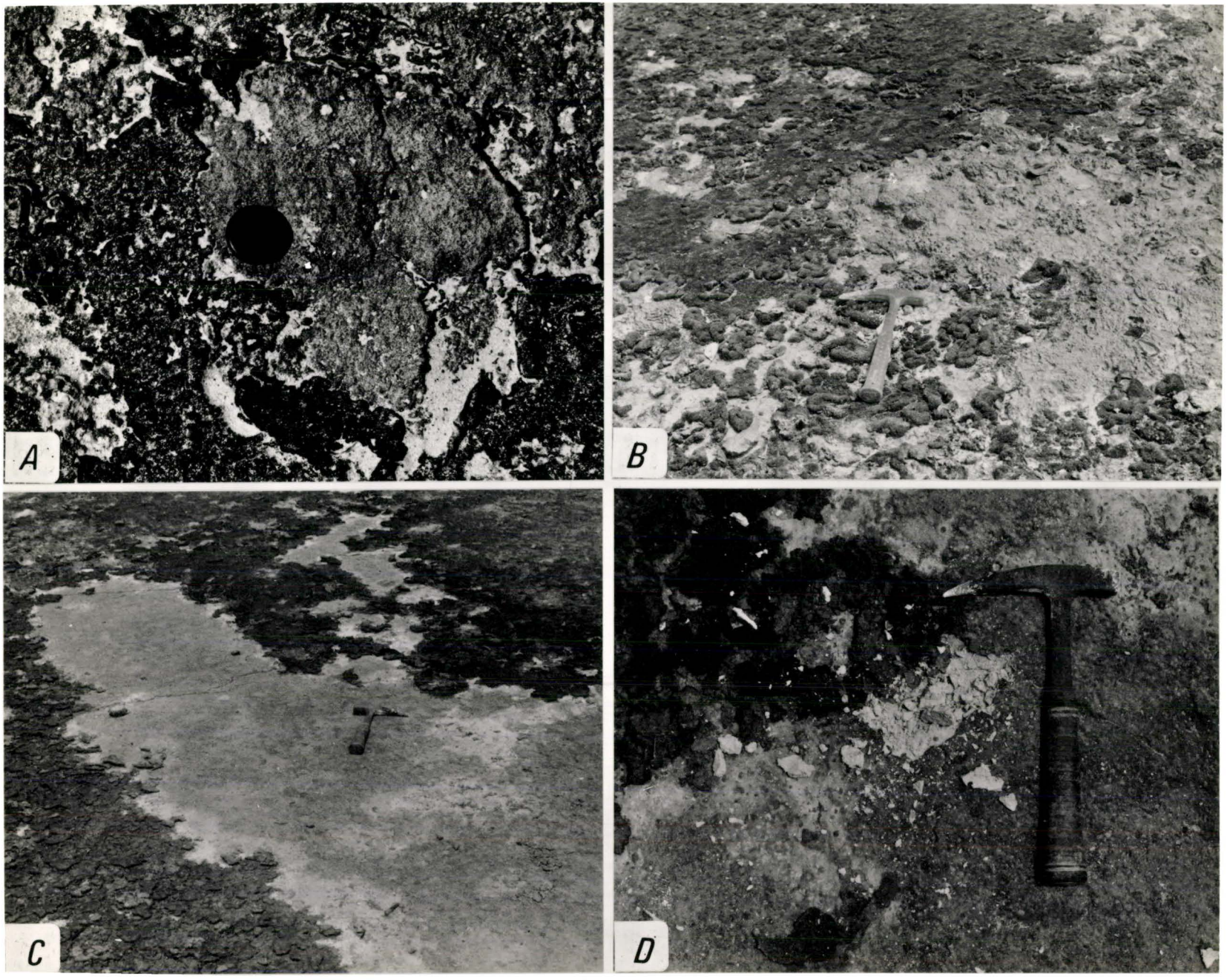
A
B
C
D

Figure 34:

Indurated crust, Boca Jewfish

A. Indurated crust pavement, site C. The crust has been broken and has buckled into a teepee structure. Intraclasts of crust and tufted mat litter the surface.

B. Lumpy surface of crust pavement that resembles tufted mat surface.

C. Section through indurated crust and underlying unconsolidated sediment (Knife handle is about 10 cm long).

D. Thin section (crossed polars) of indurated crust. Mollusc fragment (lamellar structure) and peloids (dark cryptocrystalline aragonite) are cemented by cryptocrystalline aragonite (light grey in colour) (Scale bar is 32 μm).

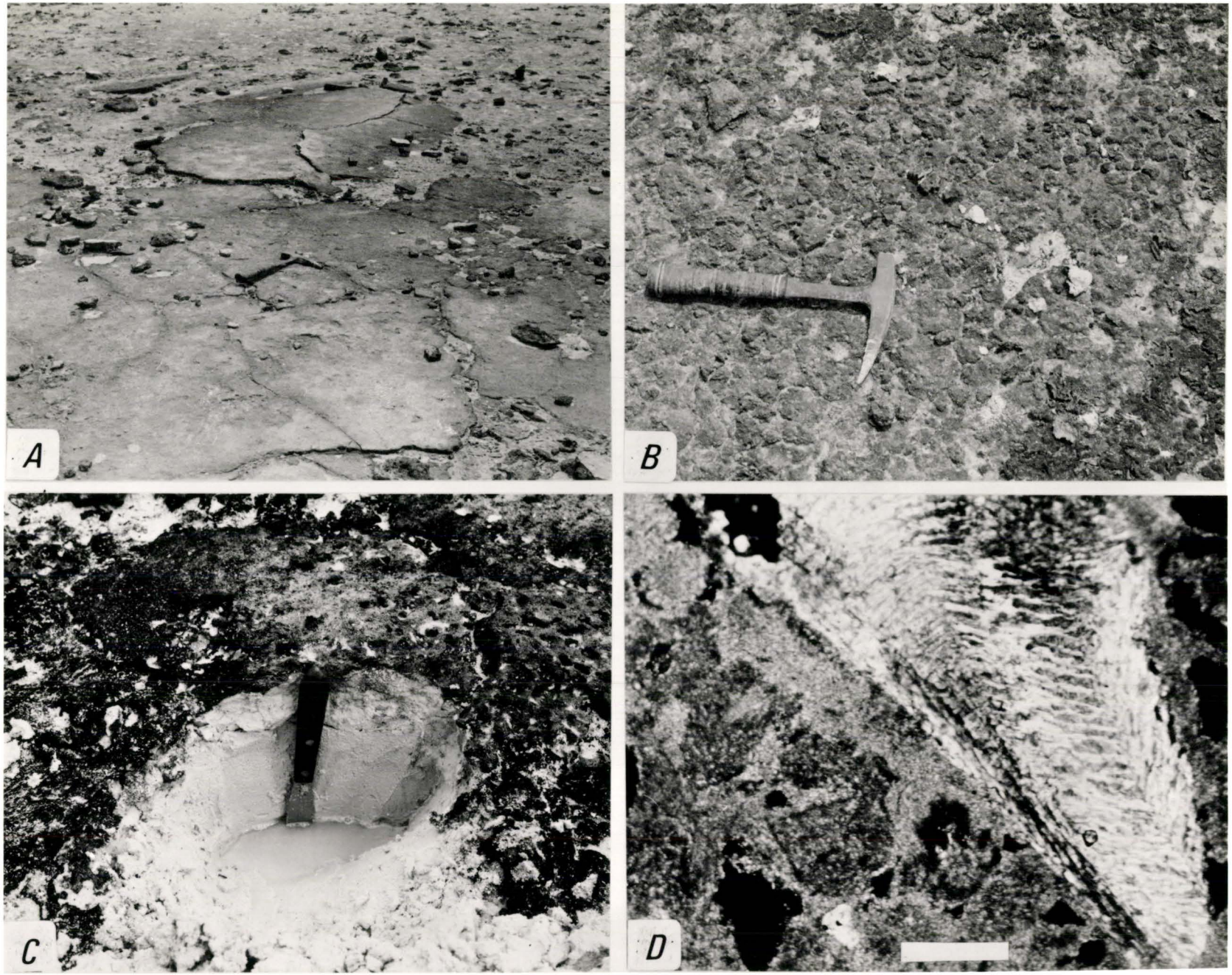
A
B
C
D

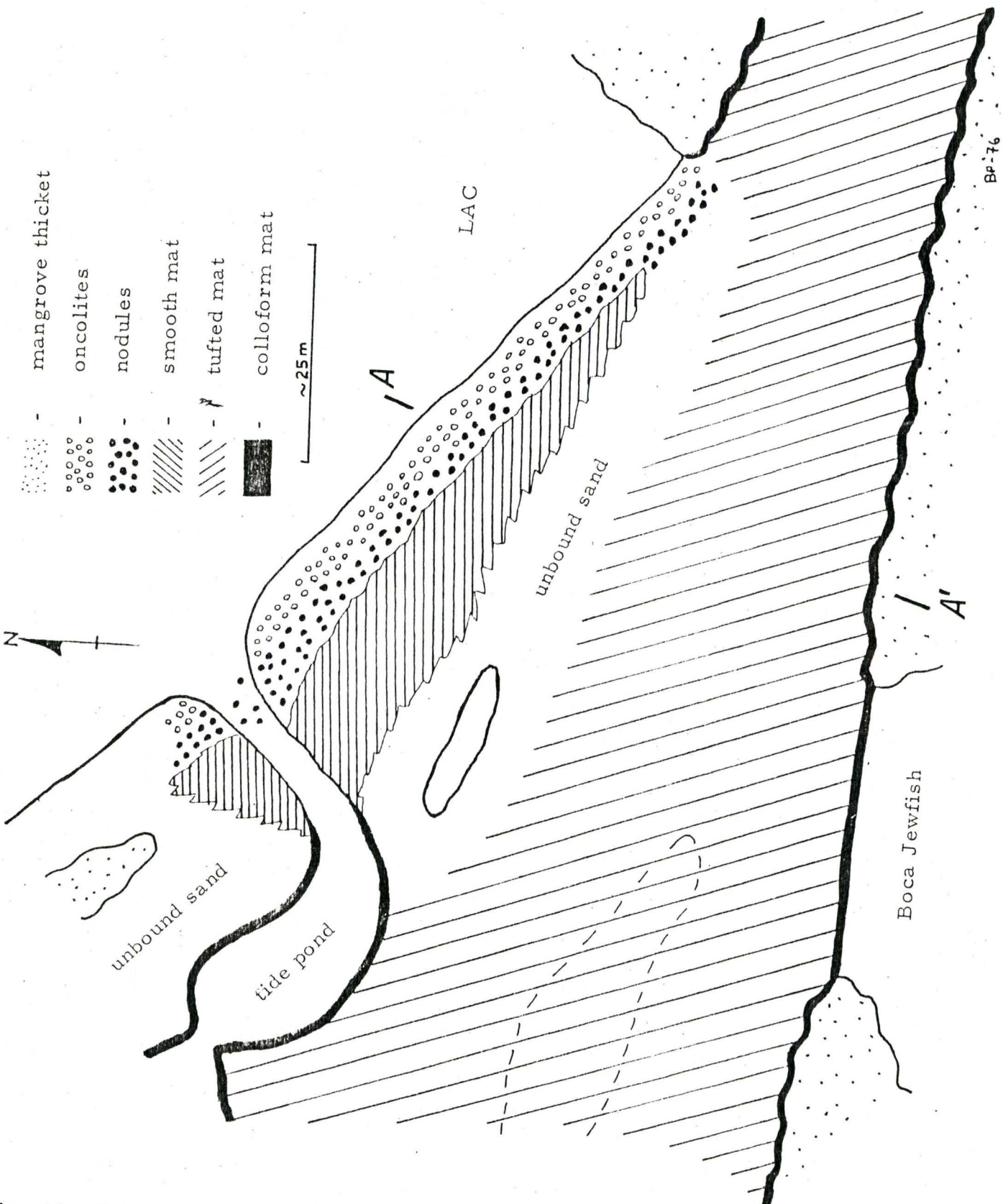

Fig. 36: Boca Jewfish site A, showing areal distribution of cryptalgal structures and position of cross-section A-A' (Figure 37).

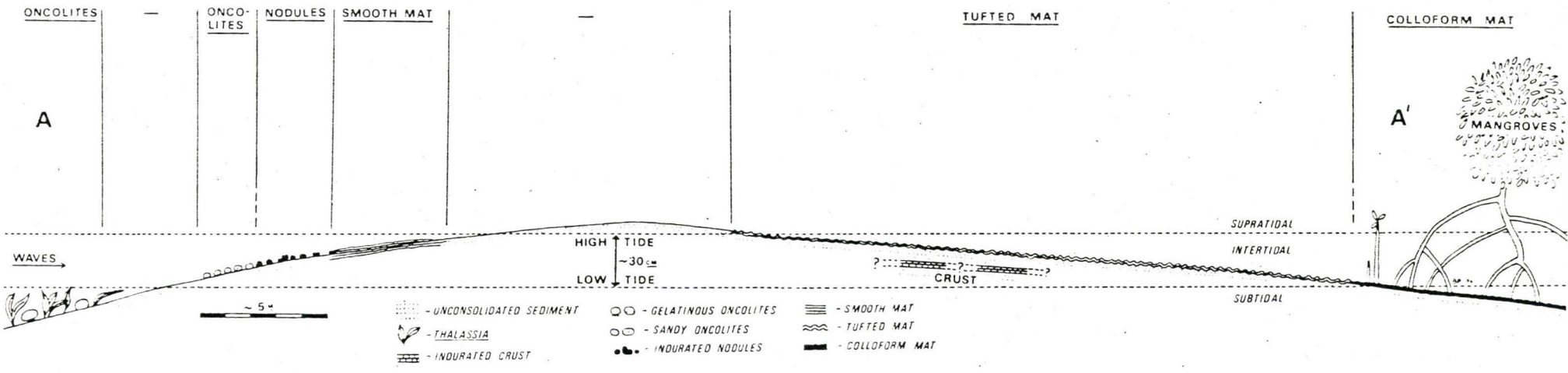

Fig. 37: Cross section A-A' across site A, showing zonation of cryptalgal structures.

into a ridge of supratidal unbound salt-encrusted sand. On the protected side of the ridge, a zone of tufted mats extends from the low supratidal to the subtidal mangroves. These tufted mates are highly desiccated in the supratidal and high intertidal areas. The tufted mat is a continuous sheet in the lower, damper areas near the mangroves. At the lowest point in the intertidal, the tufted mat zone grades into the gelatinous colloform mat which continues into the subtidal of the mangroves and tide ponds. The colloform mat ranges from a loose fragile covering to a fairly cohesive layer that can be removed from the water.

The indurated crust underlies some of the area and outcrops as a weathered pavement in the tufted mat zone.

The smooth mat zone is not present at sites B and C. The zonation of cryptalgal structures is less pronounced than at site A. The various types of cryptalgal structures can be zoned according to tidal height (Figure 38).

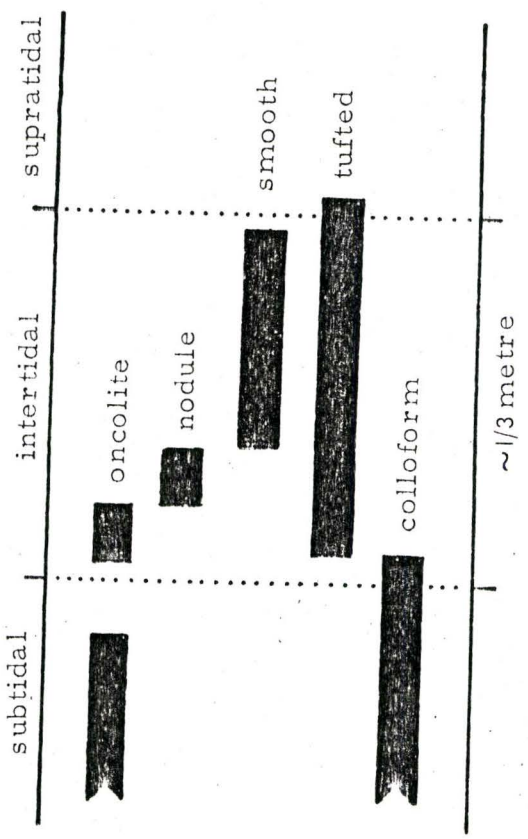

Fig. 38: Zonation of cryptalgal structures in relation to tidal heights.

Coring of the algal mats (smooth, tufted, colloform) across site A indicates that cryptalgal fabric is present only in the upper 1 or 2 cm or less of the sediment underlying the mats (Figure 39).


A
B
C
D
E
T 6
T 5
B 5
B 6
T 2

CHAPTER IV

DISCUSSION

Environmental Controls On Mat Type

A number of environmental factors are known to play important roles in determining the fabrics and morpholoies of cryptalgal structures, and the algal species present within the mat. Mats may be accreting or being eroded; erosion is by both physical destructive processes, such as waves, and biological destructive processes, such as grazing by herbivorous organisms.

Of basic importance in the algal composition of the mat, blue-green algae generally have wide environmental tolerances, and mats are often composed of several co-existing species (Ginsburg et al, 1954). Usually only a few species of algae are dominant mat-formers and other species, though present, do not play a significant role in the sediment - accreting capabilities of the mat (Sorensen and Conover, 1962). Different blue-greens are better suited than others for trapping and binding sedimentary particles in different environments (Monty, 1971). Robust erect filaments (such as Microcoleus spp.) are able to physically trap sediment grains which also adhere to the mucilagenous sheaths covering the trichomes. Fine filaments such as Schizothrix secrete copious amounts of mucilagenous material and sedimentary particles are agglutinated by this material (Monty, 1965a, 1967).

Desiccation

The length of time that an algal mat is exposed to air is a measure of possible desiccation. Blue-green algae have several mechanisms of defence against fatal dehydration, as outlined by Monty (1965a). Blue-green algae can produce a thick mucilagenous sheath around individual cells or around the whole colony. Not only does this decrease water loss but also can protect against light intensity if the sheath is stained. Blue-greens can also resist drought by the production of resting spores or hormocysts which are enlarged cells full of food reserves; these can remain dormant for long periods and are able to germinate at a later more favourable time. The mode of growth of the algal colonies also affords protection against dehydration. In some cases a species will grow in a lower part of the mat beneath another species for protection. A tufted mode where filaments are erect and project into the air allows absorption of atmospheric moisture and also moisture from the ground by capillary action. An adhesive mode, where a gelatinous film is produced, such as oncolites, allows preservation of internal moisture.

Besides the ecological tolerance of blue-green algae to desiccation, one must also consider the effect of desiccation on the physical nature of mats. Mats are continuous sheets when permanently damp; when significant dehydration occurs, algal sheaths lose water and contract. Desiccated mats will separate polygonally and shrink, sometimes detaching themselves

from the underlying sediment. These features are potentially preservable by lithification.

Salinity

Blue-green algae are able to tolerate wide variations in salinity from brackish to hypersaline levels. Cryptalgal structures from fresh water environments have been described by Monty (1965a, 1967). Algal mats in hypersaline conditions have been described from Hamelin Pool, Western Australia, where salinites reach 90 (Logan et al, 1974), Gulf of Aqaba, Red Sea which reach 146 (Friedman et al, 1973) and Mauritania, West Africa, which reach 125 (Schwarz et al, 1975). Naturally during low tide, evaporation of seawater will give rise to high salinites within the upper part of the mat.

The water of the Lac and Boca Jewfish have approximately normal oceanic salinity (Wagenaar Hummelinck and Roos, 1968), though evaporation of pore waters and tidal ponds will produce locally slightly hypersaline conditions. Salinites of this range are probably not important factors in cryptalgal structure type.

Currents

Wave and tidal currents are important erosive agents of cryptalagal structures. Topographic relief in the form of heads, domes, and pustules can be a response to eroding currents. Currents can also tear up horizontal mats, especially after they have been cracked by desiccation. The resistance of these structures depends on several factors such as degree of lithification and cohesiveness of the algal mat itself. The cohesiveness of algal mats depnds basically on its specific composition (Golubic, 1973).

Gebelein (1969), Neumann et al (1970), and Scoffin (1970), have studied the effect of bottom currents on subtidal cryptalgal structures from Bermuda and the Bahamas. Current measurements in the field and experimental flume studies indicate that mats of different compositions and morphologies have differing resistance to currents. Where the algal mat is disrupted by burrowing organisms, it becomes less stable (Neumann et al, 1970; Scoffin, 1970). Bathurst (1967) showed that loose flocculent mats can stabilize the sediments and prevent the formation of ripples.

Subtidal mats therefore are more continuous in areas that are most protected from currents; subtidal oncolites on the other hand require agitation. The floors of tide ponds and mangrove - protected areas of the Lac are colonized by subtidal colloform mats which are less cohesive than the tufted and smooth mats. Colloform mats cannot grow in the lagoon because of relatively strong wave action there.

Tidal currents are also important in determining the type of intertidal mat in the Boca Jewfish area. Tufted mats of site A are protected from

strong wave action by the supratidal barrier; those at sites B and C are protected by mangroves. Even so, shrunken areas of the tufted mats are further damaged by currents which fold pieces over and carry fragments off. The smooth mat on the windward side of the sand barrier is exposed to stronger wave action. The seaward edge of this mat is eroded.

Oncolites of the subtidal and intertidal areas are exposed to wave and tidal currents which aid in their accretion by stirring up sediment and overturning the structures.

Internal Fabric

Episodic sediment influx alternating with periods of algal growth gives rise to laminations in cryptalgal structures (Black, 1933; Ginsburg et al, 1954). Algal mats may also be laminated because of alternation of two species or groups of species (Black, 1933; Sorensen and Conover, 1962); laminated cryptalgal carbonates formed by precipitation of high-Mg calcite and aragonite laminae have been reported by Friedman et al (1973).

Laminations of alternating sediment-rich layers capped by algal-rich layers have been shown in some cases to be diurnal (Monty, 1965a,b, 1967; Gebelein, 1969). The sediment-rich layer forms mainly during the day when grains are trapped by erect filaments and an algal rich layer is formed by horizontal growth at night (Gebelein, 1969). Monty (1965a,b, 1967) showed that laminations are formed by algal growth during the day and slow growth with sedimentation later in the day and at night. Lamination may also be due to tidal cycles (Gebelein and Hoffman, 1968) or periodic storm influx (Ginsburg et al, 1954; Walter et al, 1973).

An irregular lamination or alignment of fenestrae (unsupported voids) is typical of many cryptalgal structures, both modern and ancient. Fenestral fabric results from interaction of desiccation, oxidation of organic matter, grain size and cementation (Logan, 1974). The sediments bound by the smooth mat and tufted mat of the Boca Jewfish area possess an irregular fenestral grain framework fabric, where fenestrae occur at intergranular voids and link other intergranular spaces.

Grazing and Burrowing

Burrowing organisms physically damage algal mats. Deposit feeding worms and crustaceans create burrows in bound sediments, destroying internal fabric and disrupting the mat surface. Burrowing worms have been reported to markedly influence the morphology of cryptalagal structures of the Persian Gulf (Shinn, 1972). Burrowing organisms bring surface oxidizing conditions into the reducing zone underneath (Davies, 1970). Burrowing worms cause extensive bioturbation of the unbound sands of the Boca Jewfish beach. They also disrupt and bioturbate the loose gelatinous colloform mat of the protected low intertidal and subtidal areas. Subtidal oncolites have been bored by worms (?) which have cross-cut the laminations. Burrowing fiddler crabs (Uca sp.) create burrows in the

lower intertidal and distribute fecal pellets and burrowed sand over the mat surface.

Algae play a basic vital role in the tropic structure of marine environments (Turpaeva, 1957). Subtidal benthic blue-green algae are the main food source for herbivorous browsing molluscs, echinoderms, crustaceans, fish and polychaetes (Bathurst, 1967). Strong currents in areas of oncolite growth probably prevent significant grazing and settling of burrowing organisms (Garrett, 1970). Because of the harsher environment of the intertidal zone, grazing is limited to mobile organisms that move with the tides, or to organisms that can resist desiccation during intertidal exposure. Schwarz et al (1975) have shown that grazing fish can have significant effect on the morphology of intertidal stromatolites. Cerithid gastropods grazing on intertidal mat surfaces have been reported from many areas such as the Bahamas (Garrett, 1970), Ceylon (Gunatilaka, 1975) and the Coorong of South Australia (Walter et al, 1973). These gastropods can prevent the formation of intertidal mats if uninterrupted grazing occurs (Garrett, 1970). Grazing gastropods are not found in Hamelin Pool, Western Australia because of its hypersalinity (Logan, 1961; Logan et al, 1974). This is one factor that accounts for the prolific stromatolitic growth there (Garrett, 1970).

Biogenic destruction of algally bound sediments in the supratidal is limited to burrowing by insects and worms (Garrett, 1970).

There is evidence that suggests that antipathetic relationships between algal mats and mat-destroying organisms has existed in ancient environments. Cussey and Friedman (1976) describe possible algal mat growth affected by burrowers and browsers which are restricted by high salinites, from the Jurassic of Paris. Kepper (1974) has described similar relationships between Cambrian trilobites, mats and salinity.

Conspicuous is the lack of grazing gastropods such as cerithids in the Lac intertidal. This fact was also pointed out by Sibley and Murray (1972). Cerithids are present in the salt pans near the Cai of the northern part of the Lac (Wagenaar Hummelinck and Roos, 1968). Several empty shells of the subtidal species Melongena melongena, Cittarium pica and Voluta musica were found at site A and had probably been carried in with the tide. Lack of grazing gastropods in the intertidal may be in part due to inability to withstand dehydration during intertidal periods.

Lithification

Penecontemporaneous cementation of living marine cryptalgal structures has been reported from Shark Bay, Western Austrailia (Logan, 1961; Logan et al, 1974). In this locality, stromatolites are lithified in the subtidal and intertidal zone by growth of aragonite cement from hypersaline waters (Logan, 1974). Lithification of stromatolites preserves their cryptalgal fabric and increases their resistance to erosion by waves and currents. Stromatolitic columns may in fact be inclined towards the erosive currents and waves (Hoffman, 1967; Hoffman, 1973, Logan et al, 1974).

Evamy (1973) describes calcarenitic cryptalgal structures from the Persian Gulf preserved by aragonite cementation. Surface ridges, wrinkles and polygons are preserved, but the algae of the mat are dead and decayed. The cement is believed to have been precipitated in response to the direct evaporation of marine water in the intertidal zone, and lithified cryptalgal structures are observed to grade with unlithified living algal mats.

Precipitation of aragonite by the evaporation of seawater has been shown to produce spheroidal "algal lapilli" (Rothe, 1970). These structures are pieces of desiccated mat that have been curled up and detached from the underlying sediment; they are filled with aragonite that had originally precipitated on top of the mat (Rothe, 1970).

Friedman et al (1973) and Dalrymple (1965) have demonstrated that blue-green algae are able to precipitate calcium carbonate within algal mats when, during photosynthesis in hypersaline waters, CO_2 is removed from solution. Carbonate algalaminites of the Gulf of Agaba, Red Sea are composed of alternating laminae of cryptocrystalline and fibrous aragonite (Friedman et al, 1973). Later cementation of this internal structure could produce the finely laminated carbonates observed in many fossil cryptalgal structures (Friedman et al, 1973). Monty (1965a, 1967) showed that calcium carbonate is precipitated within the algal mats of the freshwater environment of Bahamas, but lithification does not occur. Other freshwater cryptalgal structures are lithified (e.g., Clark, 1900; Roddy, 1915; Mawson, 1929). In an experimental study, Gebelein and Hoffman (1973) have shown that high-magnesium calcite is precipitated onto blue-green algal (Schizothrix calcicola) mucilagenous sheaths. Magnesium is concentrated by the algae and it is suggested that alternating sediment-rich and algal-rich layers can give rise, after later diagenetic alteration, to alternating limestone and dolomite laminations often observed in fossil cryptalgal structures.

The indurated nodules of site A, Boca Jewfish are lithified cryptalgal structures. Their internal fabric is preserved by cementation. However, lithification is not observed in other cryptalgal structures of the Boca Jewfish, though there is some evidence from scanning electron microscopic observations that does suggest in situ precipitation of calcium carbonate on organic algal material.

During the processes of fossilization, organic layers will decay. Decay of algal layers may leave fenestrae, which, along with other primary pore spaces in the sediment, may become filled by secondary calcite cementation. Sparry calcite-filled vugs such as fenestrae are birdseye structures, and are common in fossil cryptalgal structures (Shinn, 1968). Hubbard (1972) has outlined other petrographic characteristics of cryptalgal fabrics. Hand specimens of algalaminites (Figure 40) may look deceptively similar to laminated rocks not algal in origin. Fossil and recent oncolites (Figure 41) have been compared by Ginsburg (1960).

A subtidal oncolite from the Lac was dehydrated in an oven to examine the resulting structure which might be what one would expect to see preserved. The organic laminations disappeared from loss of water, and the mucilagenous material glued the sediment grains firmly together. The sediment laminations are preserved without significant crinkling, though the oncolite decreased in volume by about one half. The morphological changes during the dehydration process are identical to the inferred changes in gross morphology associated with burial and diagenesis as figured by Hofmann (1973: Figure 11).

Figure 40:

Fossil cryptalgal carbonate structures (algalaminites).

A. Algalaminite composed of alternating limestone and dolomite laminations, partly replaced by chert (in upper right corner). LLH type stromtolites (lower part of the photograph) gradually change to horizontal laminations (algalaminite). Lower Ordovician, Shakopee Formation, Utica, Illinois. Specimen courtesy of F. Hein. (Coin is 1.9 cm in diameter).

B. Algalaminite composed of dolomite, showing fenestral porosity; the pore spaces are filled with oil which is concentrated in bands of highest porosity. Upper Silurian (Cayugan), Maumee, Ohio.

C. Algalaminite composed of dolomite showing hydrocarbon-rich wavy laminations (hydrocarbons also concentrated along stylolites). Upper Silurian (Cayugan), Maumee, Ohio.

C. Algalaminite composed of dolomite. The laminations are outlined by dark-colored organics, and show a structure which may have been a folded over flap of algal mat. Lower Devonian Detroit River Formation, Wabash, Indiana.

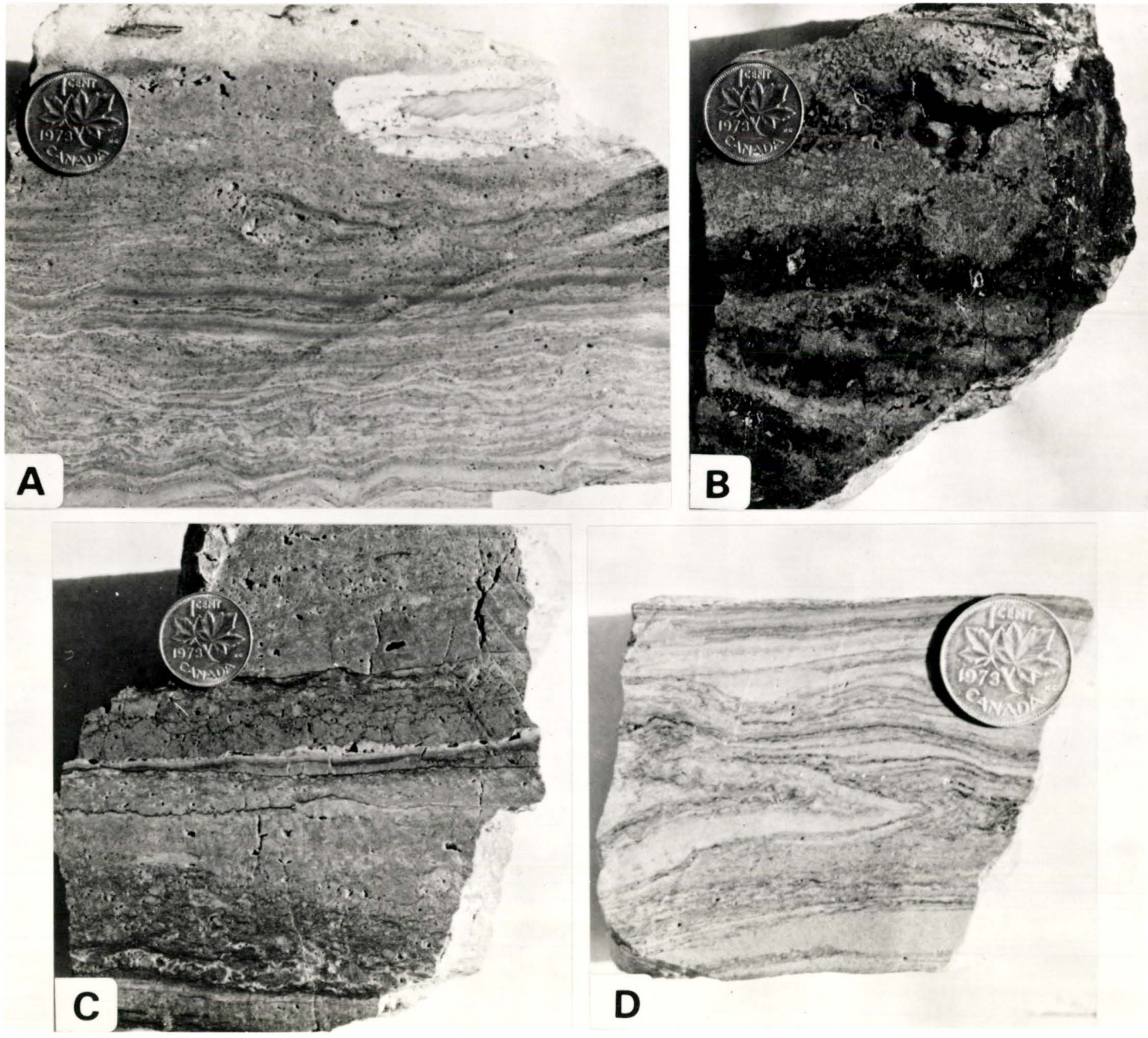
A
B
C
D

Figure 41:

Oncolites, both modern and ancient.

A. Gelatinous subtidal oncolite, Lac, Bonaire (Coin is 1.9 cm in diameter.

B. Intertidal oncolite with a fragment of indurated nodule as a nucleus, site A, Boca Jewfish, Bonaire (Diameter of the specimen is approximately 7 cm).

C. Indurated oncolite nodule, intertidal, site A, Boca Jewfish, Bonaire.

D. Fossil oncolites, Mississippian Ste. Genevieve Limestone, Illinois. Specimens courtesy of F. Hein.

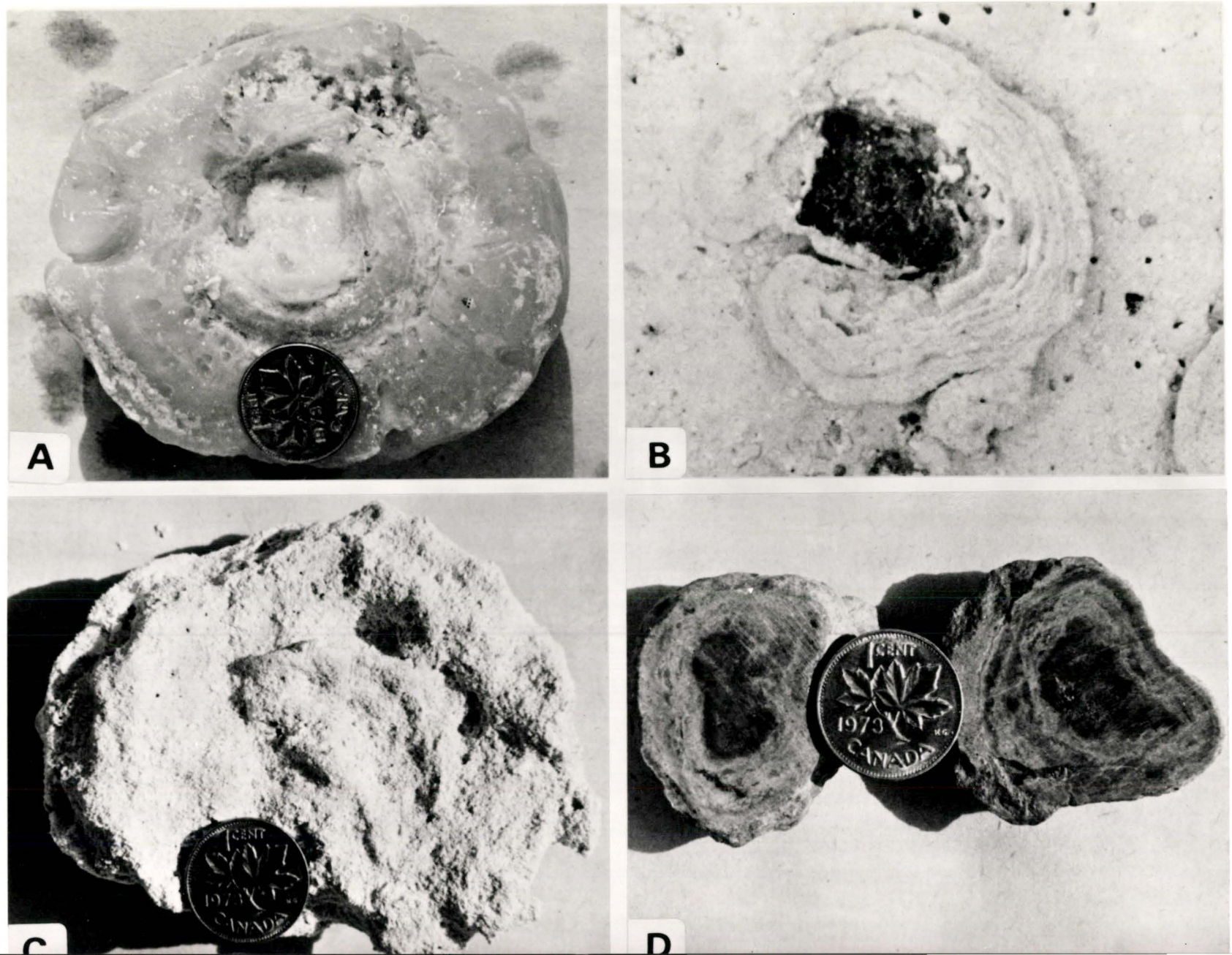
A
B
C
D
1973
CANADA

INDIVIDUAL CRYPTALGAL STRUCTURES

Oncolites

The subtidal oncolites of the Lac, the intertidal oncolites of site B and the sandy oncolites of site A are very similar to structures described by Ginsburg (1960) and Frost (1974) from Florida, Monty (1965a, b) from Bahamas and Gebelein (1969) from Bermuda. These structures are the stacked hemispheroids (SH) and spheroidal structures (SS) of Logan et al (1964) and have been called algal biscuits (Ginsburg 1960; Gebelein, 1969).

These forms appear to be formed by agglutination of particles onto the mucilagenous mass secreted by Schizothrix calcicola filaments. Further algal growth during periods of less sedimentation causes alternating sediment-rich and mucilage-rich laminations. The laminae of the stationary intertidal oncolites of site B are evenly spaced from the nucleus outwards, suggesting that the periods of sedimentation have been at regular intervals. It is not clear what episodic conditions can account for this; if they were diurnal, then the structures would be less than a month old.

The subtidal oncolites have more closely spaced laminae in their centres. The intertidal calcarenitic oncolites are found only on the small stretch of beach of site A. It is possible that, in the subtidal, small oncolites are more mobile and accretion is by means of rolling on the bottom. When they grow larger, it is more difficult to overturn them, and sediment agglutination may occur less frequently. Small subtidal oncolites may be cast onto the beach at site A by strong waves, and accretion continues by periodic rolling and sediment movement by waves. Many of the calcarenitic oncolites have cores of pieces of cryptalgal nodules, which suggests that oncolites may be forming in situ.

Cryptalgal Nodules

The progressively indurated nodules of site A appear to be lithified oncolites and chunks of smooth mat. Cementation by aragonite is probably analogous to intertidal cementation of cryptalgal structures from Shark Bay (Logan, 1974), where precipitation of aragonite is due to evaporation of seawater.

The outer surface of these nodules is colonized by filamentous blue-green algae and thus the nodules can be considered as living, one-layer thick stromatoids (H. J. Hoffmann, pers. comm., 1975). Small pieces form the nuclei of many of the gelatinous calcarenitic oncolites lower in the intertidal.

The nodules appear to be somewhat similar to detached cryptalgal lumps that have broken off the smooth mat of Shark Bay (Logan et al, 1974).

Smooth Mat

The smooth mat consists of about 1 cm to 2 cm of sand with a laminoid fenestral fabric. Below this, the sands are not algally bound. Accretion is by tight binding of sedimentary particles by a mesh of fine filaments (Schizothrix sp. ?). Binding is such that the mat is rigid, though no cement is observed. This mat may be too well drained when the tide is out for cement to precipitate. The seaward edge of the mat is eroded in places; broken pieces become indurated nodules. The mat is not found elsewhere in the Boca Jewfish Area.

A smooth mat formed by a species of Schizothrix is also described from Shark Bay (Logan et al, 1974). This mat is also characterized by lamination and laminoid fenestral fabric. Penecontemporaneous cementation occurs in Shark Bay smooth mat structures but not in the Boca Jewfish. In both areas the deposition of sediment layers is irregular in time; particles are trapped onto mucilage and binding is accomplished by growth of a filament mesh through the grain framework.

Tufted Mat

The erect tangles and mucilagenous sheaths of Microcoleus filaments of the tufted mat trap and bind sediment grains. In protected areas of little sedimentation, such as behind mangrove thickets of Sorobon (site B), the mat is a thick felt of erect filaments. Elsewhere, the mat is thin and leathery or brittle. Only the upper 1 to 2 cm of the sediment under the mat is cryptalgal; probably the growth of this mat has been a fairly recent phenomenon. Marine regression is occurring, and the Lac is gradually being filled in (Wagenaar Hummelinck and Roos, 1969). The mangrove thickets are expanding and colonizing the ground as it becomes suitable. Formation of tufted mats occurred on emergence of intertidal flats. Accretion is irregular and laminations are not very clear because sediment influx is patchy. Tufted mats are also found in the Cas di Meeuchi Area of the southeast part of the Lac (Sibley and Murray, 1972).

Similar Microcoleus mats have been reported by Davies (1970) and Logan et al (1974) from Shark Bay where they have a scalloped internal fabric, from France by Hommeril and Rioult (1965), from West Africa by Schwarz et al (1975), from Ceylon by Gunatilaka (1975), from South Australia by Walter et al (1973), from Florida and Laguna Madre, Texas by Ginsburg et al (1954).

Colloform Mat

This mat is similar to quiet subtidal mats of Shark Bay (Logan et al, 1974), Bermuda (Gebelein, 1969), Bahamas (Neumann et al, 1970; Scoffin, 1970) and Florida. The mat is loose, friable and the internal sediments do not show distinctive cryptalgal fabric. It grades with the tufted mat by a gradual increase in the amount of Microcoleus filaments higher in the intertidal. This mat is a sediment stabilizer in protected areas of tide ponds and mangrove thickets. Accretion is limited by low sediment influx and periodic destruction of the mat by storms.

Indurated Crust

An indurated aragonitic crust has been reported as occurring 35 cm below the sediment surface of Cas di Meeuchi by Sibley and Murray (1972). This crust does not have any internal laminoid fabric and seems similar to the two cemented intraclasts found in the core at sample station T7 (site A). Sibley and Murray (1972) did not record the presence of indurated crust pavements from the Boca Jewfish Area.

At site C, the supratidal crust is broken and thrust upwards into teepee structures. Similar structures in supratidal crust pavements have been reported from the Persian Gulf (Evamy, 1973), Shark Bay (Davies, 1970; Logan, 1974) and in subtidal crust of the Persian Gulf by Shinn (1969). Suggested mechanisms for the fracturing and thrusting are brecciation due to thermal expansion and thrusting due to volume increases caused by precipitation of cement, or gravitational instability caused by denser indurated slabs on top of underlying unconsolidated sediment. Smith (1974) described Permian teepee structures and attributed them to expansion due to growth of interstitial cement.

Supratidal crusts of the Persian Gulf (Evamy, 1973), Shark Bay (Davies, 1970; Logan, 1974) and Bahamas (Shinn et al, 1965) are considered to have been formed in the intertidal and supratidal zones by evaporation of marine pore waters, causing precipitation of aragonite cement. The cement in the site C crust is cryptocrystalline aragonite. Logan (1974) considered a cryptocrystalline aragonite cement as a diagenetic feature of hypersaline conditions, commonly of intertidal and supratidal settings. The planar upper surface of some parts of the pavement, lumpy irregular surface (resembling tufted mat blisters) of other parts and the internal fenestral fabric of the site C crust suggest an intertidal or low supratidal origin, rather than a submarine origin. It is not clear whether these criteria are adequate proof of the suggested origin of the Boca Jewfish crust, and further study would be necessary.

Algal Mat Zonations

Zonations of algal mat types are pronounced in areas of extensive intertidal flats, such as Cape Sable, Florida (Gebelein and Hoffman, 1968), Abu Dhabi, Persian Gulf (Kendall and Shipwith, 1968), Shark Bay, Western Australia (Davies, 1970; Logan et al, 1974), Ceylon (Gunatilaka, 1975); Mauritania, West Africa (Schwarz et al, 1975), and Bahamas (Monty, 1965a, 1967). Zonations from subtidal to supratidal conditions are caused by differing algal tolerances of environmental changes, such as degree of desiccation. Zonations are also caused by changes from the subtidal to supratidal environment in the effect of destructive and constructive aspects, such as gastropod grazing of subtidal mats and wave action. The zonation of cryptalgal structures at site A is a function of environmental factors such as drainage, degree of desiccation and wave and current action.

Although cryptalgal morphology is controlled by environmental variables, care must be exercised in interpreting fossil structures. Zonations of various morphologies have been reported from Proterozoic and Paleozoic carbonates (e.g., Laporte, 1963; Ahr, 1971; Hoffman, 1974). Hoffman (1974) shows a platform to basin lithofacies change coupled with a change in stromatolite morphologies from the Proterozoic Pethei Group. Ahr (1971) illustrated gradual shallowing which caused changes in Cambrian cryptalgal morphologies. Differing cryptalgal morphologies of the Devonian Manlius Formation have been interpreted as indicating changes in environment (Laporte, 1963) though this conclusion has been disputed by Monty (1965a).

CHAPTER VI

CONCLUSIONS

Several different types of cryptalgal carbonate structures are found in the Boca Jewfish area. These are oncolites, indurated nodules, tufted mat, smooth mat and colloform mat. An indurated crust, possibly cryptalgal, is also present.

Blue-green algae colonize sediment surfaces in the subtidal to low supratidal areas of the Boca Jewfish. Growth is inhibited by several environmental factors, such as desiccation, grazing by herbivores, and wave and tidal currents. In the intertidal of the Boca Jewfish, grazing molluscs do not seem to be present, and thus grazing is not a limiting factor here.

Environmental parameters influence the composition of the blue-green algal communities. Microcoleus has the greatest tolerance of desiccation. Lyngbya of the colloform mats requires damp or wet conditions. Schizothrix also thrives best in damp or wet areas.

The morphology and internal fabric of cryptalgal structures is controlled by environmental conditions as well as the algal composition of the mats. Hemispherical oncolitic structures are found in the subtidal and low intertidal; they cannot form in areas of long periods of desiccation. These cryptalgal structures have internal concentric laminations of sediment - rich and mucilage - rich layers caused by episodic sediment incorporation. The internal laminations of subtidal oncolites can be disrupted by burrowing organisms. Intertidal calcarenitic oncolites of site A can be fragmented by strong wave action. Cryptalgal nodules retain the morphology and internal fabric of the smooth mat or calcarentic oncolites from which they are derived. Aragonite cementation is due to evaporation of marine pore waters at low tide. The smooth mat is found only on the well-drained intertidal Boca Jewfish beach. The internal laminated fabric is due to episodic sediment trapping and the mode of binding by the algal community. Tufted mats grow from low intertidal to low supratidal of areas protected from strong wave and current action. The mat owes its surface features to degree of desiccation, sediment influx and tidal current direction. Internal lamination is not found because the sediments are too coarse and sediment influx is not episodic. The colloform mat of permanently damp, protected areas of tidal ponds and mangroves is a sediment stabilizer but is disrupted by burrowing organisms and physical erosion.

Because the environmental factors vary from subtidal to supratidal, there is a zonation of different types of algal mats and cryptalgal structures of the Boca Jewfish.

By understanding the environmental and sedimentological factors that are responsible for the morphologies and fabrics of cryptalgal structures, and their distribution, in the modern, ancient examples can be interpreted and the paleoenvironments of deposition better understood.

REFERENCES

1. Ahr, W. M., 1971, Paleoenvironments, Algal Structures and Fossil Algae in the Upper Cambrian of Central Texas; Jour. Sed. Pet., 41, pp. 205-216.

2. Aitken, J. D., 1967, Classification and Environmental Significance of Cryptalgal Limestones and Dolomites With Illustration from the Cambrian and Ordovician of Southwestern Alberta; Jour. Sed. Pet. 37, pp. 1163-1178.

3. Barghoorn, E. S. and Schopf, J. W., 1966, Microorganisms Three Billion Years old From the Precambrian of South Africa; Science, 132, pp. 758-763.

4. Barghoorn, E. S. and Tyler, S. A., 1965, Microorganisms from the Gunflint Chert; Science, 147, pp. 563-577.

5. Bathurst, R. G. C., 1967, Subtidal Gelatinous Mat, Sand Stabilizer and Food, Great Bahama Bank; J. Geol., 75, pp. 736-738.

6. Black, Maurice, 1933, The Algal Sediments of Andros Island, Bahamas; Royal Soc. London Philos. Trans., Ser. B, 222, pp. 165-192.

7. Bosellini, A. and Ginsburg, N. R., 1971, Form and Internal Structure of Recent Algal Nodules (Rhodolites) from Bermuda; Jour. Geology, 79, pp. 619-682.

8. de Buisonjé, P. H., 1974, Neogene and Quaternary Geology of Aruba, Curacao and Bonaire; Natuurwetenschappelijke Studiekring voor Surename en de Nederlandse Antille, Utrecht, No. 78, p. 293.

9. Chapman, V. J. and Chapman, D. J., 1973, The Algae; MacMillan, London, p. 497.

10. Clark, J. M., 1900, The Water Biscuit of Squaw Island, Canandaigua Lake, N.Y., N.Y. State Mus. Bull. 39, pp. 195-198.

11. Cohn, F., 1862, Über die Algen des Karlsbaden Sprudels mit Rücksicht auf die Bildung des Sprudelsinters; Abh. Schles. Gesell. Vaterl. Cult., Naturwiss. Medicin, 2, pp. 35-55.

12. Cussey, R. and Friedman, G.M., 1976, Antipathetic Relations Among Algal Structures, Burrowers and Grazers in Dogger (Jurassic) Carbonate Rocks, Southeast of Paris, France; Am. Assoc. Pet. Geol., Bull. 60, pp. 612-616.

13. Dalrymple, D. W., 1965, Calcium Carbonate Deposition Associated With Blue-Green Algal Mats, Baffin Bay, Texas; Pub. Inst. Mar. Sci., Univ. Texas, 10, pp. 187-200.

14. Davies, G. R., 1970, Algal-laminated Sediments, Gladstone Embayment, Shark Bay, Western Australia. in Carbonate Sedimentation and Environments, Shark Bay, Western Australia; Am. Assoc. Pet. Geol., Mem. 13, pp. 169-205.

15. Dawson, J. W., 1875, The Dawn of Life; Dawson Brothers, Montreal, p. 239.

16. Deffeyes, K. S., Lucia, F. J. and Weyl, P. K., 1965, Dolomitization of Recent and Plio-Pleistocene Sediments by Marine Evaporite Waters on Bonaire, Netherlands Antilles; in Dolomitization and Limestone Diagensis; Pray, L. C. and Murray, R. C., eds., SEPM Spec. Publ. No. 13, pp. 71-88.

17. Dunham, R. J., 1962, Classification of Carbonate Rocks According to Depositional Texture. in Classification of Carbonate Rocks; Am. Assoc. Pet. Geol., Mem. No. 1, pp. 108-121.

18. Evamy, B. D., 1973, The Precipitation of Aragonite and its Alteration to Calcite on the Trucial Coast of the Persian Gulf; Purser, B. H., ed., The Persian Gulf, pp. 329-342.

19. Folk, R. L., 1959, Practical Petrographic Classification of Limestones; Am. Assoc. Pet. Geol. Bull., 43, pp. 1-38.

20. Folk, R. L., 1962, Spectral Subdivision of Limestone Types. in Classification of Carbonate Rocks; Am. Assoc. Pet. Geol. Mem. 1, pp. 62-84.

21. Friedman, G. M., 1959, Identification of Carbonate Minerals by Staining Methods; J. Sed. Pet., 29, pp. 87-97.

22. Friedman, G. M., Amiel, A. J., Braun, M. and Miller, D. S., 1973, Generation of Carbonate Particles and Laminites in Algal Mats - Example From Sea - Marginal Hypersaline Pool, Gulf of Aqaba, Red Sea; Am. Assoc. Pet. Geol. Bull., 57, pp. 541-557.

23. Frost, J. G., 1974, Subtidal Algal Stromatolites from the Florida Backreef Environment; Jour. Sed. Pet., 44, pp. 532-537.

24. Garrett, P., 1970, Phanerozoic Stromatolites: Noncompetitive Ecologic Restriction by Grazing and Burrowing Animals; Science, 169, pp. 171-173.

25. Gebelein, C. D., 1969, Distribution, Morphology and Accretion Rate of Recent Subtidal Algal Stromatolites, Bermuda; Jour. Sed. Pet., 39, pp. 49-69.

26. Gebelein, C. D. and Hoffman, P., 1968, Intertidal Stromatolites From Cape Sable, Florida (Abst.); Geol. Soc. Am., Progr. Ann. Meet, p. 109.

27. Ginsburg, R. N., 1960, Ancient Analogues of Recent Stromatolites; 21 Int. Geol. Cong., Ses. 21, Pt. 22, pp. 26-35.

28. Ginsburg, R. N., Isham, L. B., Bein, S. J. and Kuperberg, J., 1954, Laminated Algal Sediments of South Florida and Their Recognition in the Fossil Record; Mar. Lab. Univ. Miami, Unpub. Rep. No. 54-21, p. 33.

29. Golubic, S., 1973, The Relationship Between Blue-Green Algae and Carbonate Rocks. in The Biology of Blue-Green Algae; Botanical Monographs, 9, pp. 434-472.

30. Gunatilaka, A., 1975, Some Aspects of the Biology and Sedimentology of Laminated Algal Mats from Mannar Lagoon, Northwest Ceylon; Sedim. Geol., 14, pp. 275-300.

31. Gürich , G., 1907, Spongiostromidae-eine neue Familie krustenbildener Organismen aus dem Kohlenkalk von Belgien; N. Jb. Mineral., Geol., Paläont., 1, p. 131.

32. Hall, J., 1883, Cryptozoon; N.Y. State Mus., 36th Ann. Rep., Plate 6, description of plate.

33. Henderson, J. B., 1975, Archean Stromatolites in the Northern Slave Province, Northwest Territories, Canada; Can. Jour. Earth Sci., 12, pp. 1619-1630.

34. Hoek, C. v.d., Colijn, F., Cortel-Breeman, A. M. and Wanders, J. B., 1972, Algal Vegetation-Types Along the Shores of Inner Bays and Lagoons of Curaçao and of the Lagoon Lac (Bonaire), Netherlands Antilles; Verhand. Kon. Ned. Akad. Wetensch., Afd. Natuurkunde, 2 veks, D. 61, No. 2, p. 72.

35. Hoffman, P., 1967, Algal Stromatolites: Use in Correlation and Paleocurrent Determinations; Science, 157, pp. 1043-1045.

36. Hoffman, P., 1973, Recent and Ancient Algal Stromatolites: Seventy Years of Pedogogic Cross-Pollenation; in Evolving Concepts in Sedimentology, Ginsburg, R. N., ed., The Johns Hopkins University Studies in Geology, No. 21, pp. 178-191.

37. Hoffman, P., 1974, Shallow and Deepwater Stromatolites in Lower Proterozoic Platform-To-Basin Facies Change, Great Slave Lake, Canada; Am. Assoc. Pet. Geol., 58, pp. 856-867.

38. Hofmann, H. J., 1969, Attributes of Stromatolites; Geol. Surv. Can., Paper 69-39, p. 77.

39. Hofmann, H. J., 1971, Precambrian Fossils, Pseudofossils and Problematica in Canada; Geol. Surv. Can., Bull. 189, p. 146.

40. Hofmann, H. J., 1973, Stromatolites: Characteristics and Utility; Earth-Sci. Rev., 9, pp. 339-373.

41. Hofmann, H. J., 1974, The Stromatolite Archoaeozoon acadiense from the Proterozoic Green Head Group of Saint John, New Brunswick; Can. Jour. Earth Sci., 11, pp. 1098-1115.

42. Hofmann, H. J., 1975, Stratiform Precambrian Stromatolites, Belcher Islands, Canada: Relations Between Silicified Microfossils and Microstructure; Am. J. Sci., 275, pp. 1121-1132.

43. Hommeril, P. and Rioult, M., 1965, Etude de la Fixation des Sédiments Meubles par Deux Algues Marines: Rhodothamniella floridula (Dillwyn) J. Feldm. et Microcoleus chthonoplastes Thur., Mar. Geol., 3, pp. 131-155.

44. Hubbard, J. A. E., 1972, Stromatolitic Fabric: a Petrographic Model; 24 Int. Geol. Cong., Ses. 24, Sect. 7, pp. 380-396.

45. Johnson, J. H., 1961, Limestone Building Algae and Algal Limestones; Col. Sch. Mines, p. 297.

46. Kahle, C. F., Eustler, R. and Huh, J., 1973, Nature and Significance of Borings and Other Structures On and Within Oolite Allochems (abst.); Am. Assoc. Pet. Geol. Bull., 57, p. 787.

47. Kalkowsky, E., 1908, Oolith und Stromatolith im norddeutschen Bundsandstein; Zeitsch. Deutsch. Geol. Ges., 60, pp. 68-125.

48. Kendall, C. G. St. C. and Skipwith, P. A. d'E., 1968, Recent Algal Mats of a Persian Gulf Lagoon; Jour. Sed. Pet., 38 pp. 1040-1058.

49. Kepper, J. C., 1974, Antipathetic Relation Between Cambrian Trilobites and Stromatolites; Am. Assoc. Pet. Geol. Bull., 58, pp. 141-143.

50. Kobluk, D. R., 1976, Micrite Envelope Formation, Grain Binding and Porosity Modification by Endolithic (Boring) Algal in Calcarenites in Modern and Ancient Reef Environments (abst.); Geol. Assoc. Canada Program with Abstracts, 1., p. 78.

51. Laporte, L. F., 1963, Codiacean Algae and Algal Stromatolites of the Manlius Formation (Devonian) of New York; J. Paleont., 37, pp. 643-647.

52. Laporte, L. F., 1967, Carbonate Deposition Near Mean Sea-Level and Resultant Facies Mosaic: Manlius Formation (Lower Devonian) of New York State; Am. Assoc. Pet. Geol. Bull. 51, pp. 73-101.

53. Logan, B. W., 1961, Cryptozoon and Associated Stromatolites from the Recent, Shark Bay, Western Australia; Jour. Geol. 69, pp. 517-533.

54. Logan, B. W., 1974, Inventory of Diagenesis in Holocene-Recent Carbonate Sediments, Shark Bay, Western Australia; Am. Assoc. Pet. Geol., Mem 22, pp. 195-249.

55. Logan, B. W., Hoffman, P. and Gebelein, C. D., 1974, Algal Mats, Cryptalgal Fabrics and Structures, Hamelin Pool, Western Australia; Am. Assoc. Pet. Geol., Mem. 22, pp. 140-194.

56. Logan, B. W., Rezak, R. and Ginsburg, R. N., 1964, Classification and Environmental Significance of Algal Stromatolites; Jour. Geol., 72, pp. 68-83.

57. Lucia, F. J., 1968, Recent Sediments and Diagenesis of South Bonaire, Netherlands Antilles; J. Sed. Pet., 38, pp. 845-858.

58. Lucia, F. J., 1972, Recognition of Evaporitic-Carbonate Shoreline Sedimentation. in Recognition of Ancient Sedimentary Environments; Spec. Pub. 16, pp. 160-191.

59. Lukas, K. J., 1973, Taxonomy and Ecology of the Endolithic Microflora of Reef Corals with a Review of the Literature on Endolithic Microphytes; PhD Thesis, Univ. of Rhode Island.

60. Mawson, D., 1929, Some South Australian Algal Limestones in Process of Formation; Quart. Jour. Geol. Soc. London, 85, pp. 613-620.

61. Meer Mohr, C. G. v.d., 1972, Recent Carbonates from the Netherlands Antilles: Hypersaline to Open Marine Environments; Annales Soc. Géol. Belgique, 95, pp. 407-412.

62. Milliman, J. D., 1974, Marine Carbonates; Recent Sedimentary Carbonates, Pt. 1, Springer-Verlag, p. 374.

63. Monty, C., 1965a, Geological and Environmental Significance of Cyanophyta; PhD Thesis, Princeton University.

64. Monty, C. L. V., 1965b, Recent Algal Stromatolites in the Windward Lagoon, Andros Island, Bahamas; Ann. Soc. Géol. Belgique, 88, pp. 269-276.

65. Monty, C. L. V., 1967, Distribution and Structure of Recent Stromatolitic Algal Mats, Eastern Andros Island, Bahamas; Ann. Soc. Géol. Belgique, 90, p. 55-100.

66. Monty, C. L. V., 1972, Recent Algal Stromatolitic Deposits, Andros Island. Preliminary Report; Geol. Rund., 61, pp. 742-783.

67. Murray, R. C., 1969, Hydrology of South Bonaire, N.A. - a Rock Selective Dolomitization Model; J. Sed. Pet., 39, pp. 1007-1013.

68. Neumann, A. C., Gebelein, C. D. and Scoffin, T. P., 1970, Composition, Structure and Erodability of Subtidal Mats, Abaco, Bahamas; Jour. Sed. Pet., 40, pp. 274-297.

69. Pia, J., 1927, Thallophyta in Handbuch de Paläobotanik, 1, Oldenburg, München and Berlin.

70. Reis, O. M., 1908, Über Oolith und Stromatolith im norddeutschen Bundsandstein; N. Jb. Mineral., Geol., Palaont., 2, pp. 114-138.

71. Roddy, H. J., 1915, Concretions in Streams Formed by the Agency of Blue-Green Algae and Related Plants; Proc. Amer. Philos. Soc., 54, pp. 246-258.

72. Roehl, P. O., 1967, Stony Mountain (Ordovician) and Interlake (Silurian) Facies Analogs of Recent Low-Energy Marine and Subaerial Carbonates, Bahamas; Am. Assoc. Pet. Geol. Bull. 51, pp. 1979-2032.

73. Rothe, P., 1970, Aragonitic "Algal Lapilli" from Lagoonal Environment (Lobos, Canary Islands); Jour. Sed. Pet., 40, pp. 497-499.

74. Schopf, J. W., Haugh, B., Molnar, R. E. and Satterthwait, D. F., 1973, On the Development of Metaphytes and Metozoans; J. Paleo., 47, pp. 1-9.

75. Schopf, J. W., Oehler, D. Z., Horodyski, R. J. and Kvenvolden, K. A., 1971, Biogenicity and Significance of the Oldest Known Stromatolites; J. Paleo., 45, pp. 477-485.

76. Schroeder, J. H., 1972, Calcified Filaments of an Endolithic Alga in Recent Bermuda Reefs; N. Jb. Geol. Palaont., Mh., pp. 16-33.

77. Schwarz, H.-U., Einsele, G. and Herm, D., 1975, Quartz-Sandy, Grazing-Contoured Stromatolites from Coastal Embayments of Mauritania, West Africa; Sediment., 22, pp. 539-561.

78. Scoffin, T. P., 1970, The Trapping and Binding of Subtidal Carbonate Sediments by Marine Vegetation in Bimini Lagoon, Bahamas; Jour. Sed. Pet., 40, pp. 249-273.

79. Seely, H. M., 1906, Beekmantown and Chazy Formations in the Champlain Valley, Contribution to Their Geology and Paleontology; Rep. Vermont St. Geol., 1905-1906, 5, pp. 174-187.

90. Shinn, E. A., 1968, Practical Significance of Birdseye Structures in Carbonate Rocks; Jour. Sed. Pet., 38, pp. 215-223.

91. Shinn, E. A., 1969, Submarine Lithification of Holocene Carbonate Sediments in the Persian Gulf; Jour. Sed. Pet., 12, pp. 109-144.

92. Shinn, E. A., 1972, Worm and Algal-Built Columnar Stromatolites in the Persian Gulf; Jour. Sed. Pet., 42, pp. 837-840.

93. Shinn, E. A., Ginsburg, R. N. and Lloyd, R. M., 1965, Recent Supratidal Dolomite from Andros Island, Bahamas; SEPM Spec. Pub. 13, pp. 112-123.

94. Sibley, D. F. and Murray, R. C., 1972, Marine Diagenesis of Carbonate Sediment, Bonaire, Netherlands Antilles; J. Sed. Pet., 42, pp. 168-178.

95. Smith, D. B., 1974, Origin of Teepees in Upper Permian Shelf Carbonate Rocks of Guadalupe Mountains, New Mexico; Am. Assoc. Pet. Geol., Bull., 58, pp. 63-70.

96. Sorensen, L. O. and Conover, J. T., 1962, Algal Mat Communities of LyngbyacConfervoides (C. Agardh) Gomont; Pub. Inst. Mar. Sci., Univ. Texas, 8, pp. 60-74.

97. Steel, J. H., 1825, A Description of the Oolite Formation Lately Discovered in the County of Saratoga and State of New York; Am. J. Sci., Ser. 1, 9, pp. 16-19 (and pl. opp. p. 208).

98. Steinman, G., 1911, Über Gymnosolen ramsayi, eine Colenterate von der Halbinsel Kanin; Fennia, 31, pp. 18-23.

99. Toomey, D. F., 1975, Rhodoliths from the Upper Paleozoic of Kansas and the Recent - A Comparison; N. Jb. Geol. Paläont. Mh., pp. 242-255.

100. Turpaeva, E. P., 1957, Food Interrelationships of Dominant Species in Marine Benthic Biocenoses; in Nikitin, B. N., ed., Marine Biology; Trans. Inst. Oceanol. Mar. Biol., U.S.S.R. Acad. Sci., pp. 137-148.

101. Wagenaar Hummelinck, P. and Roos, P. J., 1959, Een Natuurwetenschappelijk Onderzoeck Gericht op het Behoud van het Lac op Bonaire; Natuurwetenschappelijke Werkgroep Nederlandse Antillen, No. 18, p. 28.

101. Walcott, C. D., 1914, Pre-Cambrian Algonkian Algal Flora; Smithsonian Inst. Misc. Coll., 64, pp. 77-156.

102. Walker, K. R., 1972, Communi ty Ecology of the Middle Ordovician Black River Group of New York State; Geol. Soc. Am. Bull., 83, pp. 2499-2524.

103. Walter, M. R., Golubic, S. and Preiss, W. V., 1973, Recent Stromatolites from Hydromagnesite and Aragonite Depositing Lakes Near the Coorong Lagoon, South Australia; Jour. Sed. Pet., 43, pp. 1021-1030.

104. Weed, W. H., 1889, On the Formation of Siliceous Sinter by the Vegetation of Thermal Springs; Am. J. Sci., Ser. 3, 137, pp. 351-359.

105. Zaneveld, J. S., 1958, A Lithothamnion Bank at Bonaire (Netherlands Antilles); Blumea Suppl., 4, pp. 206-219.